# OIL RETENTION AND PRESSURE DROP OF R1234YF AND R134A WITH POE ISO 32 IN SUCTION LINES

BY

ANKIT SETHI

THESIS

Submitted in partial fulfillment of the requirements
for the degree of Master of Science in Mechanical Engineering
in the Graduate College of the
University of Illinois at Urbana-Champaign, 2011

Urbana, Illinois

Adviser:

Professor Predrag S. Hrnjak

## Abstract

In most of the refrigeration systems a small quantity of oil is carried out of the compressor by high velocity vapor leaving the compressor discharge in the form of a mixture with the refrigerant. The circulating liquid which is a mixture of oil and refrigerant has the highest viscosity in the suction line to the compressor due to which it has the highest potential for oil retention. R1234yf is a new alternative refrigerant of low global warming potential (GWP) which has been developed for automobile air conditioners as a drop-in replacement for R134a in order to meet European Union's low GWP requirement. A quantitative comparison of oil retention and pressure drop characteristics of R1234yf and R134a with POE32 oil in 10.2 mm inside diameter horizontal and vertical suction lines at saturation temperature of 13$^{o}$C with 15$^{o}$C of superheat is presented. The effect of pipe inclination on oil retention was also investigated. High speed videos of the flow were taken to relate flow regimes to the oil retention data. Test results show that for same system cooling capacity, R1234yf and R134a have very similar oil retention; however, the use of R1234yf results in 20-30% higher pressure drop. It was also found that inclined suction lines retain more oil than vertical lines. A semi-empirical model for prediction of oil retention and pressure drop in vertical suction lines in annular flow regime is presented. The model predicts 90% of the oil retention and pressure drop within ± 20% and ± 30% of the experimental data. The model is used to propose a new criterion for minimum refrigerant mass flux which could be useful as an improved guideline for sizing of vertical suction lines.

*To My Parents and Sister*

\

## Acknowledgement

This research project would not have been possible without the support of many people. I would like to thank my advisor, Professor Predrag S. Hrnjak for his support and guidance throughout this project. I would like to thank Scott Wujek and Augusto Zimmermann for their tremendous support and help throughout this project. I would like to thank Aravind Ramakrishnan for his help in performing out the experiments. I would also like to thank the members of the Air Conditioning and Refrigeration Center at the University of Illinois for their support. Finally, I would like to thank my parents, my sister and all my friends for their love and support.

# Table of Contents

**List of Tables** ..... **vii**

**List of Figures** ..... **viii**

**Nomenclature** ..... **x**

**Chapter 1-INTRODUCTION** ..... **1**

1.1 Overview ..... 1

1.2 Literature Review ..... 2

1.2.1 Studies for determining minimum refrigerant velocity for oil return ..... 2

1.2.2 Studies for determining oil retention in suction lines ..... 5

1.2.3 Oil Retention Studies at ACRC, University of Illinois ..... 8

1.2.4 Studies for modeling of oil retention in suction lines ..... 10

1.3 Project Objectives ..... 12

**CHAPTER 2- EXPERIMENTAL TEST SETUP** ..... **13**

2.1 Description of the experimental facility ..... 13

2.2 Test Conditions ..... 17

**CHAPTER 3- EXPERIMENTAL RESULTS** ..... **19**

3.1 Flow Regimes and Flow Visualization ..... 19

3.1.1 Horizontal Pipe Visualization and Flow Regimes ..... 19

3.1.2 Vertical Pipe Visualization and Flow Regimes ..... 24

3.1.3 Inclined Pipe Visualization and Flow Regimes ..... 27

3.2 Oil Retention and Pressure Drop ..... 29

3.2.1 Oil Retention and Pressure Drop for R134a/POE32 ..... 29

3.2.1.1 Vertical Pipe ..... 31

3.2.1.2 Horizontal Pipe ..... 33

3.2.2 Oil Retention and Pressure Drop for R1234yf/POE32 ..... 34

3.2.2.1 Vertical Pipe ..... 36

3.2.2.2 Horizontal Pipe ..... 37

3.3 Comparison of R134a/POE 32 and R1234yf/POE 32 ..... 38

3.4 Oil Retention in Inclined Pipes ..... 42

**CHAPTER 4- MODELING OF OIL RETENTION AND PRESSURE DROP IN VERTICAL SUCTION LINES ..... 44**
4.1 Development of the model ..... 44
4.1.1 Navier-Stokes equation for liquid film ..... 45
4.1.2 Momentum Balance for the Refrigerant Vapor Core ..... 48
4.1.3 Correlation for interfacial friction factor ..... 49
4.1.4 Procedure for calculating oil retention and pressure drop in suction lines ..... 51
4.2 Validation of the model ..... 53
4.3 Parametric Study ..... 61
4.3.1 Effect of reducing the cooling capacity ..... 61
4.3.2 Effect of pipe diameter ..... 62
4.3.3 Effect of suction line superheat ..... 63
4.4 Model for prediction of minimum refrigerant mass flux for oil return ..... 65
4.4.1 Development of Model ..... 65
4.4.2 Procedure for calculating minimum refrigerant mass flux for vertical suction lines ... 71
**CHAPTER 5- SUMMARY AND CONCLUSIONS ..... 72**
5.1 Conclusions from experimental study ..... 72
5.2 Conclusions from modeling efforts ..... 73
**APPENDIX A ..... 75**
**APPENDIX B ..... 77**
**APPENDIX C ..... 81**
**REFERENCES ..... 84**

# List of Tables


| | | |
|---|---|---|
| Table 2.1 | Mass flux test conditions for R134a/POE 32…….. | 18 |
| Table 2.2 | Mass flux test conditions for R1234yf/POE 32…….. | 18 |
| Table 4.1 | Statistical comparison between experimental data and model predictions for oil retention…… | 55 |
| Table 4.2 | Statistical comparison between experimental data and model predictions for pressure drop……. | 55 |
| Table 4.3 | Density of refrigerant vapor and viscosity of liquid film at different superheats at $10^{o}$C evaporation temperature for R134a/POE ISO 32 mixture…… | 64 |
| Table 4.4 | Minimum Refrigeration Capacity in kW for Oil Entrainment up Suction Risers based on the proposed model (OCR 0.3%)……. | 68 |
| Table 4.5 | Minimum Refrigeration Capacity in kW for Oil Entrainment up Suction Risers based on the proposed model (OCR 0.5%)……. | 69 |
| Table 4.6 | Minimum Refrigeration Capacity in kW for Oil Entrainment up Suction Risers based on the proposed model (OCR 1.0%)……. | 70 |
| Table A-1 | Repeatability tests 10.2 mm tube…….. | 76 |

# List of Figures


Figure 2.1 Schematic of the facility……..... 14

Figure 3.1 Flow pattern map for R134a-POE32 in 10.2mm I.D. horizontal pipe (Taitel, Dukler 1976) ..... 19

Figure 3.2 Flow pattern map for R134a-POE 32 in 10.2mm I.D. horizontal pipe (Baker 1954)..... 20

Figure 3.3 Description of flow visualization images…… 21

Figure 3.4 R1234yf/POE 32 flow visualization in horizontal pipe for different mass flux and OCR…….. 21

Figure 3.5 R134a/POE 32 flow visualization in horizontal pipe for different mass flux and OCR……..... 22

Figure 3.6 R1234yf/POE 32 flow visualization in vertical pipe for different mass flux and OCR…….. 24

Figure 3.7 R134a/POE 32 flow visualization in vertical pipe for different mass flux and OCR…….. 25

Figure 3.8 Flow visualization in inclined pipes with R1234yf/POE 32…… 28

Figure 3.9 Oil retention as a function of mass flux for three different OCRs for R134a/POE 32 in 10.2 mm I.D. pipe……... 30

Figure 3.10 Pressure drop as a function of mass flux for three different OCRs for R134a/POE 32 in 10.2 mm I.D. pipe……..... 30

Figure 3.11 Oil retention as a function of mass flux for three different OCRs for R1234yf/POE 32 in 10.2 mm I.D. pipe…… 35

Figure 3.12 Pressure drop as a function of mass flux for three different OCRs for R1234yf/POE 32 in 10.2 mm I.D. pipe…… 36

Figure 3.13 Comparison of oil retention for R134a/POE 32 and R1234yf/POE32 for 1% OCR……... 40

Figure 3.14 Comparison of pressure drop for R134a/POE 32 and R1234yf/POE32 for 1% OCR …… 41

Figure 3.15 Effect of angle of inclination from the horizontal on oil retention for R1234yf/POE 32…… 43

Figure 3.16 Effect of angle of inclination from the horizontal on liquid hold-up for air/water (Beggs, Brill 1973)…… 43

Figure 4.1 Force balance on the refrigerant vapor core in annular flow……... 45

Figure 4.2 Experimental validation of the model based on oil retention per unit length of vertical suction pipe..... 53

Figure 4.3 Pressure drop model validation for unit length of vertical suction pipe ……. 54

Figure 4.4 Model predictions with experimental data for oil retention as a function of mass flux for three OCRs in vertical pipe for R134a/POE …… 56

Figure 4.5 Model predictions with experimental data for oil retention as a function of OCR and mass flux as parameter in vertical pipe for R134a/POE ……. 56

Figure 4.6 Model predictions with experimental data for pressure drop as a function of mass flux for three OCRs in vertical pipe for R134a/POE ……. 57

Figure 4.7 Model predictions with experimental data for oil retention as a function of mass flux for three OCRs in 7.1 mm I.D. vertical pipe for R410A/POE …….. 58

Figure 4.8 Model predictions with experimental data for oil retention as a function of OCR and mass flux as parameter in 7.1 mm I.D. vertical pipe for R410A/POE …… 58

Figure 4.9 Model predictions with experimental data for oil retention as a function of OCR and mass flux as parameter in 18.5 mm I.D. vertical pipe for R410A/POE ……. 59

Figure 4.10 Model predictions with experimental data for pressure drop as a function of mass flux for three OCRs in vertical pipe for R410A/POE …… 59

Figure 4.11 Comparison of Radermacher et al. (2006) and proposed model for R22/MO data from Cremaschi et al. (2005)……. 60

Figure 4.12 Effect of cooling capacity reduction on oil retention and pressure drop based on the proposed model……... 62

Figure 4.13 Effect of diameter on oil retention and pressure drop based on the proposed model……. 63

Figure 4.14 Effect of suction line superheat on oil retention and pressure drop based on the proposed model. 64

Figure 4.15 Oil retention data for R134a/POE 32 in 10.2 mm I.D. vertical pipe with various minimum mass flux limits……... 66

Figure 4.16 Pressure drop data for R134a/POE 32 in 10.2 mm I.D. vertical pipe with various minimum mass flux limits…… 66

# Nomenclature

| | | | | | |
|---|---|---|---|---|---|
| a | = | constant | $\dot{m}$ | = | mass flow rate, kg/s |
| b | = | constant | MO | = | mineral oil |
| c | = | constant | ISO | = | International Organization for Standardization |
| A | = | inner area of pipe, $m^2$ | OCR | = | oil in circulation ratio |
| AB | = | alkyl benzene | P | = | pressure, Pa |
| D | = | diameter, m | $P_{sat}$ | = | saturation pressure, Pa |
| EES | = | Engineering Equation Solver | PAG | = | polyalkylene glycole oil |
| $f_i$ | = | interfacial friction factor | POE | = | polyol ester oil |
| $f_s$ | = | smooth pipe friction factor | r | = | radial distance from axis |
| g | = | gravity, $m/s^2$ | R | = | pipe radius, m |
| GWP | = | global warming potential | Re | = | Reynolds number |
| G | = | mass flux, $kg/m^2s$ | SUS | = | saybolt universal seconds |
| HFC | = | hydrofluorocarbon | $T_{bub}$ | = | bubble temperature, $^oC$ |
| HFO | = | hydrofluoroolefins | u | = | velocity |
| j* | = | dimensionless superfacial velocity | $w_{local}$ | = | local oil concentration in liquid film |
| K | = | constants | We | = | Weber number |
| L | = | length of suction pipe, m | x | = | quality |
| $m_{oil}$ | = | mass of oil, kg | z | = | axial distance |

## Greek Symbols

| | | | | | |
|---|---|---|---|---|---|
| $\alpha$ | = | void fraction | $\rho$ | = | density, $kg/m^3$ |
| $\delta$ | = | liquid film thickness, m | $\sigma$ | = | surface tension, N/m |
| $\delta^+$ | = | dimensionless film thickness | $\tau$ | = | shear stress, Pa |
| $\mu$ | = | dynamic viscosity, Pa-s | $\tau_i$ | = | interfacial shear stress, Pa |
| $\upsilon$ | = | kinematic viscosity, $m^2/s$ | | | |

## Subscripts

| | | | | | |
|---|---|---|---|---|---|
| A | = | air | v | = | refrigerant vapor |
| c | = | refrigerant vapor core | W | = | water |
| l | = | liquid film | z | = | axial coordinate |
| r | = | radial coordinate | | | |

# Chapter 1-INTRODUCTION

## 1.1 Overview

There has been extensive research in studying oil holdup in different components of a refrigeration system for over four decades. The positive displacement compressors used in refrigeration systems need oil for lubrication of the parts that slide in the compression chamber. A small amount of oil is carried out of the compressor by high velocity vapor leaving the compressor discharge in the form of a mixture with the refrigerant. This liquid mixture (primarily oil) has highest viscosity in suction line of a refrigeration system due the low temperature and high quality conditions prevalent there. Hence the suction line has the highest potential for oil retention in the entire system. In order to ensure that a refrigeration system operates properly measures need to be taken for returning this oil back to the compressor, otherwise depleted oil levels and consequently poor lubrication could lead to its failure. With the advent of various energy saving measures like variable speed compressors, the oil return becomes a big problem in these suction lines especially under part load conditions due to low vapor velocities. Moreover, the presence of oil in the suction lines has a detrimental effect on the system performance as it leads to increase in pressure drop. Refrigerants such as R11 and R12 have already been phased out due to their high global warming and ozone depletion potential and R22 is also being phased out throughout the world. HFC's (Hydrofluorocarbons) such as R410A, R407C and R502 were introduced as replacement for R22. However these refrigerants were immiscible with mineral oil (MO) due to which the oil film has a higher viscosity and therefore had poor oil return characteristics (Sundaresan, Radermacher 1996). Hence new miscible synthetic lubricants such as polyolesters (POEs) and polyalkylene glycols (PAGs) were

developed which exhibited good oil return characteristics (Sundaresan, Radermacher 1996). Recently there has been further push towards development of refrigerants with even lower global warming potential as compared to HFC's. HFO's (Hydrofluoroolefins) like R1234yf and R1234ze have been developed which have 300 times lower GWP as compared to R134a. R1234yf has been developed as a drop-in replacement for R134a in order to meet European Union's low GWP requirement for automotive air-conditioning systems and is expected to be used extensively in these and other refrigeration systems. The purpose of this study is to compare the oil retention and pressure drop characteristics of R1234yf and R134a.

## 1.2 Literature Review

### 1.2.1 Studies for determining minimum refrigerant velocity for oil return

It was believed that ASHRAE (1973) data on oil transport in vertical risers did not have sufficient experimental validation. An experimental study was carried out by Jacobs et al. (1976) to verify the data reported by ASHRAE and to establish analytical conditions for good oil return by refrigerant vapor. The refrigerants used were R12 and R22 along with 150 and 300 SUS napthenic oils. Oil was injected into the test section at the bottom and oil transport was observed through the sight glass following the point of injection. The vapor refrigerant flow rate was decreased until liquid accumulation was observed in the sight glass indicating lack of oil transport. This was referred to as refrigerant mass flux required for good oil return. Typical compressor suction and discharge conditions were simulated. The experimental results were correlated using flooding correlations proposed by Wallis (1969). Within the range of experimental data collected a conservative bound for guaranteeing oil return was suggested by authors as

$$j_v^{*\frac{1}{2}} = 0.85 \quad (1.1)$$

Where dimensionless j* relates momentum flux of the vapor to the gravitational and buoyant forces. This bound was suggested entirely on the basis of visual observation. This criterion was recast into a more convenient form in terms of minimum refrigerant mass flux required for oil return.

$$G = \left(j_v^{*\frac{1}{2}}\right)^2 \left[\rho_v g D(\rho_l - \rho_v)\right]^{0.5} \quad (1.2)$$

The authors further presented the data as minimum tonnage required to ensure oil return and presented it in form of charts which indicated the minimum diameter of suction risers for ensuring oil return. The correlation suggested by the authors did not take into account the effect of lubricant concentration nor does it includes the effect of viscosity changes in oil.

An experimental and theoretical investigation oil return characteristics in vertical suction risers was carried out by Mehendale and Radermacher (2000). The objective of this study was to determine the critical refrigerant mass flow rates required to ensure oil return and compare the results with predictions of Jacobs et al. (1976). Two kinds of tests were carried out a) Flow reversal tests in which the onset of flow reversal was observed and b) falling film tests in which oil film front was seen moving downwards. Five different combinations of refrigerant oil mixtures were compared R22, R407A, R410A with MO and R407C, R410A with POE. Injection separation method was used and two different sight glasses at top and bottom of the vertical test section were used to visualize the flow. They observed that as the refrigerant mass flow rate was reduced below the critical value the stable upward oil film started oscillating and became unstable and eventually reversed its direction of motion. They observed that critical

refrigerant mass flow rate for oil transport by superheated vapor was higher than that suggested by Jacobs et al. (1976). The authors also developed an analytical model to predict critical refrigerant mass flow rate for oil return in annular flow. Wallis (1969) correlation for interfacial friction factor was used in developing the model. The predictions from the model were within -4% and +7% of the experimental data. A parametric study of the variation of critical refrigerant mass flow rate was carried out using the analytical model. They reported that the critical refrigerant flow rate should decrease with increasing film viscosity or vapor quality. On the other hand critical refrigerant flow rate should increase as the pipe diameter or the vapor density increases.

An analytical study to investigate the minimum refrigerant mass flux for carrying the lubricating oil up in the vertical suction lines was carried out by Kesim at al. (2000). They applied Navier-Stokes and continuity equations to the liquid film and the refrigerant vapor and arrived at a set of equations. These equations were closed by relating frictional pressure drop to refrigerant vapor velocity using an empirical expression for interfacial friction factor. The authors used the Blasius correlation (Hager 2003) for turbulent flow in smooth pipe for determining the interfacial friction factor. It was assumed that in the limiting condition case, the volumetric flow rate of oil would be equal to zero. The authors formulated tables indicating minimum cooling capacity needed for entraining oil up the suction risers and hot gas risers. The tables were presented for R-134a refrigerant for copper tubing of different internal diameters and saturation suction temperatures of -35, -25, -15, -5 and 5$^{o}$C while the condensing temperatures was kept at 40$^{o}$C. For condensing temperatures different than 40$^{o}$C correction factors were provided. In arriving at these tables the authors assumed that oil film thickness was 1/50$^{th}$ of the internal diameter of the tube as a conservative estimation of the practically worst condition at which it may still be expected that

oil is carried up with refrigerant vapor. Though this study takes into account the effect of lubricant concentration and viscosity of liquid, the assumption that the interfacial friction can be represented by Blasius correlation may not be accurate, as near the conditions of liquid film reversal the liquid vapor interface is rough due to the presence of interfacial waves whereas Blasius correlation was developed for turbulent flow in smooth pipes. The lack of any experimental validation is another limitation of this study.

### 1.2.2 Studies for determining oil retention in suction lines

Oil return characteristics of R407C/MO, R407C/POE and R22/MO was studied by Sundaresan, and Radermacher (1996) in a split three-ton heat pump system. They reported that R22/MO and R407C/POE have similar oil return characteristics and were expected to be equally reliable. However, in case of R407C/MO a significant amount of oil was logged in the system outside the compressor. This was because the new HFC blends were immiscible with MO leading to high liquid film viscosity and consequently larger retention in condenser, evaporator and suction line. They suggested further experiments were needed have a better understanding of oil return characteristics.

An experimental investigation of oil accumulation characteristics in a vertical suction line was carried out by Lee et al. (2001). Three different types of refrigerant oil mixtures were investigated R134a with AB ISO-8, AB ISO-10 and MO ISO-10. Conditions similar to those which exist in residential refrigerators and freezers were simulated. Injection-extraction technique was used to measure the amount of oil accumulated in the vertical test section. Oil was injected at the bottom of a pure refrigerant suction line and was separated at the top of the suction line by using oil separators. The mass of oil retained in the test section was the difference between the total mass of oil injected into the test section and the total amount of oil that was

extracted from the test section. Large amounts of oil accumulated in test section for MO and high viscosity AB oil and about 2 to 17% of the oil initially charged in the compressor was found in the test section. The results were also presented as mean oil film thickness ratio (MOFTR) which is the ratio of average film thickness and radius of the pipe. The high viscosity AB ISO-10 oil has higher MOFTR as compared to AB ISO-8. It was also observed that MO has around 3 times higher MOFTR as compared to AB ISO-8 at refrigerant vapor velocity of 1 m/s due to its poor solubility with R134a. However at high vapor velocities of 4.6 m/s the MOFTR was not influenced by oil type and viscosity. The MOFTR increases as the oil flow rate increases and decreases as vapor velocity increases. The authors suggested using lower viscosity AB oil instead of MO for safe oil return. The authors also carried out flow visualization studies and observed only annular flow and churn flow patterns within the range of refrigerant mass flow rate and oil mass flow rate investigated. At high refrigerant Reynolds numbers (Re=13,000 and Re=16,000) the flow pattern was an annular flow regime for all oil types with oil film continuously flowing upwards. On the other hand at low refrigerant Reynolds numbers (Re=4,000) the flow pattern was churn flow for all oil types and oil flow rates. The authors recommended that the churn flow pattern be avoided because the oil transport in a vertical tube is very unstable.

An experimental and theoretical investigation of oil retention in several components of a carbon dioxide air conditioning system was performed by Lee (2003). PAG oil was used as the lubricant which was partially miscible with $CO_2$. The oil injection-extraction technique similar to one used by Lee et al. (2001) was used for measuring the oil retention in different components. The oil retention was expressed as oil retention volume ratio which was the ratio of oil volume retained to oil volume initially charged in a typical automotive air conditioning system which was

assumed to be 250 ml. The oil in circulation ratio which was defined as the ratio of oil mass flow rate to total mass flow rate of refrigerant and oil mixture was varied from 1-7 wt%. The suction line was horizontal with an inside diameter of 7.1 mm and length of 3.8 m. They observed that the oil retention volume ratio in horizontal suction line increased from 0.05 to 0.15 as oil in circulation ratio was increased from 1.4 to 6 wt% at refrigerant mass flux of 290 kg/($m^2$s). They also observed that as the refrigerant mass flux was increased from 290 kg/($m^2$s) to 559 kg/($m^2$s), the oil retention volume ratio in the suction line decreased from 0.1 to 0.04 at oil in circulation ratio of 2 wt%. It was observed that as vapor quality at the inlet to the suction line increased the oil retention volume also increased. This happened because the local liquid viscosity increases due to increase of oil concentration in the liquid film.

An extensive experimental study for measuring oil retention in different components of air conditioning system was carried out by Cremaschi et al. (2005). Injection-extraction technique similar to the one used by Lee et al. (2001) was used to determine the amount of oil retained in condenser, liquid line, evaporator and suction line. Five different refrigerant oil mixtures R22/MO, R410A/MO, R410A/POE, R134a/POE and R134a/PAG were investigated. Oil retention in both horizontal and vertical suction lines was investigated. The oil mass fraction was varied from 0.7 to 8 wt% and refrigerant mass flux from 150 to 400 kg/($m^2$s). The variation of oil retention with refrigerant mass flux, orientation of pipe, oil-refrigerant mixture viscosity and degree of mutual miscibility and solubility of oil and refrigerant mixture was discussed. They found that at an oil mass fraction of 5% increasing mass flux from 150 to 206 kg/($m^2$s) led to decrease in oil retention volume by about 30% in horizontal test section. It was also found that at oil mass fraction of 3% an increase in oil refrigerant mixture viscosity by a factor of 3 leads to oil retention volume increasing by a factor of 4. At same oil mass fraction refrigerant oil

mixtures such as R134a/POE and R134a/PAG have 20% lower oil retention than R22/MO due to their lower liquid film viscosity as compared to R22/MO. The oil retention in the upward vertical suction line was about 50% more than horizontal line at same refrigerant mass flux and oil mass fraction due to the effect of gravity on liquid film.

### 1.2.3 Oil Retention Studies at ACRC, University of Illinois

Oil retention in horizontal suction pipes with 9 mm inside diameter for a typical refrigeration system was studied by Crompton et al. (2004) . Experiments were carried out with internally smooth pipes and enhanced pipes with internal helical microfins. Five different refrigerant oil mixtures were investigated R134a/POE, R134a/PAG, R134a/alkylbenzene, R22/ alkylbenzene and R410A/POE. The refrigerant mass flux was varied from 75-150 kg/($m^2$s), inlet vapor quality from 0-100% and oil concentration from 0-5%. Oil retention was measured by the technique of direct measurement. The refrigerant and oil mixture was mixed in liquid line and the mixture was allowed to run through the evaporator. The system was allowed to reach at equilibrium and while the system was running the valves on both ends of the test section were closed simultaneously. The test section was removed and weighed. Then the test section was put under vacuum to remove the entire refrigerant and the test section was weighed again to determine the mass of oil retained. It was found that the oil retention decreases as vapor quality increases reaches a minimum at around mid qualities of around 0.4-0.6 and increases again as quality increases further because the viscosity of oil starts dominating the behavior of liquid flow. The oil retention increases as the refrigerant mass flux decreases and the enhanced pipes were also found to have higher oil retention. However, tube surface was found to an influence on oil retention only at high qualities. They also reported that immiscible oil refrigerant mixture had

higher oil retention as compared to a miscible mixture under similar conditions. It was found that higher refrigerant mass flux tend to have higher void fraction if all other conditions are similar.

Oil retention in horizontal and vertical suction lines with R410A/POE refrigerant oil mixture was studied by Zoellick and Hrnjak (2010). Two different pipe diameters 7.1 mm and 18.5 mm were investigated. The refrigerant mass flux was varied from 100-250 kg/($m^2$s) for 7.1 mm pipe and from 50-100 kg/($m^2$s) for 18.5 mm pipe. The OCR (oil in circulation ratio) was varied from 1-5% and two different evaporator superheat 10$^o$C and 15$^o$C were investigated. Oil retention was measured by direct measurement similar to Crompton et al. (2004). The study focused on studying the variation of oil retention with mass flux, OCR and superheat. It was found that the oil retention in vertical pipe increased substantially as the mass flux was reduced and Jacobs limit was approached. Some hysteresis in the transition of flow from annular to churn flow regime near the Jacobs limit was also observed and he suggested that vertical suction lines should be sized for mass flux 30% above the Jacobs limit. He also reported that increasing the OCR from 1% to 5% led to around 20% to 50% increase in oil retention. The vertical suction pipe had 10% higher oil retention than horizontal pipe at high refrigerant vapor velocities. He also reported that a 5$^o$C increase in superheat from 10$^o$C to 15$^o$C led to 15% increase in oil retention as the viscosity of liquid film increases as superheat increases.

This review of literature illustrates that studies on oil retention in suction lines can be broadly divided into two groups one using injection-extraction methods and others using direct measurement techniques. The injection-extraction method may not be very accurate as it generates non-equilibrium condition inside the suction riser, as some refrigerant will be dissolving into oil during the test. The efficiency of oil separators used to separate oil at the exit of the test section reduces drastically as the oil concentration is reduced which reduces the

accuracy of measurement. However, injection-extraction technique is very useful for studying oil retention in different components of an air-conditioning system like condenser and evaporator as it may be difficult to remove and weigh these components although some results were presented (Peuker and Hrnjak 2010). Direct measurement may be a better technique for measuring oil retention in any component of an air-conditioning system. However, it is very time consuming and it may be difficult to use this approach to measure oil retention in condenser and evaporator. This technique is very suitable for measuring oil retention in the suction lines if they can be removed, weighed and reinstalled easily. The objective of the current work was to study and compare oil retention of R1234yf and R134a with POE 32 oil in horizontal and vertical suction lines under similar conditions since former is supposed to be a drop in replacement of the latter. The project was aimed at studying the effect of refrigerant mass flux, oil in circulation ratio and pipe orientation on oil retention. The method of direct measurement by weighing the suction lines was used to measure the oil retention. An experimental investigation of the effect of inclination on oil retention was also carried out.

### 1.2.4 Studies for modeling of oil retention in suction lines

Various studies have focused on modeling of oil retention in suction lines. The models have been developed for annular flow regime since it is most commonly observed in suction lines. Several researchers have developed models by applying Navier-Stokes and continuity equations to the liquid film and the refrigerant vapor. The system of equations thus obtained are solved using closure equation by relating interfacial shear stress to the vapor momentum using interfacial friction factor. A semi-empirical model for prediction of oil retention in horizontal suction line with $CO_2$/PAG mixture was proposed by Lee (2003). An empirical expression for interfacial friction factor relating it to refrigerant vapor Reynolds number and dimensionless film thickness

was proposed. A similar model for horizontal suction line was proposed by Radermacher et al. (2006) using experimental data obtained by Cremaschi et al. (2005) for various refrigerant oil mixtures. They proposed a new empirical expression for interfacial friction factor as a function of refrigerant vapor Reynolds number, Weber number of the mixture and dimensionless film thickness. Their model was applicable for the refrigerant vapor Reynolds number in the range $1.7*10^4<Re_v<4*10^4$ and liquid film thickness ranged from $0.001<\delta/D<0.06$. The model predictions for oil retention in horizontal pipes were within ±31% of the experimental results. They recommended further investigation on oil retention in vertical pipe as they could not verify the applicability of their model for mixtures other than R22/MO. The accuracy of model in prediction of the pressure drop in suction lines was not discussed. Zoellick and Hrnjak (2010) studied oil retention with R410A/POE mixture in 7.1 mm and 18.5 mm diameter horizontal and vertical suction pipes. He proposed an empirical correlation relating dimensionless film thickness with liquid film Reynolds number similar to approach followed by van Rossum (1959). He used Wallis (1969) correlation for relating interfacial friction factor with film thickness. His correlations were able to predict oil retention within ±20% for both horizontal and vertical suction pipes. However he did not discuss accuracy of his model in prediction of the pressure drop in suction lines.

## 1.3 Project Objectives

The primary objective of this research was to study and compare oil retention and pressure drop of R1234yf and R134a with POE 32 oil in suction lines under similar conditions since former is supposed to be a drop in replacement of the latter. The project was aimed at studying the effect of refrigerant mass flux, oil in circulation ratio and pipe orientation on oil retention. Oil retention was measured in horizontal, vertical and inclined pipes. The method of direct measurement by weighing the suction lines was used to measure the oil retention. Transparent suction pipes were used and high speed videos of the flow were taken in order to relate the oil retention with flow regimes. A new analytical/semi-empirical model was to be developed to predict oil retention and pressure drop in suction lines using the experimental data. The final aim was to provide system designers with tools and guidelines which could enable better design of suction lines.

# CHAPTER 2- EXPERIMENTAL TEST SETUP

## 2.1 Description of the experimental facility

An experimental facility was developed by Zoellick and Hrnjak (2010) to study oil retention in horizontal and vertical suction lines, thereby simulating the suction line of a typical R410A air conditioning system. The facility was modified and a condensing unit was installed to increase the range through which the refrigerant mass flow rate could be varied to study different flow regimes. Figure 2.1 shows a schematic of the modified facility. The fluids investigated in this study were R134a and R1234yf with nominally 32 cSt POE oil. There was one vertical and horizontal test section made of clear PVC tubes, each of which was about 2 m long. The internal diameter of the test sections was 10.2 mm. The system was modified so that the vertical test sections could be inclined at any angle to study the effect of inclination on oil retention. The method of direct measurement was used to determine the oil retention by weighing the test sections. There were ball valves on both sides of the test sections, which were closed simultaneously during steady state conditions to measure the mass of oil retained inside of the test sections. In order to measure the pressure drop across the test sections pressure taps were provided at both ends of test section. In order to prevent any disturbance to the flow, 1.6 mm diameter holes were drilled in 12.7 mm unions and copper pressure tap pipes were brazed to the union. The ball valves were chosen so that the orifice of the valves was very close to the internal diameter of the test sections in order to prevent any disturbance to the flow.

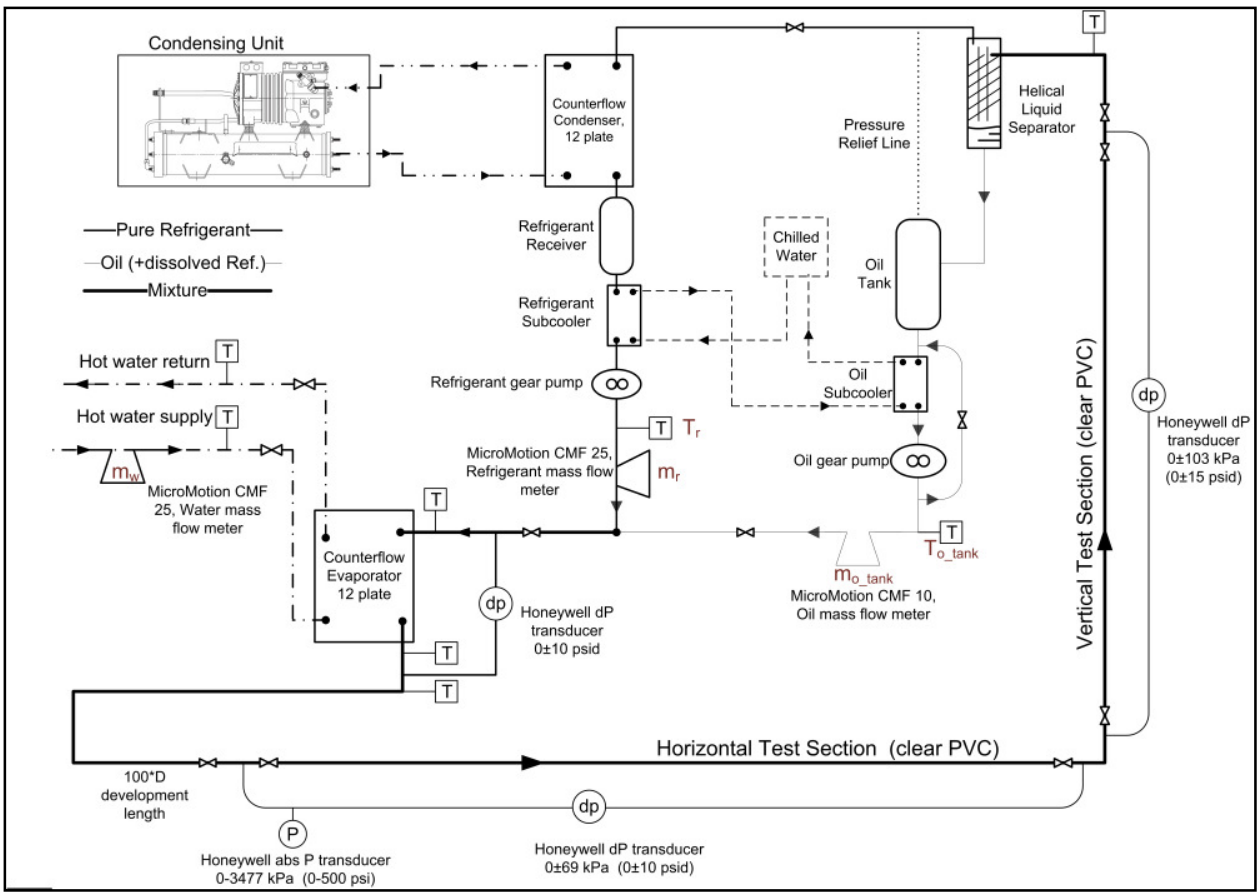


Figure 2.1 - Schematic of the facility

The pure liquid refrigerant was pumped by a gear pump which was driven by a variable speed motor. A subcooler was provided at the inlet to the refrigerant pump to prevent cavitation. A MicroMotion CMF25 Coriolis flow meter was used to measure the flow rate and density of liquid refrigerant. The accuracy and repeatability of the mass flow measurements are ±0.1% and ±0.05% of the flow rate reading respectively. The accuracy of the CMF25 density measurement is ±0.5 kg/m$^3$.

The oil tank contained oil with some dissolved refrigerant. A gear pump was used to pump the oil-refrigerant mixture from the tank. The pump was driven by a fixed frequency AC motor and a bypass valve was used to control the flow rate. A subcooler was provided to increase subcooling and reduce the fluctuations in the flow rate. The flow rate and density of oil rich mixture was

measured using a MicroMotion CMF10 Coriolis flow meter. The accuracy and repeatability of the mass flow measurements are ±0.1% and ±0.05% of the flow rate reading respectively. The accuracy of the density measurement is ±0.5 kg/m$^3$. A T-type thermocouple (±0.5 °C) measured the temperature of the oil flow at the entrance to the flow meter. The concentration of refrigerant dissolved in the oil flow was calculated from the temperature and density of the oil mixture as described in Zoellick and Hrnjak (2010). The OCR (oil in circulation ratio) at the inlet of the test section was controlled by adjusting the flow rate of the pure refrigerant stream and the oil stream. A typical OCR measurement with associated uncertainty would be 0.05 ± 0.001.

The pure refrigerant and oil rich mixture were mixed and then flowed into the evaporator. A 12 plate counter flow plate heat exchanger was used as the evaporator. The superheat at the exit of the evaporator was controlled by varying the temperature and flow rate of hot water entering the evaporator. In order to ensure that the oil rich liquid and vapor leaving the evaporator are in equilibrium, temperature at the exit of the evaporator was measured at the center of the tube and on the outside of the tube wall underneath the insulation. In order to ensure that the flow is thermally and hydrodynamically fully developed before it enters the test section a 100 diameter long development length was provided. As the temperature of the mixture at the outlet of the evaporator and the saturation pressure determined the concentration of oil in the liquid phase, both of them were maintained within ±3% or ±1 °C of the set value during a test. Since the oil and refrigerant were completely mixed before they entered the test sections it can be assumed that equilibrium conditions prevailed inside the test sections as opposed to injection-extraction technique in which non-equilibrium conditions may be generated due refrigerant being dissolved in oil in test sections.

The liquid and vapor leaving the test section were separated by using a helical separator provided at the exit of the vertical test section. The oil rich liquid flowed into the oil tank and the pure refrigerant vapor flowed into a 12-plate counter flow plate heat exchanger which served as condenser. This condenser served as an evaporator for R-22 condensing unit. The capacity of condensing unit was varied by varying the compressor speed. The compressor speed was varied in order to maintain the required saturation temperature and to ensure that all vapor is condensed to liquid. The condensed liquid fell directly into a receiver due of gravity from where it was pumped by the refrigerant gear pump.

A Honeywell Sensotec TJE absolute pressure transducer with a range 0 to 3477 kPa and accuracy ± 8.6 kPa was used to measure the saturation pressure at the inlet to the horizontal test section. A Honeywell Sensotec Z differential pressure transducer with a range 0 ± 69 kPa and accuracy ± 0.1 kPa was used to measure the pressure drop across the horizontal test section. A Honeywell Sensotec Z differential pressure transducer with a range 0 ± 103 kPa and accuracy ± 0.26 kPa was used to measure the pressure drop across the vertical test section. The oil holdup measurements throughout this investigation have been found to have an uncertainty of ±0.08g, which is a maximum percent error of 2% at an oil holdup of 4.72g.

A Yokogawa HR1300 data-logger was used to read the outputs from all thermocouples, pressure transducers, and Coriolis flow meters. The data-logger interfaces with a computer running a LabView program to display and record all measured data.

A detailed description of experimental facility and the testing procedure is presented in Zoellick and Hrnjak (2010) .

## 2.2 Test Conditions

In the current study two different refrigerants, R134a and R1234yf with POE ISO 32 oil were investigated. The saturation temperature was maintained at 13$^{o}$C and the superheat was 15$^{o}$C. The test section inside diameter was 10.2 mm and tests were run with mass flux varying from 170 kg/m$^2$s for R1234yf and 140 kg/m$^2$s for R134a, upto Jacobs et al. (1976) minimum limit. The mass flux presented here is obtained by dividing the total mass flow rate of refrigerant vapor and oil rich liquid by the internal area of the pipe. The length of both horizontal and vertical test sections was around 2 m. The vertical test section was inclined to angle of inclination of 45$^{o}$ and 60$^{o}$ from the horizontal to study oil retention in inclined pipes. Tables 2.1 and 2.2 illustrate the mass flux studied and corresponding superficial vapor velocities for R134a/POE and R1234yf/POE respectively. The OCR (oil in circulation ratio) was defined as the ratio of the mass flow rate of oil to the total mass flow rate of oil and refrigerant and it was varied from 1-5%. High speed videos of the flow inside the transparent test section were taken in order to relate oil retention to flow regimes.

Table 2.1- Mass flux test conditions for R134a/POE 32

| D=10.2 mm | |
|---|---|
| **Superficial Vapor Velocity** | Mass Flux |
| **[m/s]** | [kg/m$^2$s] |
| **1.5** | 33 (Jacobs Limit) |
| **2.5** | 50 |
| **3** | 60 |
| **4** | 80 |
| **5** | 100 |
| **6** | 120 |
| **7** | 140 |

Table 2.2-Mass flux test conditions for R1234yf/POE 32

| D=10.2 mm | |
|---|---|
| **Superficial Vapor Velocity** | Mass Flux |
| **[m/s]** | [kg/m$^2$s] |
| **1.5** | 36 (Jacobs Limit) |
| **2** | 50 |
| **2.5** | 60 |
| **3** | 80 |
| **4** | 100 |
| **5** | 120 |
| **6** | 140 |
| **7** | 170 |

# CHAPTER 3- EXPERIMENTAL RESULTS

## 3.1 Flow Regimes and Flow Visualization

### 3.1.1 Horizontal Pipe Visualization and Flow Regimes

In this study high speed videos of the flow were taken in order to identify the flow regime. Two adiabatic flow maps Baker (1954) and Taitel-Duckler (1975) were chosen to investigate their applicability to refrigerant and oil mixtures. The vapor quality entering the test section was more than 90% for all the experimental data points. The quality at inlet to the test section is defined as the ratio of mass flow rate of vapor to the total mass flow rate entering the test section. Figure 3.1 shows the Taitel-Duckler flow map and Figure 3.2 illustrates modified Baker's map with experimental data obtained for R134a with POE oil.

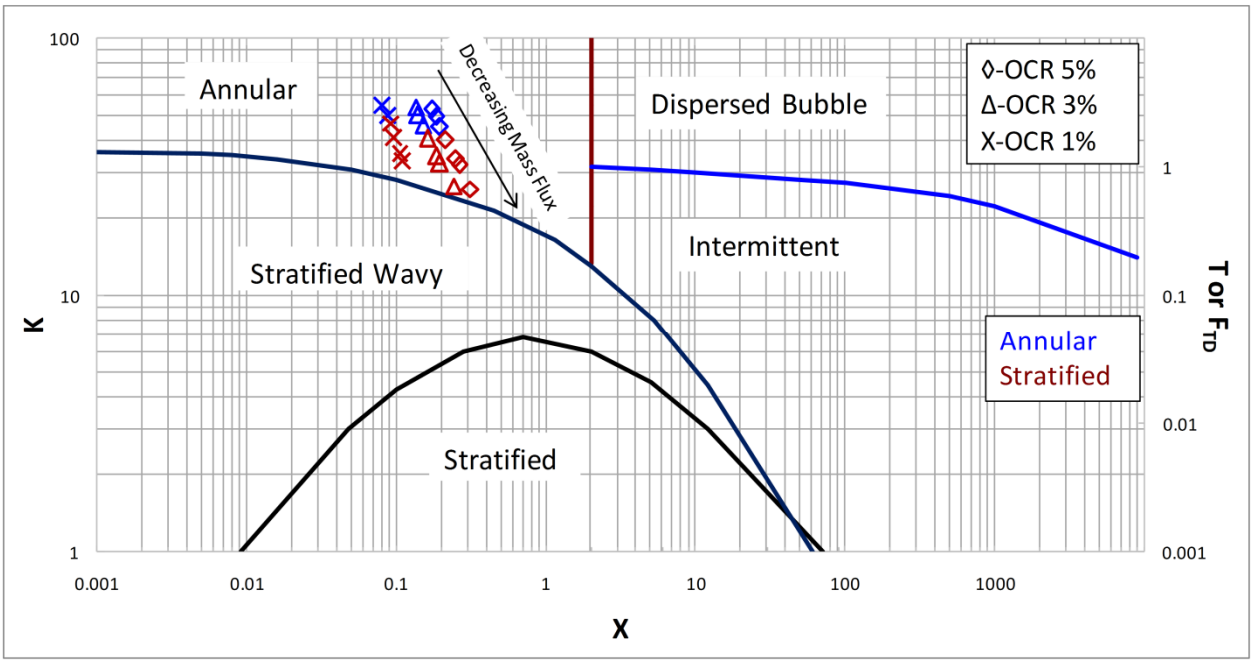


Figure 3.1- Taitel and Dukler (1976) flow pattern map for R134a-POE32 in 10.2mm I.D. diameter horizontal pipe

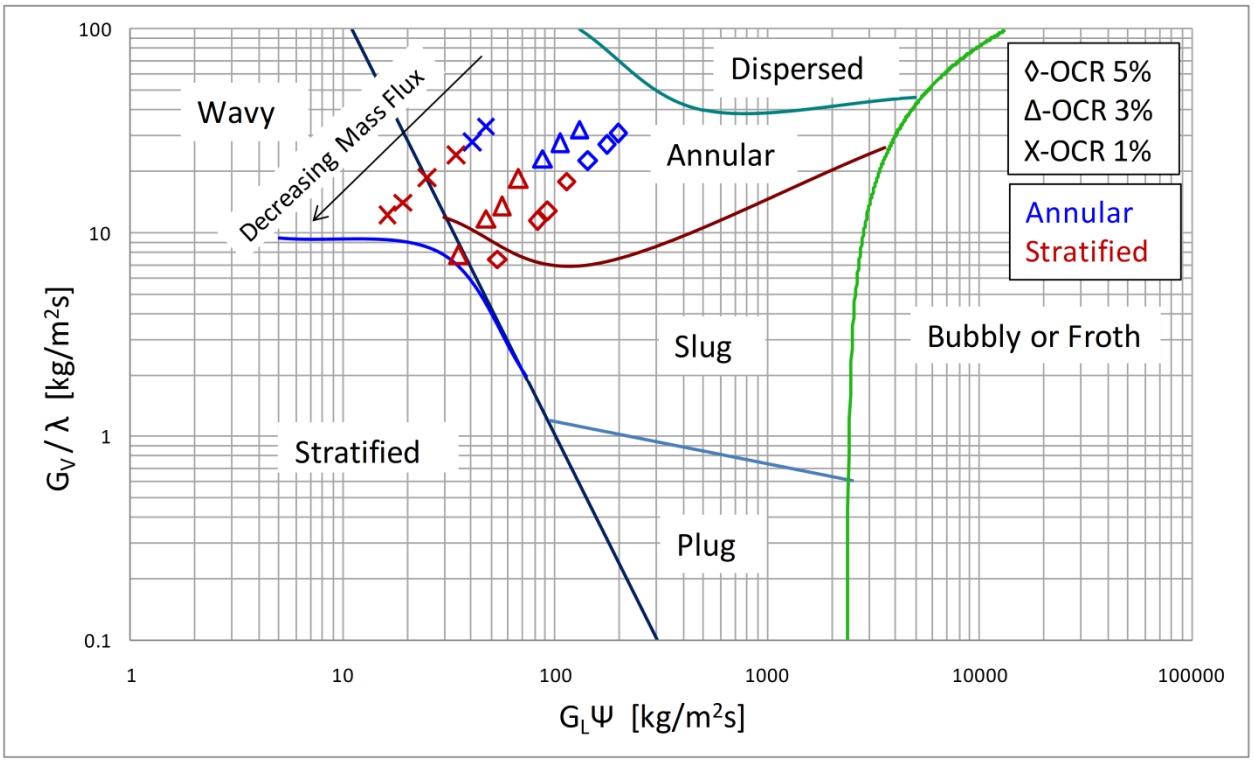


Figure 3.2 - Baker (1954) flow pattern map for R134a-POE 32 in 10.2mm I.D. horizontal pipe

Figure 3.3 indicates the outside edge of the tube and the top of the liquid layer in the images of the flow for horizontal, vertical and inclined tubes. In stratified flow regime the top of the liquid layer can be seen easily. However, for the annular flow one cannot see the inside edge of the liquid film due to the waviness of the film. Figures 3.4 and 3.5 show the still images from high speed videos taken for the flow under different conditions of mass flux and OCR for R1234yf/POE and R134a/POE mixtures respectively. It was observed that only annular and stratified-wavy flow patterns exist in the horizontal pipe. Annular flow was observed for superficial vapor velocities greater than 5 m/s for both the refrigerants. As the mass flux was reduced, the flow regime transitioned from annular to stratified-wavy. It is worth mentioning here that the stratified-wavy flow regime had been defined as one in which no film is present on the top of the pipe and waves are seen on the liquid film (Weisman, Kang 1981). The transition

of flow from annular to stratified-wavy flow regime appears to be affected by OCR. Figure 3.5 illustrates that at a mass flux of 100 kg/m$^2$s the flow at 5% and 3% OCR is annular whereas the flow at 1% OCR is stratified-wavy.

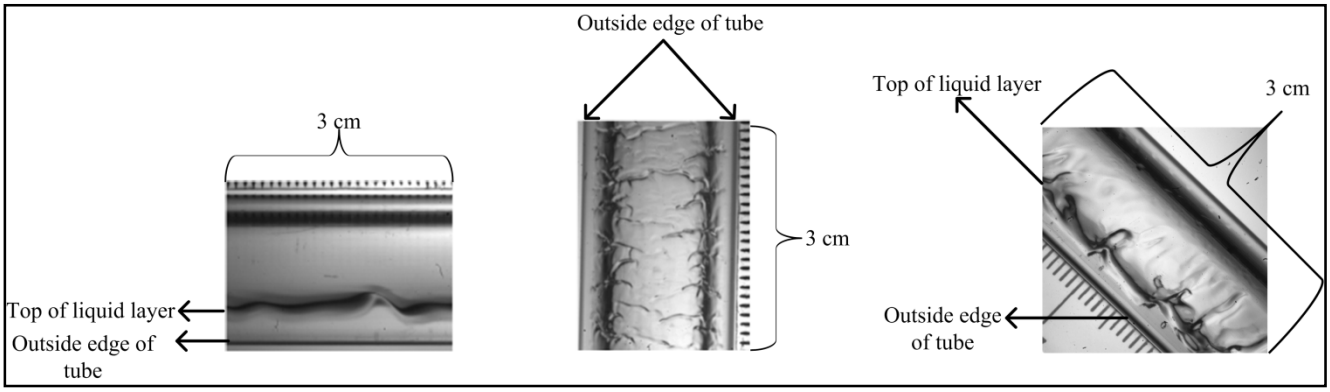


Figure 3.3- Description of flow visualization images

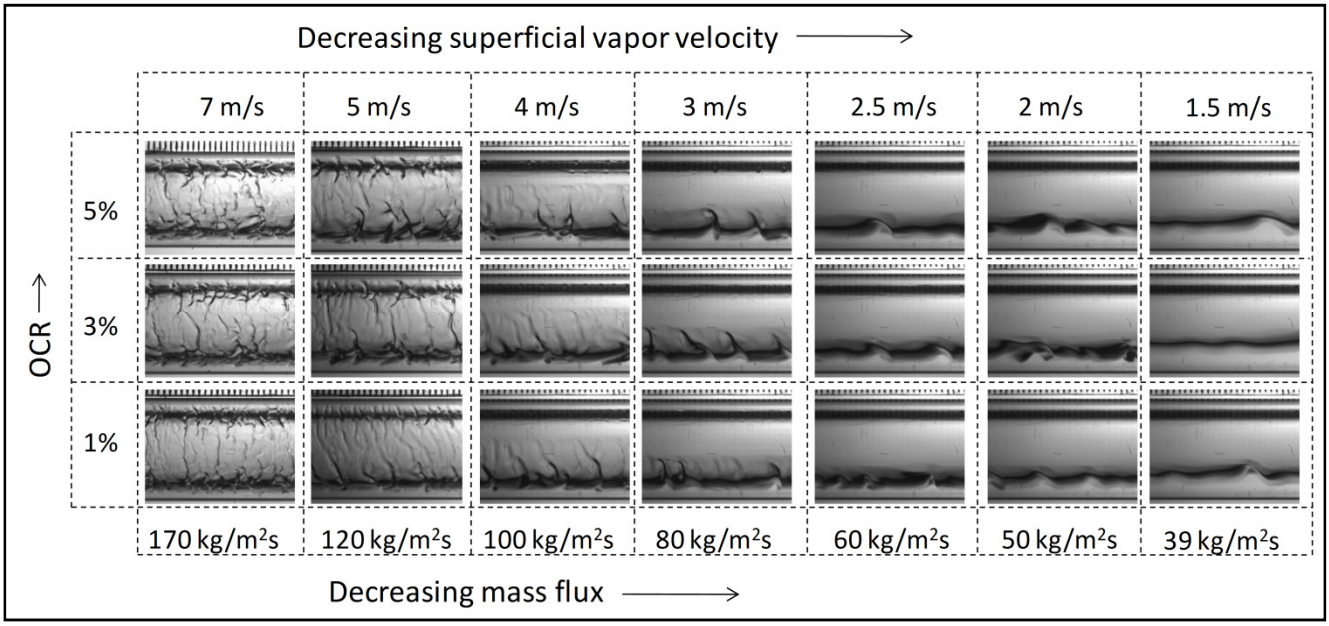


Figure 3.4- R1234yf/POE 32 flow visualization in horizontal pipe for different mass flux and OCR

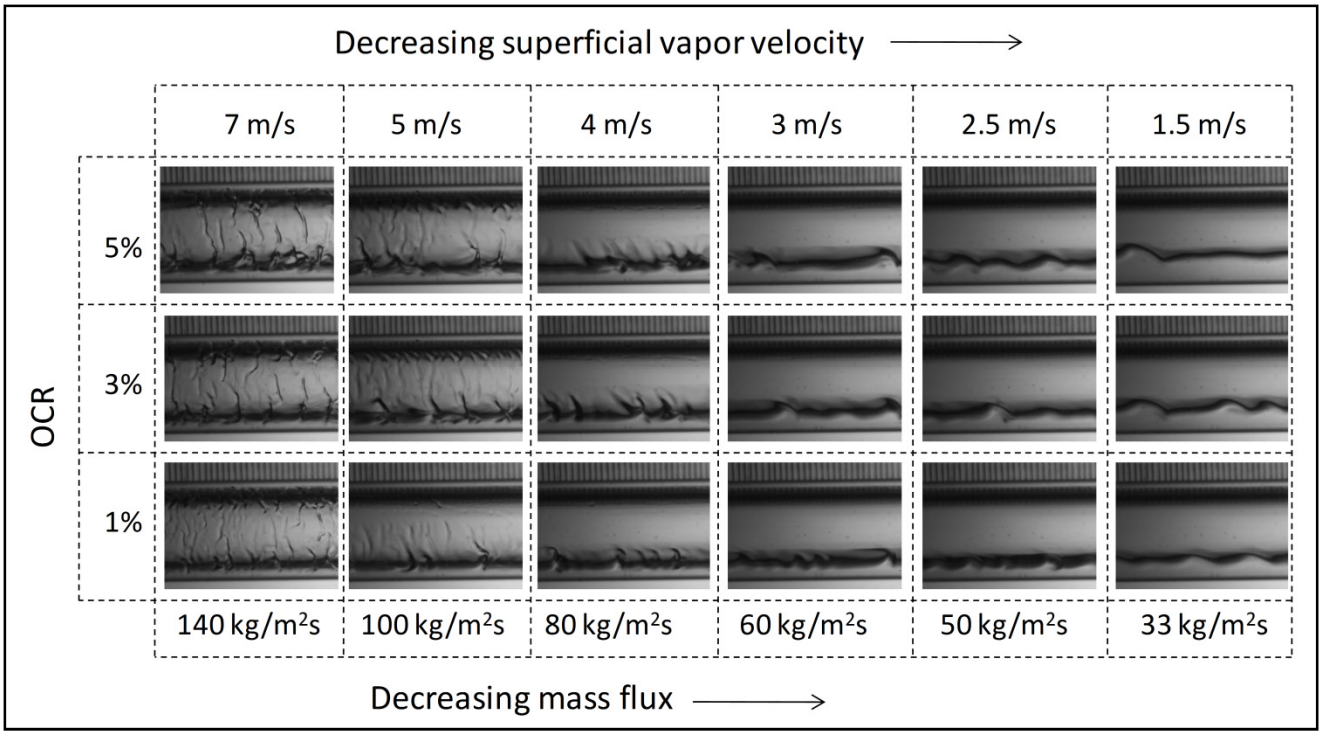


Figure 3.5- R134a/POE 32 flow visualization in horizontal pipe for different mass flux and OCR

This indicates that as the OCR is reduced the transition from annular to stratified-wavy flow regime takes place at a higher mass flux. This could be due to the fact that at lower OCR there is less amount of liquid available which cannot from the film around the pipe leading to stratified-wavy flow regime. It can also be observed from the images that for fixed OCR, the liquid level is very similar at mass flux of 80 kg/m$^2$s, 60 kg/m$^2$s and 50 kg/m$^2$s for both R1234yf/POE and R134a/POE and it increases as mass flux is reduced to 39 kg/m$^2$s and 33 kg/m$^2$s for R1234yf and R134a respectively. This indicates that the oil retention should be very similar under these conditions. This fact was also corroborated by oil retention measurements in the horizontal suction pipe which would be discussed later. It can be observed from the images that as the OCR increases, the liquid film thickness increases which leads to an increase in oil retention. Further, at high mass flux the flow at 5% OCR has larger ripple waves as compared to 1% OCR. The

presence of the larger waves as well as increased amount of retention leads to a higher pressure drop in suction lines at high OCR. It was found that the flow regimes look very similar for both R134a and R2134yf. However, the transition from annular to stratified-wavy regime takes place at a higher mass flux for R1234yf, as the refrigerant vapor density for R1234yf is greater than that of R134a. Figure 3.1 illustrates that Taitel-Ducker map predicts the flow regime to be annular for all mass fluxes and all OCR and hence does not predict the transition to stratified-wavy regime accurately. The modified Baker's map (Collier, Thome 1994) is illustrated in Figure 3.2. The x-axis represents corrected liquid mass flux and y-axis represents corrected vapor mass flux. The correction factors which were developed to extend the applicability of map to fluids other than air and water are given as follows:

$$\lambda = \left[\left(\frac{\rho_v}{\rho_A}\right)\left(\frac{\rho_l}{\rho_W}\right)\right]^{\frac{1}{2}} \tag{3.1}$$

$$\psi = \left(\frac{\sigma_W}{\sigma}\right)\left[\left(\frac{\mu_l}{\mu_W}\right)\left(\frac{\rho_W}{\rho_l}\right)^2\right]^{\frac{1}{3}} \tag{3.2}$$

The modified Baker's map is able predict the flow regime at lower mass flux to be stratified-wavy and also captures the dependence of transition mass flux on OCR and predicts a higher transition mass flux at lower OCR which is also indicated by images of the flow. Hence modified Baker's map is a reasonable flow map for identifying annular and stratified-wavy flow regimes and for prediction of transition between them for refrigerant oil flows.

### 3.1.2 Vertical Pipe Visualization and Flow Regimes

Figures 3.6 and 3.7 show the still images from high speed videos taken for the flow in vertical pipe under different conditions of mass flux and OCR for R1234yf/POE and R134a/POE mixture respectively.

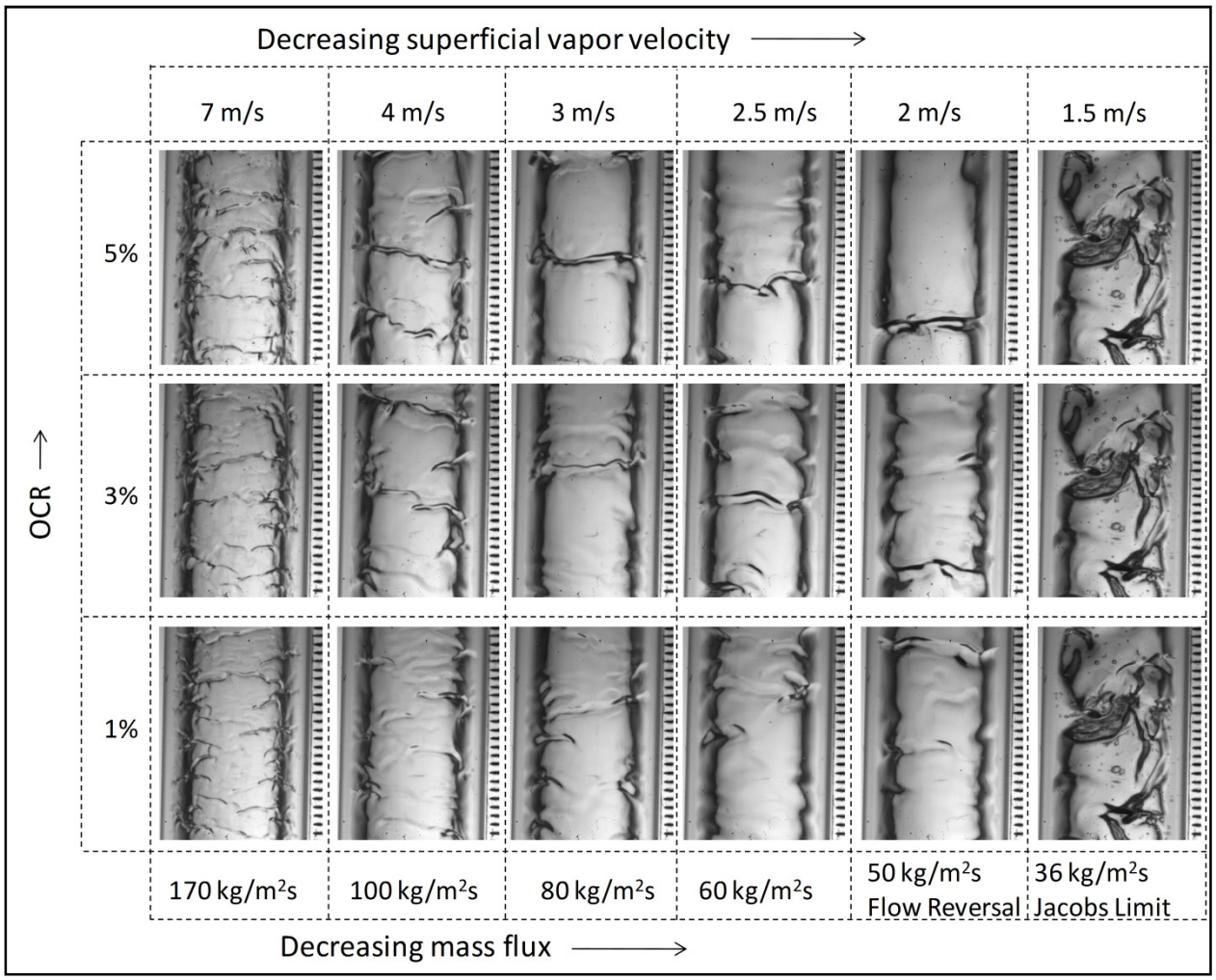


Figure 3.6- R1234yf/POE 32 flow visualization in vertical pipe for different mass flux and OCR

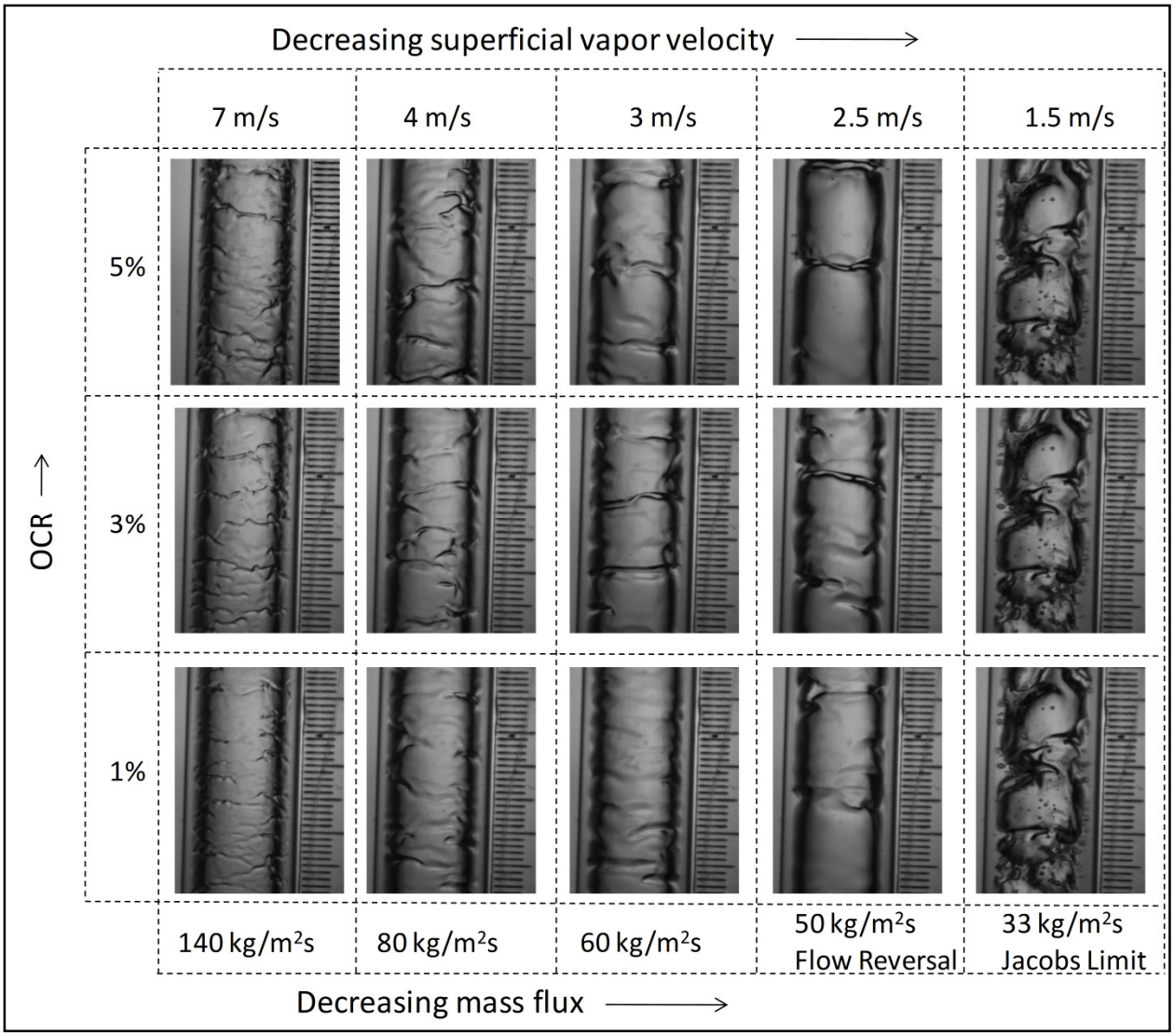


Figure 3.7- R134a/POE 32 flow visualization in vertical pipe for different mass flux and OCR

The flow regime in vertical pipe was annular for all mass fluxes above Jacobs limit and changed to churn as the Jacobs limit was reached. At high mass flux a stable upward flowing liquid film with ripples was observed. These conditions are good for oil return as there is a very thin oil film and the entire film is moving upwards. As the mass flux is reduced the liquid film thickness increases with small ripples changing to larger waves and some entrainment of droplets in the vapor core was also observed. At a mass flux of 50 kg/m$^2$s it was observed that the liquid film near the wall started reversing and partial downward flow was observed for both R1234yf and

R134a. As the mass flux was reduced to Jacobs limit the flow regime transition from annular flow to churn flow was observed. In the churn flow regime, a lot of liquid was retained in the vertical test section and liquid was observed to have intermittent upward and downward motion. This oscillatory behavior of the liquid has been reported in the literature and is a characteristic of churn flow regime (Taitel et al. 1980). These observations were consistent with Zoellick and Hrnjak (2010) who also carried out tests for R410A/POE mixture in vertical pipe near Jacobs limit in 18.5 mm diameter pipe. These observations suggest that the Jacobs limit is coincident with the transition of flow from annular to churn flow regime. It was observed that the liquid film thickness started increasing at a faster rate as the mass flux was reduced below the point at which liquid film reversal was observed. Thus, even before the Jacobs limit was reached a substantial increase in oil retention was observed. Hence designing vertical suction lines based on this criterion may lead to large amount of oil being retained in suction lines under part load conditions, even before this limit is reached. Mehendale and Radermacher (2000) proposed an improved criterion for designing vertical suction lines based on the mass flux at which film reversal begins. The flow visualization studies confirm that this is a better approach for designing vertical suction lines. It was observed that as the OCR was increased the liquid film thickness also increased, indicating higher oil retention. The flow regimes for R134a and R1234yf were very similar at high refrigerant mass flux. The only difference was that R1234yf transitioned to churn flow at higher mass flux due as its vapor has a higher density than R134a vapor.

### 3.1.3 Inclined Pipe Visualization and Flow Regimes

The variation of flow regime with angle of inclination from the horizontal, mass flux and OCR for R1234yf/POE 32 is shown in Figure 3.8. Apart from horizontal and vertical test sections two other angle of inclinations, $45^o$ and $60^o$ from the horizontal were also investigated. For mass fluxes greater than 100 kg/m$^2$s the flow regime was annular for all angles of inclination. For $45^o$ inclined pipe it was observed that the flow transitioned to stratified-wavy between a mass flux of 100 kg/m$^2$s and 80 kg/m$^2$s. It was observed that in $60^o$ inclined pipe the flow regime was annular until a mass flux of 50 kg/m$^2$s and changed to intermittent at a mass flux between 50 kg/m$^2$s and 36 kg/m$^2$s. The stratified-wavy flow regime was completely absent in the $60^o$ pipe since a thin liquid film was always present at the top of the pipe. This observation is consistent with Weisman and Kang (1981) who also reported the absence of stratified-wavy and stratified flow regimes for sharply inclined pipes. It was also observed that the liquid film close to the wall was flowing downwards at mass flux of 50 kg/m$^2$s for both $45^o$ and $60^o$ pipe. As the mass flux was reduced further it was observed in both $45^o$ and $60^o$ pipe that the flow regime changed to intermittent flow with occasional slugs of oil being carried up the pipe by the vapor. In the inclined pipes, churn flow was not observed even at very low vapor velocities. The inclination of the pipe led to total suppression of churn flow regime. Similar to observations in horizontal and vertical pipes, it was observed that in inclined pipes the film thickness increases as the OCR increases which leads to higher oil retention.

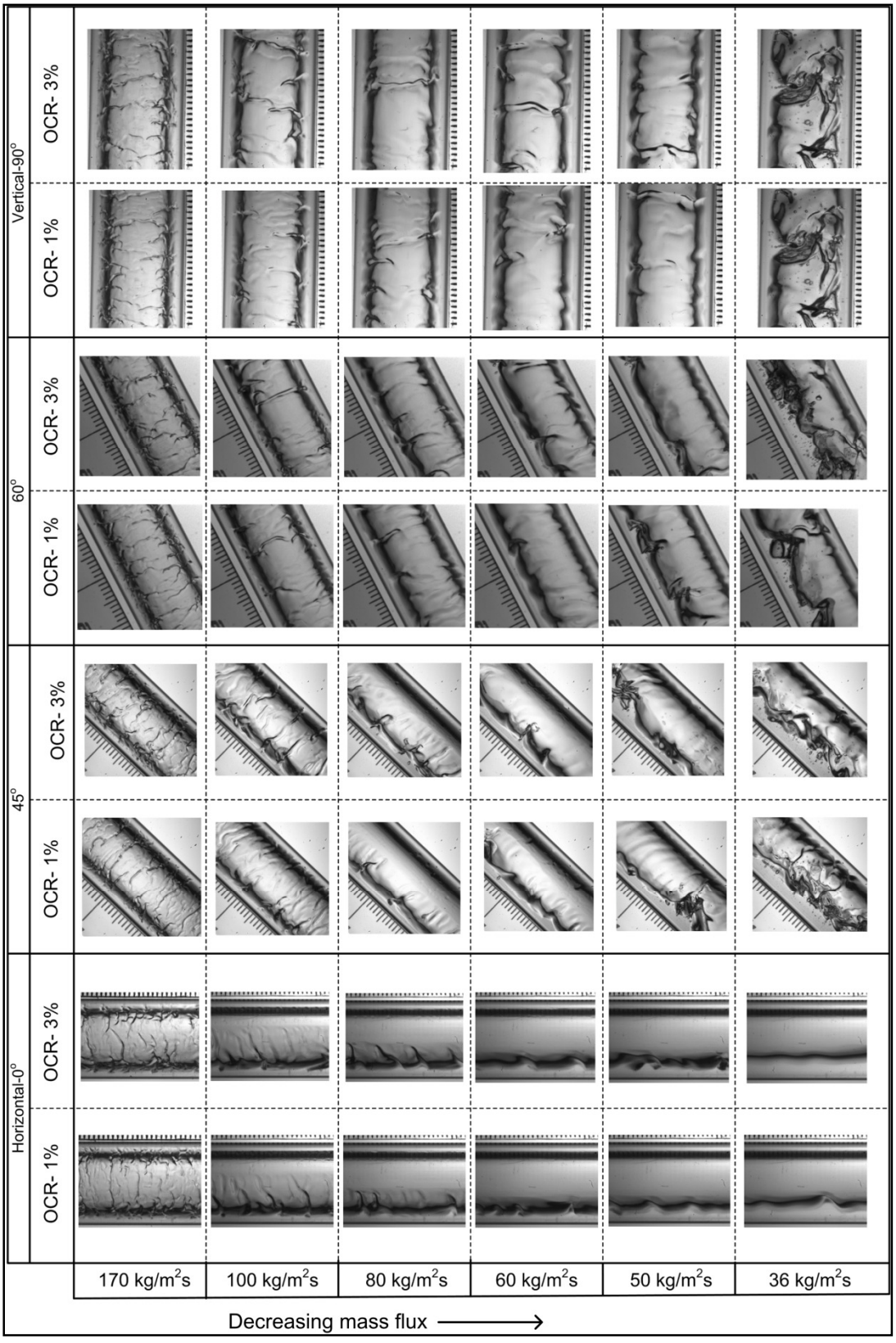


Figure 3.8– Flow visualization in inclined pipes with R1234yf/POE 32

## 3.2 Oil Retention and Pressure Drop

In this section, experimental results for oil retention and pressure drop in horizontal and vertical test section will be presented. First, the results for R134a/POE will be discussed followed by results for R1234yf/POE.

### 3.2.1 Oil Retention and Pressure Drop for R134a/POE32

The oil retention in horizontal and vertical suction lines is plotted versus mass flux in Figure 3.9. Figure 3.10 shows the variation of pressure drop versus mass flux in horizontal and vertical suction lines. The results are plotted for three different OCR's of 5%, 3% and 1%. OCR is defined as the ratio of mass flow rate of oil to the total mass flow rate of oil and refrigerant. The oil retention is presented as amount of oil retained in grams per meter of suction pipe. For 5% and 3% OCR the mass flux was varied from 33 kg/m$^2$s to 140 kg/m$^2$s whereas for 1% OCR the mass flux was varied from 50 kg/m$^2$s to 140 kg/m$^2$s. Jacobs limit was reached as mass flux was reduced to 33 kg/m$^2$s and the transition of flow from annular flow to churn flow in the vertical pipe was observed.

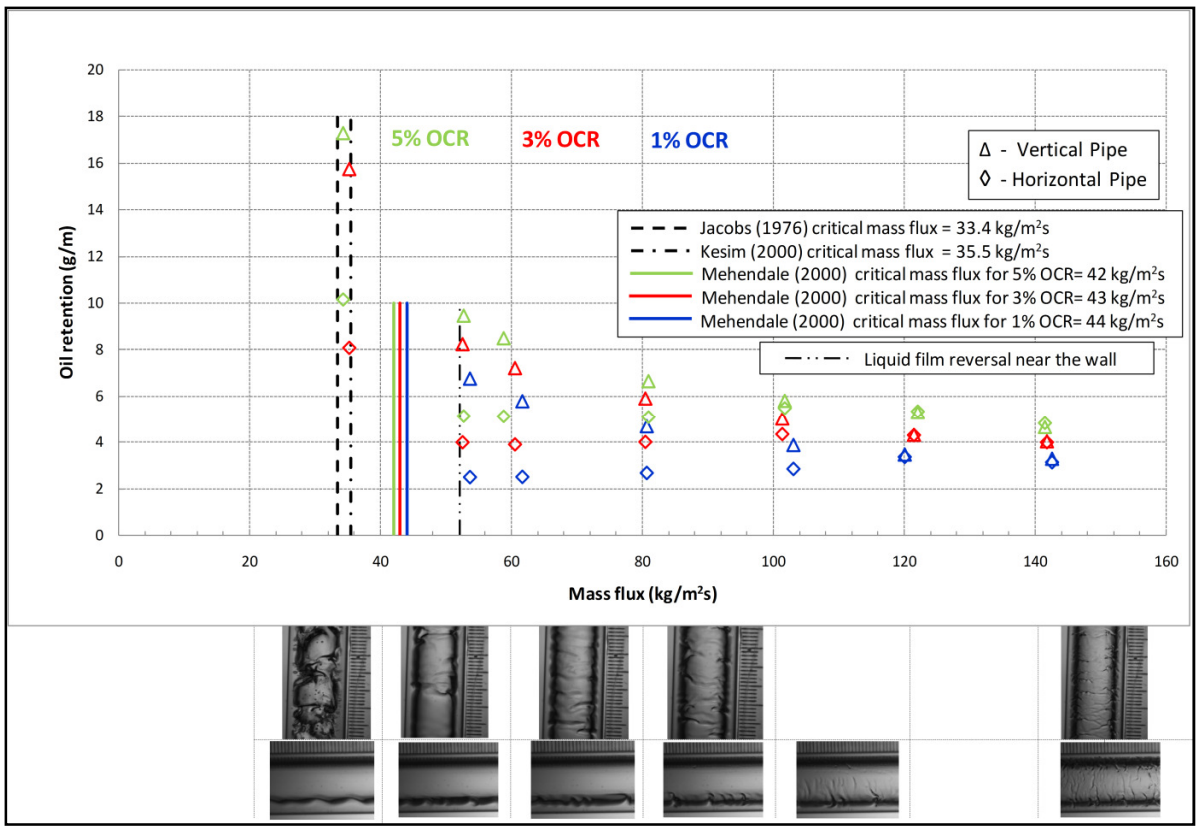


Figure 3.9- Oil retention as a function of mass flux for three different OCRs for R134a/POE 32 in 10.2 mm I.D. pipe

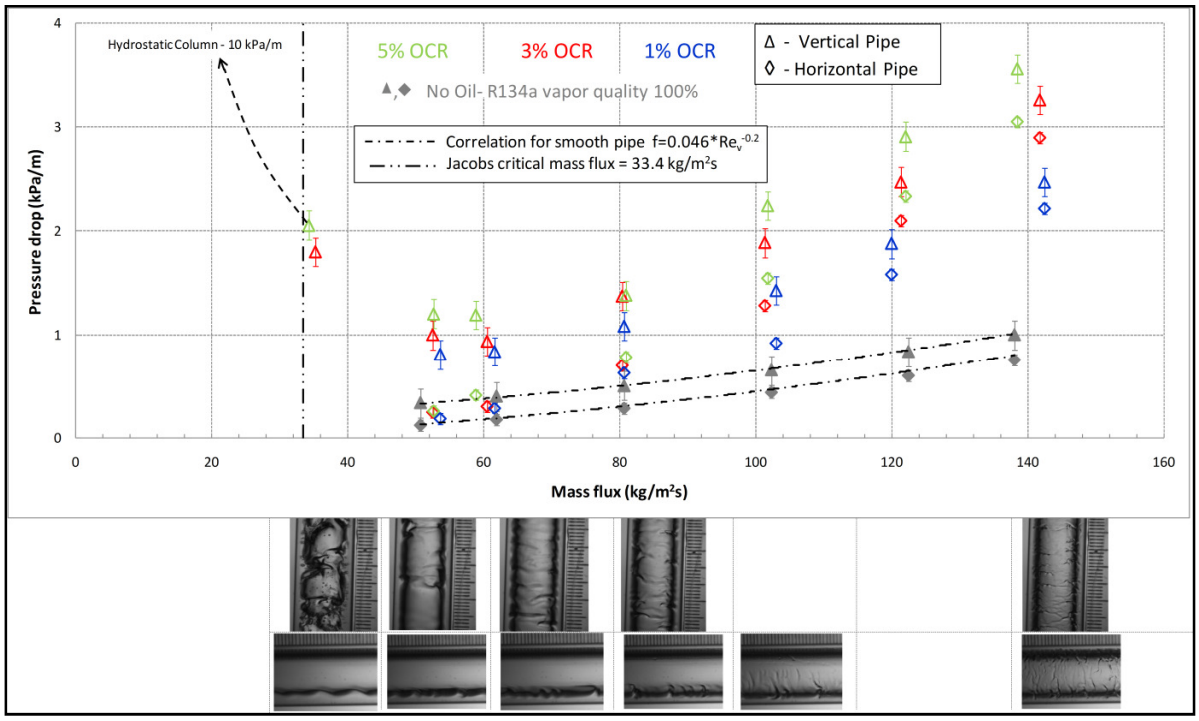


Figure 3.10- Pressure drop as a function of mass flux for three different OCRs for R134a/POE 32 in 10.2 mm I.D. pipe

#### 3.2.1.1 Vertical Pipe

In the vertical pipe, as the mass flux is reduced, the oil retention increases. For an OCR of 1%, the oil retention at mass flux of 140 kg/m$^2$s was 3.29 g/m which increased to 4.68 g/m at a mass flux of 80 kg/m$^2$s. As the mass flux was reduced below 60 kg/m$^2$s, the liquid film reversal was observed near the wall due to which oil retention jumped to 6.75 g/m at mass flux of 54 kg/m$^2$s. As the OCR increases, the oil retention increases due to the fact that more oil is circulating in the system. As the OCR is increased from 1% to 3% the oil retention increases by around 25% and as the OCR is increased from 1% to 5% the oil retention increases by around 45%. This indicates that OCR has a very significant effect on oil retention. Figure 3.9 also indicates the various limits for minimum refrigerant mass fluxes proposed by Jacobs et al. (1976), Kesim et al. (2000) and Mehendale and Radermacher (2000). The minimum mass flux serves as a design criteria for guaranteeing oil return in vertical suction lines. However, in this study it was found that oil returns at all mass fluxes, but the oil retention in the pipe increases as the mass flux is reduced. It was observed that Jacobs limit predicts the transition from annular flow to churn flow and as this limit is approached as the oil retention increases significantly. It can be seen from Figure 3.9 that oil retention is doubled as the mass flux is reduced from 50 kg/m$^2$s to Jacobs limit for OCRs of 5% and 3%. Hence the slope of oil retention versus mass flux curve increases sharply as the mass flux is reduced below 50 kg/m$^2$s where liquid film reversal near the wall was observed. This indicates that at part load conditions even if the system operates above Jacobs limit but below the point where liquid film reversal begins, a large amount of oil could be retained in the suction lines which could lead to depleted oil levels in the compressor and consequently poor lubrication and in an extreme case even lead to the its failure. Jacobs et al. (1976) limit does not take into account the effect of liquid viscosity or OCR on minimum mass flux. Kesim et al. (2000) assumed that minimum mass flux is reached at the point when net flow of liquid film is zero.

This limit is only slightly greater that Jacobs limit. This limit incorporates the effect of liquid viscosity but does not account for effect of OCR on minimum mass flux. Mehendale and Radermacher (2000) proposed that the minimum mass flux limit should be the point at which liquid film reversal begins. They proposed that at the point of liquid film reversal, the wall shear stress would become zero. This limit is greater than Kesim's limit and is closer to the point at which the actual liquid film reversal was observed by flow visualization. Mehendale's model takes into account the effect of liquid film viscosity as well as the OCR. The experiments conducted in this study suggest that Mehendale's model can be improved to establish good criterion for predicting minimum refrigerant mass flux.

Figure 3.10 shows the variation of pressure drop with mass flux for three different OCRs. The pressure drop is presented as pressure drop per unit length of suction pipe. It was observed that pressure drop decreases as the mass flux decreases and reaches a minimum between a mass flux of 50 kg/m$^2$s and 33 kg/m$^2$s. The occurrence of this minimum can be explained based on change in flow regimes. At high mass flux, the flow regime is annular and the frictional component of pressure drop is dominant over the hydrostatic component of pressure drop. As the mass flux is reduced, the vapor velocity decreases due to which the frictional component of pressure drop reduces which leads to a decrease in pressure drop. At mass flux between 50 kg/m$^2$s and 60 kg/m$^2$s, the liquid film reversal begins and as the mass flux is reduced further the flow transitions from annular to churn flow regime. In churn flow regime, the hydrostatic component of pressure drop is dominant over the frictional component and the hydrostatic component increases as the mass flux is reduced in churn flow regime because of increase in liquid accumulation in the vertical suction pipe. This increase in hydrostatic component leads to increase in overall pressure drop. If the refrigerant mass flux was to be decreased continuously, eventually the whole pipe

will be filled with oil and pressure drop would be equal to the hydrostatic head of the oil column. For 3% OCR the pressure drop at 140 kg/m$^2$s was 3.3 kPa/m which reduced to 0.9 kPa/m at a mass flux of 61 kg/m$^2$s and increased to 1.8 kPa/m at a mass flux of 35 kg/m$^2$s. It was also observed that the pressure drop in vertical suction line increases as the OCR increases for the same mass flux. A possible reason of this could be the presence of bigger ripples on the liquid film at higher OCR which leads to a larger loss of vapor momentum. As the OCR is increased from 1% to 3%, the pressure drop increased by around 30% and as the OCR is increased from 1% to 5%, the pressure drop increased by around 40%. Figure 3.10 also shows the pressure drop in suction lines without the presence of oil and it was found that the friction factor correlation for smooth pipe (Knudsen, Katz 1958) was able to predict the experimental data within ±3%.

#### 3.2.1.2 Horizontal Pipe

In the horizontal pipe, an interesting trend was observed for oil retention as the mass flux was reduced. For an OCR of 3% the oil retention at mass flux of 140 kg/m$^2$s was 4 g/m which increased to 4.35 g/m at a mass flux of 100 kg/m$^2$s. As the mass flux was reduced it was observed that, contrary to the expectations, the oil retention reduced to about 4.02 g/m at a mass flux of 80 kg/m$^2$s. As the mass flux was reduced further the oil retention was almost constant with 3.91 g/m at mass flux of 60 kg/m$^2$s and 4.00 g/m at mass flux of 52 kg/m$^2$s. As the mass flux was reduced further to 35 kg/m$^2$s the oil retention increased to 8 g/m. The high speed videos of the flow revealed that for an OCR of 3%, the flow transitioned from annular to stratified-wavy at a mass flux between 80 kg/m$^2$s and 100 kg/m$^2$s. The liquid level in the stratified-wavy flow regime remained almost constant until the mass flux was reduced to 33 kg/m$^2$s when an increase in liquid level was observed which lead to increase in oil retention. This trend was observed for all the OCRs. Similar to the observations in vertical pipe as the OCR increases, the oil retention

also increases. At a high mass flux of 140 kg/m$^2$s, as the OCR is increased from 1% to 3% the oil retention increases by 28% and as the OCR is increased from 1% to 5% the oil retention increases by 54%. At mass flux of 100 kg/m$^2$s, as the OCR is increased from 1% to 3% the oil retention increases by 53% and as the OCR is increased from 1% to 5% the oil retention increases by 93%. This indicates that the increase in oil retention with OCR is higher for lower mass flux. This may be due to the difference in the flow regime. The increase in oil retention with OCR is more for stratified wavy flow regime than annular flow regime. It was observed at a high mass flux that the oil retention in the vertical suction line was very similar to the horizontal suction line because flow regime was annular in both test sections. As the mass flux was reduced, the oil retention in vertical suction line was always greater than horizontal suction line due to the effect of gravity.

In the horizontal pipe, it was observed that the pressure drop decreases as the mass flux is reduced. In the annular and stratified-wavy flow regimes the frictional component of pressure drop is the dominant force and hence as the mass flux is reduced, the vapor velocity goes down, which leads to reduction in frictional pressure drop. For 1% OCR the pressure drop at 140 kg/m$^2$s was 2.2 kPa/m and reduced to 0.2 kPa/m at a mass flux of 54 kg/m$^2$s. The pressure drop increases as the OCR is increased due to the presence of bigger waves on the liquid film. As the OCR is increased from 1% to 3% the pressure drop increases by around 30% and as the OCR is increased from 1% to 5% the pressure drop increases by around 40%.

### 3.2.2 Oil Retention and Pressure Drop for R1234yf/POE32

Figure 3.11 shows the variation of oil retention with mass flux in horizontal and vertical suction lines. Figure 3.12 shows the variation of pressure drop versus mass flux in horizontal and vertical suction lines. The results are plotted for three different OCRs of 5%, 3% and 1%. The mass flux

was varied from 36 kg/m$^2$s to 170 kg/m$^2$s. Jacobs limit was reached as mass flux was reduced to 36 kg/m$^2$s and the flow transitioned from annular flow to churn flow in the vertical pipe.

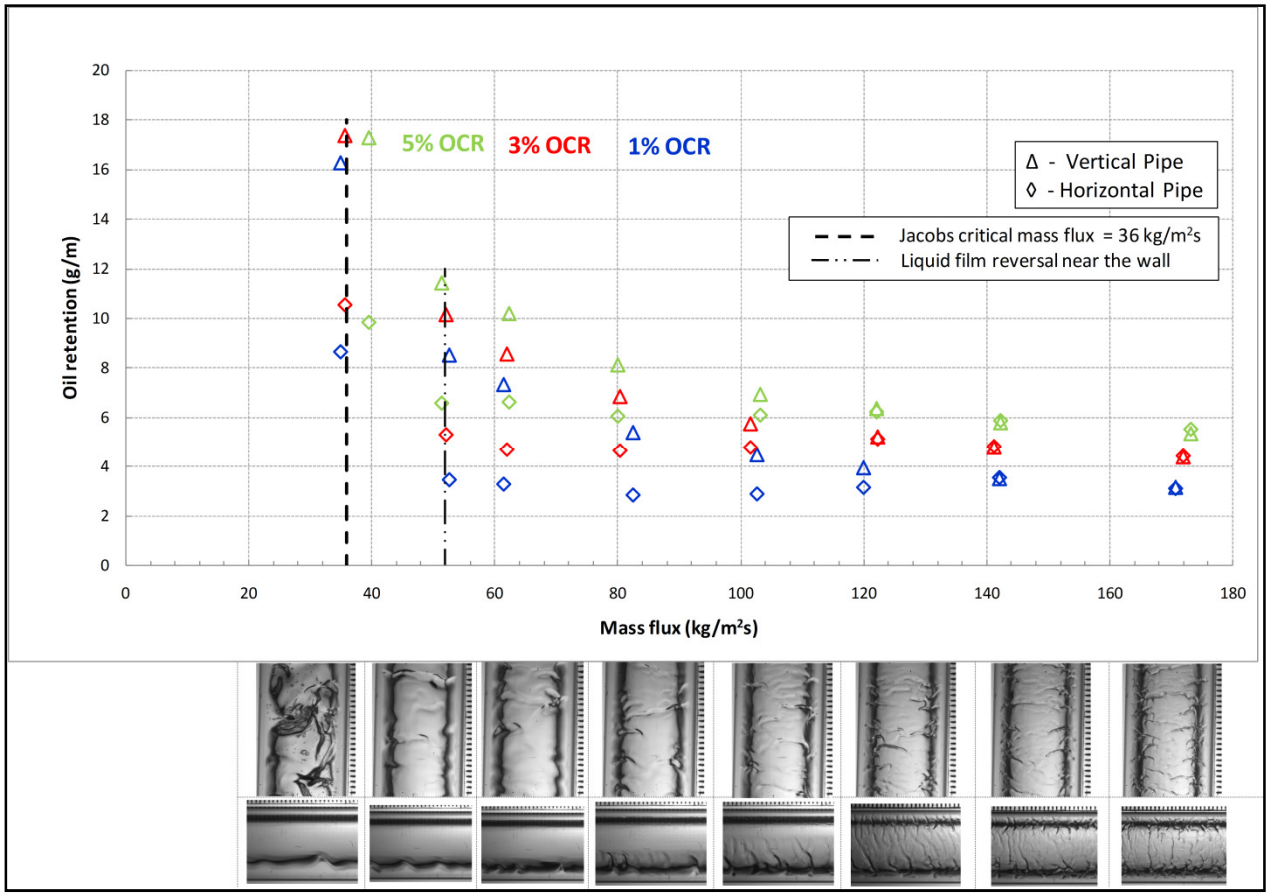


Figure 3.11- Oil retention as a function of mass flux for three different OCRs for R1234yf/POE 32 in 10.2 mm I.D. pipe

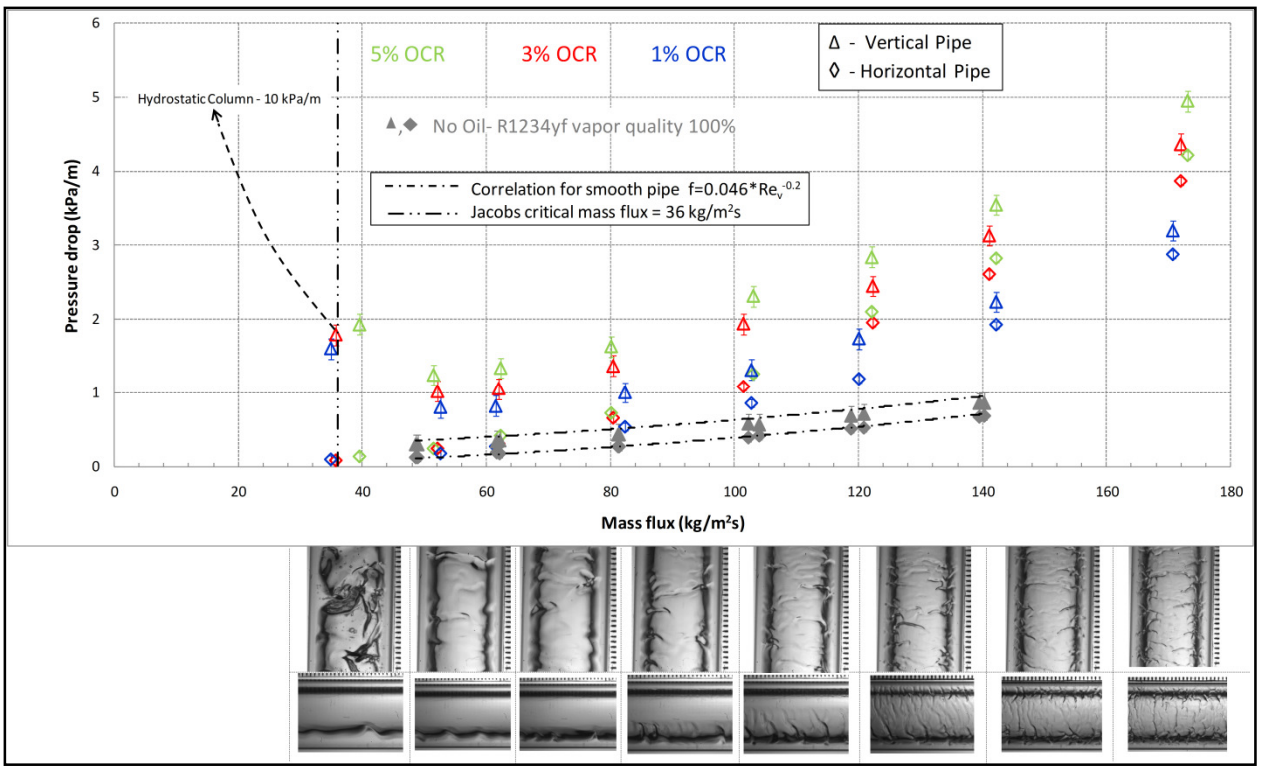


Figure 3.12- Pressure drop as a function of mass flux for three different OCRs for R1234yf/POE 32 in 10.2 mm I.D. pipe

### 3.2.2.1 Vertical Pipe

The oil retention in the vertical pipe increases as the mass flux is reduced. For an OCR of 1%, oil retention increased from 3.14 g/m at a mass flux of 170 kg/m$^2$s to 5.38 g/m at a mass flux of 82 kg/m$^2$s. As the mass flux was reduced further, the oil retention increased to 8.53 g/m at a mass flux of 52 kg/m$^2$s and liquid film reversal was observed near the wall. As the mass flux was reduced to 35 kg/m$^2$s, the Jacobs limit was reached and oil retention increased sharply to 16.25 g/m. Similar to observations with R134a, it was observed that as the Jacobs limit is reached the flow regime changes from annular to churn. As the OCR increases, the oil retention also increases due to the fact that more oil is circulating in the system at higher OCR. As the OCR is increased from 1% to 3%, the oil retention increases by around 30% and as the OCR is increased from 1% to 5% the oil retention increases by around 50% similar to the observations with R134a. It was observed that pressure drop decreases as the mass flux decreases and reaches a minimum

at a mass flux between 50 kg/m$^2$s and 35 kg/m$^2$s. For 1% OCR the pressure drop at 170 kg/m$^2$s was 3.2 kPa/m, reduced to 0.8 kPa/m at a mass flux of 52 kg/m$^2$s and increased to 1.6 kPa/m at a mass flux of 35 kg/m$^2$s . As the OCR is increased from 1% to 3% the pressure drop increases by around 40% and as the OCR is increased from 1% to 5% the pressure drop increases by around 60%.

#### 3.2.2.2 Horizontal Pipe

The trend of oil retention in horizontal pipe was very similar to the one observed for R134a/POE. For 1% OCR, the oil retention was 3.11 g/m at 170 kg/m$^2$s which increased to 3.52 g/m at 140 kg/m$^2$s. As the mass flux was reduced to 100 kg/m$^2$s the flow transitioned from annular to stratified-wavy regime and oil retention decreased to 2.88 g/m. As the mass flux was reduced further the oil retention started increasing again and reached 3.45 g/m at a mass flux of 53 kg/m$^2$s. Finally the oil retention reached 8.65 g/m at a mass flux of 35 kg/m$^2$s. Hence a local minima in oil retention was observed for R1234yf at a mass flux between 60 kg/m$^2$s and 80 kg/m$^2$s. The oil retention increases as the OCR is increased. As the OCR is increased from 1% to 3% the oil retention increases by around 50% and as the OCR is increased from 1% to 5% the oil retention was almost doubled. In the horizontal pipe it was observed that the pressure drop decreases as the mass flux is reduced similar to R134a. For 1% OCR the pressure drop at a mass flux of 170 kg/m$^2$s was 2.9 kPa/m and reduced to 0.1 kPa/m at a mass flux of 35 kg/m$^2$s. As the OCR is increased from 1% to 3% the pressure drop increases by around 30% and as the OCR is increased from 1% to 5% the pressure drop increases by around 50%.

## 3.3 Comparison of R134a/POE 32 and R1234yf/POE 32

Figure 3.13 shows the comparison of oil retention for R134a and R1234yf at an OCR of 1%. For the same flux in the same pipe the oil retention is higher for R1234yf as compared to R134a. The reason for higher oil retention for R1234yf is the higher density of the refrigerant vapor which leads to lower velocity at same mass flux. Due to the lower velocity the refrigerant vapor has a lower momentum which leads to higher oil retention for R1234yf. In the vertical pipe, R1234yf has 7% more oil retention at mass flux of 140 kg/m$^2$s, 15% more oil retention at mass flux of 80 kg/m$^2$s, and 27% higher oil retention at a mass flux of 60 kg/m$^2$s. It is evident that as the mass flux is reduced the difference in oil retention increases. In the horizontal pipe R1234yf has 13% more oil retention at mass flux of 140 kg/m$^2$s which increases to 30% higher oil retention at a mass flux of 60 kg/m$^2$s. It was found that at similar superficial vapor velocities the oil retention for R1234yf and R134a is very similar in both horizontal and vertical suction lines. For similar system cooling capacities the oil retention for R1234yf and R134a is also very similar in both horizontal and vertical suction lines. R1234yf has lower enthalpy of vaporization compared to R134a. In order to achieve similar system cooling capacity, higher mass flow rate is required for R1234yf which leads to similar vapor velocities in suction line for both R1234yf and R134a. Hence the oil retention is similar for both the refrigerants as they have similar vapor velocities in suction line at similar system cooling capacities. The system cooling capacities for both the refrigerants were calculated assuming 40$^o$C condenser temperature with no subcooling and 10$^o$C evaporator temperature with 10$^o$C of superheat.

Figure 3.14 shows the comparison of pressure drop for R134a and R1234yf for an OCR of 1%. At the same mass flux, in the same pipe R134a presents 10-15% higher pressure drop because of higher vapor velocity and larger waves on the liquid vapor interface. At the same superficial

vapor velocity in the same pipe it was observed that R1234yf shows 20-30% higher pressure drop in both horizontal and vertical suction lines due to the higher vapor density and therefore higher kinetic energy. This results in more frictional losses within the vapor. For the same system cooling capacity, it was observed that R1234yf has 20-30% higher pressure drop in both horizontal and vertical suction lines. This is due to similar vapor velocities in the suction line at same system cooling capacities as explained before when dealing with oil retention. As discussed earlier for similar vapor velocities R1234yf is expected to have higher pressure drop. The fact that R1234yf has 20-30% higher pressure drop in suction lines at same system cooling capacity in the same pipe may have an impact on system performance as R1234yf is intended to be a drop-in replacement for R134a systems.

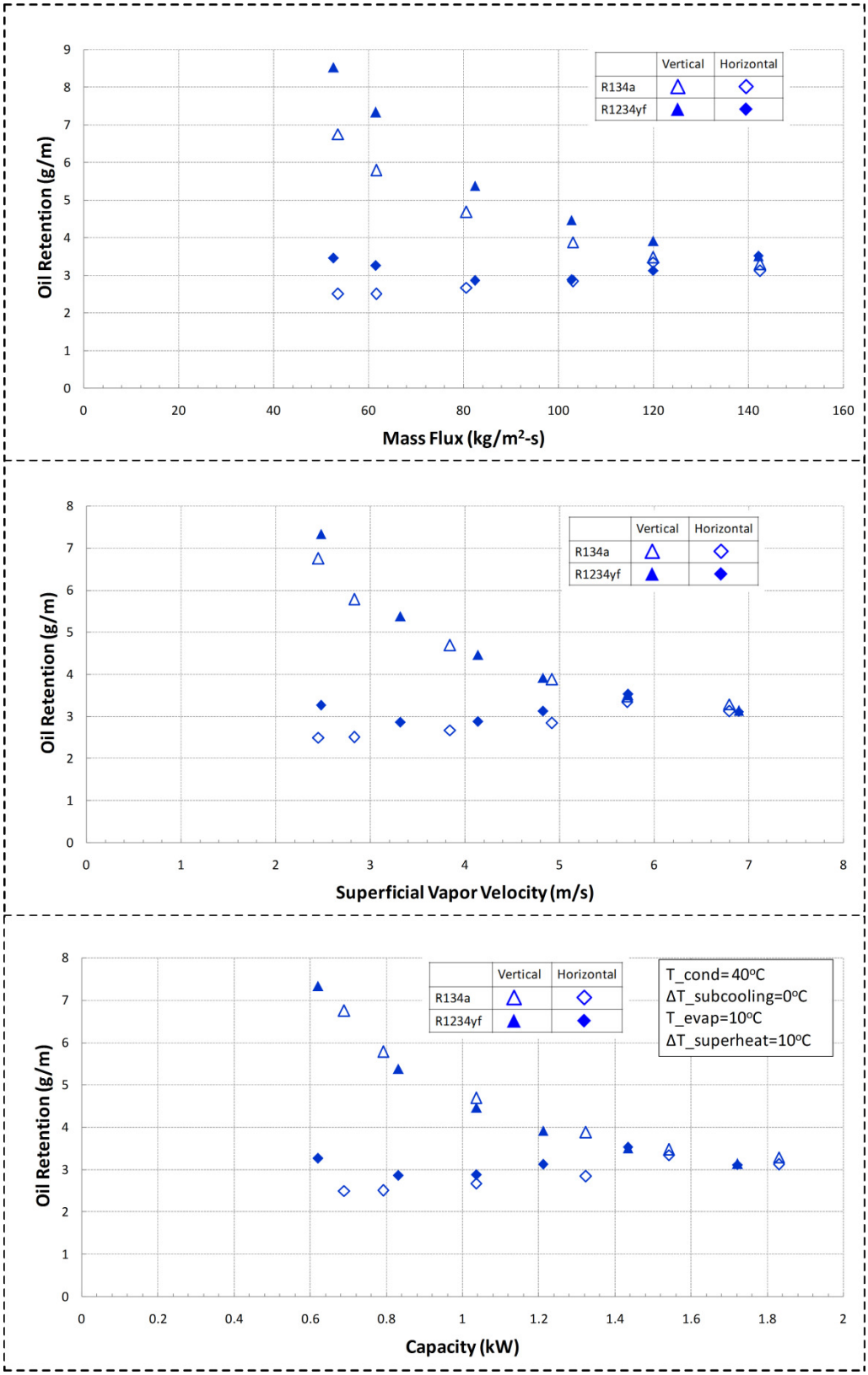


Figure 3.13- Comparison of oil retention for R134a/POE 32 and R1234yf/POE32 for 1% OCR

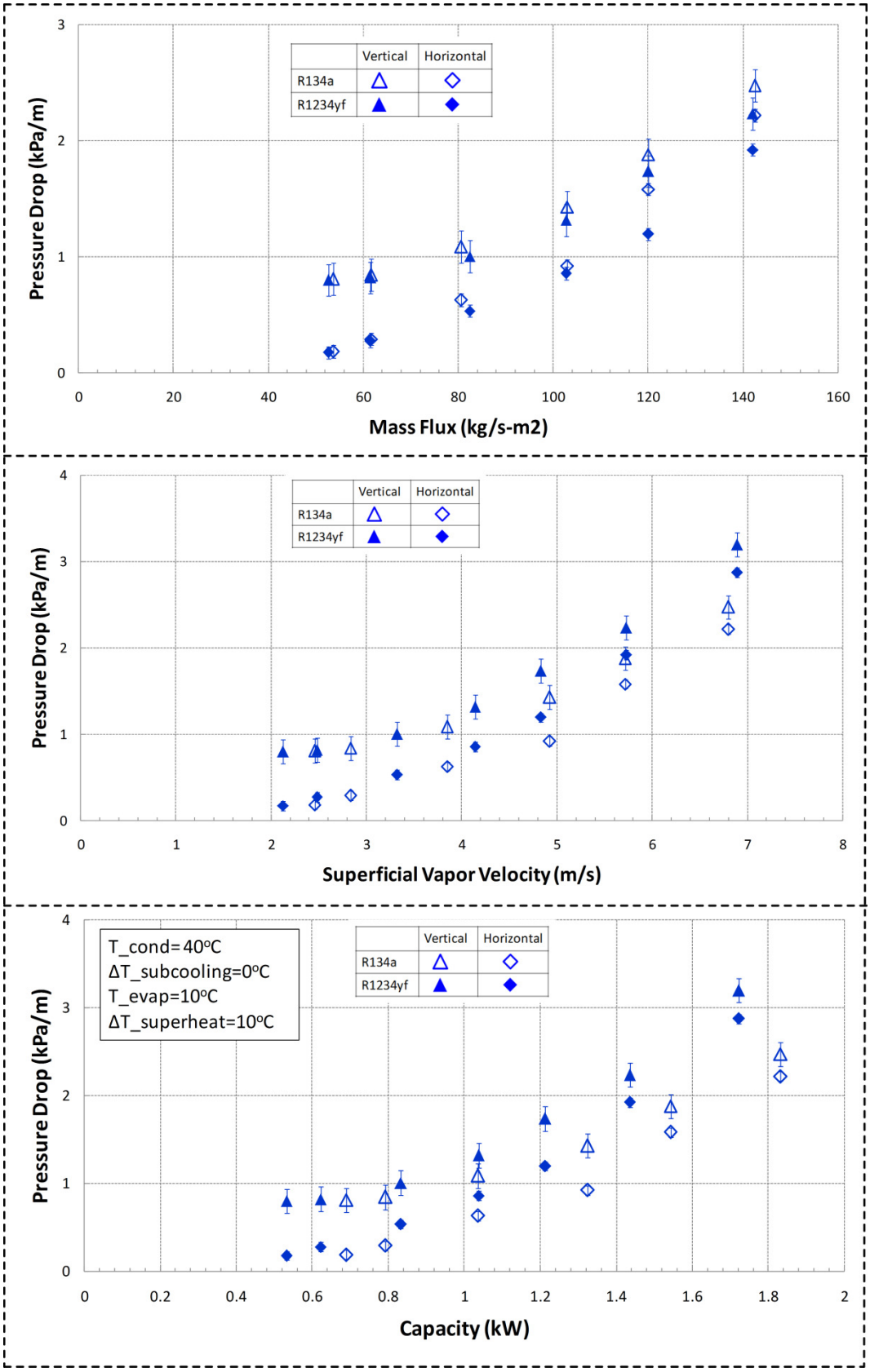


Figure 3.14- Comparison of pressure drop for R134a/POE 32 and R1234yf/POE32 for 1% OCR

## 3.4 Oil Retention in Inclined Pipes

The effect of inclination on oil retention was also studied in this work. Figure 3.15 shows the oil retention variation with angle of inclination from the horizontal for mass flux ranging from 36 kg/m$^2$s to 170 kg/m$^2$s. The results are presented for OCRs of 1% and 3%. Apart from horizontal and vertical pipes two other angle of inclinations, namely 45$^o$ and 60$^o$ from the horizontal were also studied. It was found that the oil retention was lowest in the horizontal suction pipe. As the inclination was increased the oil retention also increased. The oil retention in 45$^o$ suction pipe was more than the horizontal suction pipe. As the angle of inclination was further increased to 60$^o$ the oil retention increased further. As the angle of inclination was increased to 90$^o$ the oil retention decreased indicating that oil retention reaches a maximum value at some particular angle of inclination. This trend was observed for all the mass fluxes and OCRs investigated. Figure 3.15 also suggests that oil retention might reach a maximum value at some inclination between 45$^o$ and 90$^o$. This observation is consistent with Beggs and Brill (1973) and Mukherjee and Brill (1983) who reported that liquid hold up reaches a maximum value at an angle of inclination of approximately 50$^o$. Figure 3.16 shows the curve reported by Beggs and Brill (1973) showing variation of liquid hold-up with angle of inclination from horizontal with air water flow. The results are presented for three different liquid circulation ratios. The liquid circulation ratio was defined as the ratio of volume flow rate of water to the total volume flow rate of water and air. The trends observed in this study agree very well with those observed by Beggs and Brill (1973). It is suggested that plots similar to Figure 3.16 should be developed for refrigerant oil mixtures. This would enable a designer to decide whether to install an inclined suction pipe or a combination of vertical and horizontal suction pipe so as to minimize the amount of oil retention.

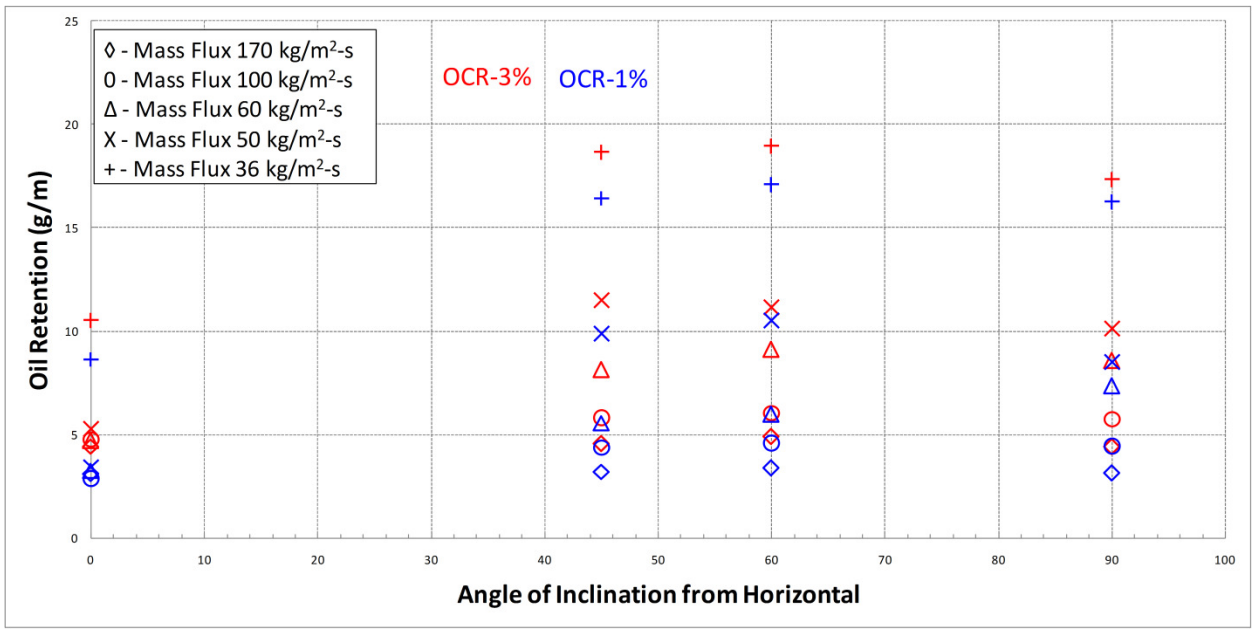


Figure 3.15- Effect of angle of inclination from the horizontal on oil retention for R1234yf/POE 32

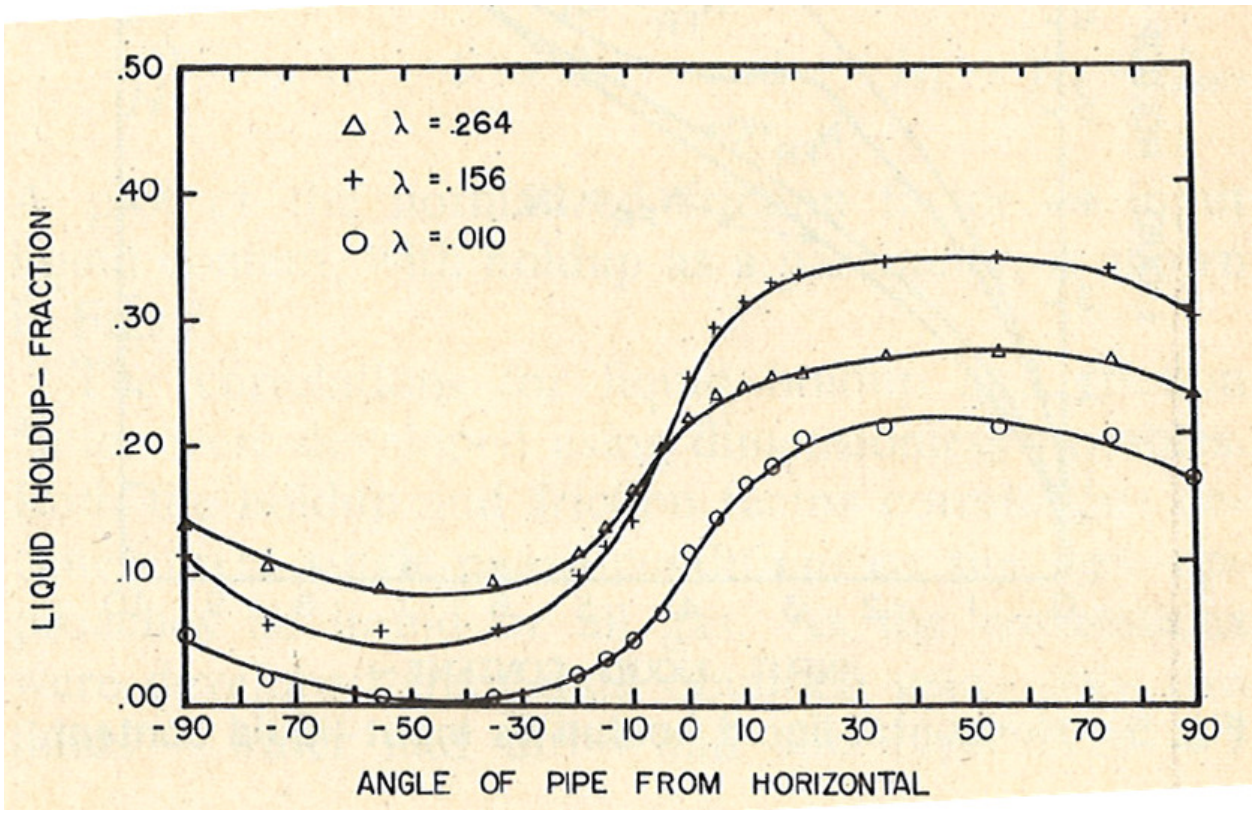


Figure 3.16- Effect of angle of inclination from the horizontal on liquid hold-up for air/water (Beggs, Brill 1973)

# CHAPTER 4- MODELING OF OIL RETENTION AND PRESSURE DROP IN VERTICAL SUCTION LINES

This chapter describes the semi-empirical model which was developed to predict the oil retention and pressure drop for vertical suction line. The model incorporates the effects of mass flux, liquid viscosity, diameter and OCR on oil retention and pressure drop. Based on the model, a criterion for predicting minimum refrigerant mass flux for design of vertical suction lines is also presented.

## 4.1 Development of the model

A semi-empirical model was developed for predicting oil retention and pressure drop in annular flow for vertical suction lines. An approach similar to Lee (2003) was used in the current study but a new correlation for interfacial friction factor was developed for the vertical pipe. The Navier-Stokes and continuity equations with appropriate assumptions were applied to the liquid film and vapor core in annular flow regime to solve for average film thickness. This liquid film thickness was then used to predict the oil retention under various conditions.

The following assumptions were used to simplify the Navier-Stokes equations

- Steady State, fully developed and adiabatic flow
- Axisymmetric flow
- The effect of oil entrainment was ignored
- The liquid film thickness is uniform around the pipe and flow pattern was annular

The Navier-Stokes equations were applied to liquid film to obtain the velocity profile in the film. The velocity profile of the liquid was integrated over the liquid film thickness to obtain mass flow rate of the film as a function of film thickness, pressure drop and interfacial shear stress. Next, a force balance was carried out for the vapor core to obtain an expression relating

interfacial shear stress to the pressure drop. The interfacial shear stress was expressed as a function of the vapor momentum using interfacial friction factor. A new expression for interfacial friction factor was developed using the experimental data for oil retention and pressure drop obtained for R134a/POE 32. The interfacial friction factor was expressed as a function of the vapor Reynolds number, dimensionless liquid film thickness and liquid film Reynolds number. A system of equations was obtained which were solved using the Engineering Equation Solver (EES) software (F-Chart 2010). The properties for refrigerant oil mixtures were obtained from ASHRAE 2002 refrigeration handbook.

### 4.1.1 Navier-Stokes equation for liquid film

Figure 4.1 shows the forces acting on an element of liquid film and on the refrigerant vapor core.

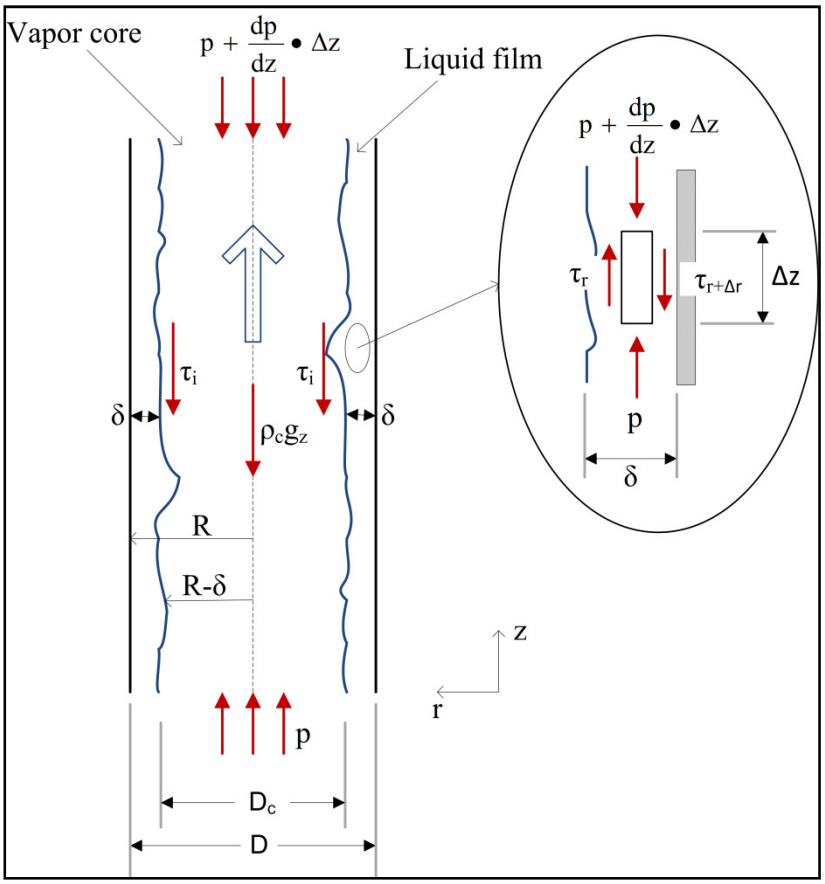


Figure 4.1- Force balance on the refrigerant vapor core in annular flow

For steady, incompressible flow the continuity equation is:

$$\frac{d(ru_r)}{dr} = 0 \tag{4.1}$$

Integrating equation (4.1) gives

$$r \cdot u_r = constant \tag{4.2}$$

Since the radial velocity is zero at the wall

$$R \cdot u_r(r = R) = 0$$

This gives

$$u_r = 0 \qquad \forall \; R - \delta \leq r \leq R \tag{4.3}$$

Applying Z direction momentum equation gives:

$$\frac{\mu_l}{r}\frac{d}{dr}\left(r\frac{du}{dr}\right) = \frac{dP}{dz} + \rho_l g_z \tag{4.4}$$

Integration of equation (4.4) gives:

$$\mu_l r\frac{du}{dr} = \left(\frac{dP}{dz} + \rho_l g_z\right).\frac{r^2}{2} + C_1 \tag{4.5}$$

Where $C_1$ is the constant of integration

For a Newtonian fluid,

$$\tau_{rz} = \tau = -\mu_l \frac{du}{dr} \tag{4.6}$$

Substituting in equation (4.5)

$$-\tau \cdot r = \left(\frac{dP}{dz} + \rho_l g_z\right).\frac{r^2}{2} + C_1 \tag{4.7}$$

Applying the boundary condition that $\tau(r = R - \delta) = \tau_i$, the interfacial shear stress leads to

$$-\tau_i(R - \delta) = \left(\frac{dP}{dz} + \rho_l g_z\right).\frac{(R - \delta)^2}{2} + C_1 \tag{4.8}$$

Eliminating the constant $C_1$ between equations (4.7) and (4.8) leads to the equation

$$\tau = \tau_i \frac{(R - \delta)}{r} - \frac{1}{2}\left(\frac{dP}{dz} + \rho_l g_z\right)\left(\frac{r^2 - (R - \delta)^2}{r}\right) \tag{4.9}$$

Using the relation between shear stress and the velocity gradient equation (4.6) in equation (4.9) leads to

$$-\mu_l \frac{du}{dr} = \tau_i \frac{(R - \delta)}{r} - \frac{1}{2}\left(\frac{dP}{dz} + \rho_l g_z\right)\left(\frac{r^2 - (R - \delta)^2}{r}\right) \tag{4.10}$$

Integrating equation (4.10) with respect to r,

$$-\mu_l u = \tau_i(R - \delta)\ln r - \frac{1}{2}\left(\frac{dP}{dz} + \rho_l g_z\right)\left(\frac{r^2}{2} - (R - \delta)^2 \ln r\right) + C_2 \tag{4.11}$$

Using the boundary condition $u(r = R) = 0$ and eliminating the constant $C_2$ leads to an expression for liquid film velocity, as follows

$$u = \frac{1}{\mu_l}\left[\left(\tau_i(R - \delta) + \left(\frac{(R - \delta)^2}{2}\left(\frac{dP}{dz} + \rho_l g_z\right)\right)\right)\ln\frac{R}{r} - \frac{1}{4}\left(\frac{dP}{dz} + \rho_l g_z\right)(R^2 - r^2)\right] \tag{4.12}$$

The mass flow rate of the liquid can be obtained by integrating the liquid film velocity profile over the film cross section as follows

$$\dot{m}_l = \int_{R-\delta}^{R} \rho_l 2\pi u r dr \tag{4.13}$$

which leads to the following expression for liquid mass flow rate

$$\dot{m}_l = \frac{2\pi\rho_l}{\mu_l}\left[\left(\tau_i(R-\delta) + \left(\frac{(R-\delta)^2}{2}\left(\frac{dP}{dz} + \rho_l g_z\right)\right)\right) \times \left(\frac{(R^2-(R-\delta)^2)}{4} - \frac{(R-\delta)^2}{2}\ln\frac{R}{R-\delta}\right)\right] - \frac{\pi\rho_l}{8\mu_l}\left(\frac{dP}{dz} + \rho_l g_z\right)(R^2-(R-\delta)^2)^2 \tag{4.14}$$

The expression for liquid mass flow contains three variables for given fluid properties and pipe diameter. These variables are the interfacial shear stress, the pressure gradient and the liquid film thickness. Hence, for a given liquid flow rate equations relating pressure gradient and interfacial shear stress to the liquid film thickness are required. The following sections describe these equations.

### 4.1.2 Momentum Balance for the Refrigerant Vapor Core

The forces acting on the refrigerant core are shown in Figure 4.1. When a force balance of the refrigerant core is carried out following equation is obtained

$$\frac{dP}{dz} + \rho_v g_z + \frac{\tau_i \pi D_c}{A_c} = 0 \tag{4.15}$$

The void fraction is defined as

$$\alpha = \frac{A_c}{A} = \left(\frac{D_c}{D}\right)^2 = \left(\frac{D - 2\delta}{D}\right)^2 \tag{4.16}$$

Substituting equation (4.16) in equation (4.15)

$$\frac{dP}{dz} + \rho_v g_z + \frac{4\tau_i}{D\sqrt{\alpha}} = 0 \tag{4.17}$$

In order to close these systems of equations a closure relationship is required which is generally expressed by relating interfacial shear stress with the pressure gradient using interfacial friction factor.

### 4.1.3 Correlation for interfacial friction factor

There are many correlations for interfacial friction factors in annular flow available in literature. The correlation proposed by Wallis (1969) has been very popular and has been used in many studies. Wallis correlation tends to under-predict the interfacial friction factor for a large film thickness ($\delta/D \geq 0.02$) and to over-predict for small film thickness ($\delta/D \leq 0.005$) (Belt et al. 2009). In this study an approach similar to Asali et al. (1985) is adopted. The ratio of interfacial friction factor and the smooth pipe friction factor is expressed as a function of the vapor phase Reynolds number, liquid film Reynolds number and dimensionless liquid film thickness. The advantage of using this form of correlation is that it captures the smooth pipe pressure drop as the film thickness goes to zero. The liquid film thickness normalized by the vapor kinematic viscosity and the friction velocity has been found to explain the effect of pipe diameter better than normalizing the film thickness using the pipe diameter (Asali et al. 1985). The non-dimensional liquid film thickness and the vapor phase Reynolds number capture the effect of vapor momentum on oil retention and pressure drop. In order to capture the effect of OCR on oil

retention and pressure drop, the liquid film Reynolds number was also included in the expression for interfacial friction factor. The following form for the interfacial friction factor was attempted:

$$\frac{f_i}{f_s} = 1 + KRe_l{}^a Re_v{}^b \delta_v^{+c} \tag{4.18}$$

Where

$$f_s = 0.046 Re_v^{-0.2} \tag{4.19}$$

$$Re_l = \frac{G(1-x)D}{4\mu_l} \tag{4.20}$$

$$Re_v = \frac{GxD}{\mu_v} \tag{4.21}$$

$$\delta_v^+ = \frac{\delta}{\nu_v}\sqrt{\frac{\tau_i}{\rho_v}} \tag{4.22}$$

The friction velocity is defined as

$$u^* = \sqrt{\frac{\tau_i}{\rho_v}} \tag{4.23}$$

The liquid film Reynolds number was evaluated based on liquid film thickness as the characteristic length and the average liquid velocity as the characteristic velocity. The interfacial shear stress is related to the vapor velocity by the following equation

$$\tau_i = \frac{1}{2} f_i \rho_v (u_v - u_l)^2 \tag{4.24}$$

Since the average vapor velocity in general is much higher than average liquid film velocity this equation can be simplified to

$$\tau_i = \frac{1}{2} f_i \rho_v \bar{u}_v^2 \tag{4.25}$$

$$\bar{u}_v = \frac{Gx}{\rho_v \alpha} \tag{4.26}$$

Optimum values of coefficients in Equation (4.18) were determined by a least square fit of collected data for R134a with POE 32 oil. The dependence of friction factor on Weber number could not be investigated as the experimental data for only R134a and POE 32 mixture was used to develop the model due to which surface tension did not change a lot. The experimental data for R1234yf and POE 32 mixture could not be used to develop the model as the thermophysical properties of the refrigerant oil mixture were not available. The final form of the correlation for vertical suction line is:

$$\frac{f_i}{f_s} = 1 + \ 0.0784 {Re_v}^{-0.3} \delta_v^{+1.4} \ {Re_l}^{-0.3} \tag{4.27}$$

This correlation is only valid for annular flow in vertical suction pipe.

### 4.1.4 Procedure for calculating oil retention and pressure drop in suction lines

1. The inputs required for calculating oil retention and pressure drop are the saturation pressure, suction line inlet temperature, total mass flow rate of refrigerant and oil entering the test section, OCR, the diameter of the suction line, and vapor and liquid thermophysical properties.
2. The quality and local oil concentration in the liquid film can be estimated from the saturation pressure, suction line inlet temperature and the OCR using method for R22 and

AB oil presented by Takaishi and Oguchi (1987), and later generalized to other refrigerants and oils by Thome (1995). The relevant equations are mentioned below

$$T_{bub} = \frac{A(w_{local})}{\ln(P_{sat}) - B(w_{local})} \tag{4.28}$$

$$A(w_{local}) = a_0 + a_1 w_{local} + a_2 w_{local}^3 + a_3 w_{local}^5 + a_4 w_{local}^7 \tag{4.29}$$

$$B(w_{local}) = b_0 + b_1 w_{local} + b_2 w_{local}^3 + b_3 w_{local}^5 + b_4 w_{local}^7 \tag{4.30}$$

$a_1$ = 182.52 $b_1$ = -0.72212

$a_2$ = -724.21 $b_2$ = 2.3914

$a_3$ = 3868.0 $b_3$ = -13.779

$a_4$ = -5268.9 $b_4$ = 17.066

As suggested by (Thome 1995), the values of constants $a_0$ and $b_0$ are found out by using a pure refrigerant vapor pressure equation at system saturation pressure.

$$w_{local} = \frac{OCR}{1 - x} \tag{4.31}$$

3. Equations (4.14), (4.16), (4.17), (4.19) to (4.27) are solved for obtaining film thickness and pressure gradient. Once the film thickness is known the amount of oil in the suction line can be estimated by the equation given below

$$m_{oil} = w_{local}.\, 2\pi R \delta L \rho_l \tag{4.32}$$

## 4.2 Validation of the model

Figure 4.2 shows the plot of predicted and experimental values for oil retention in vertical suction pipe.

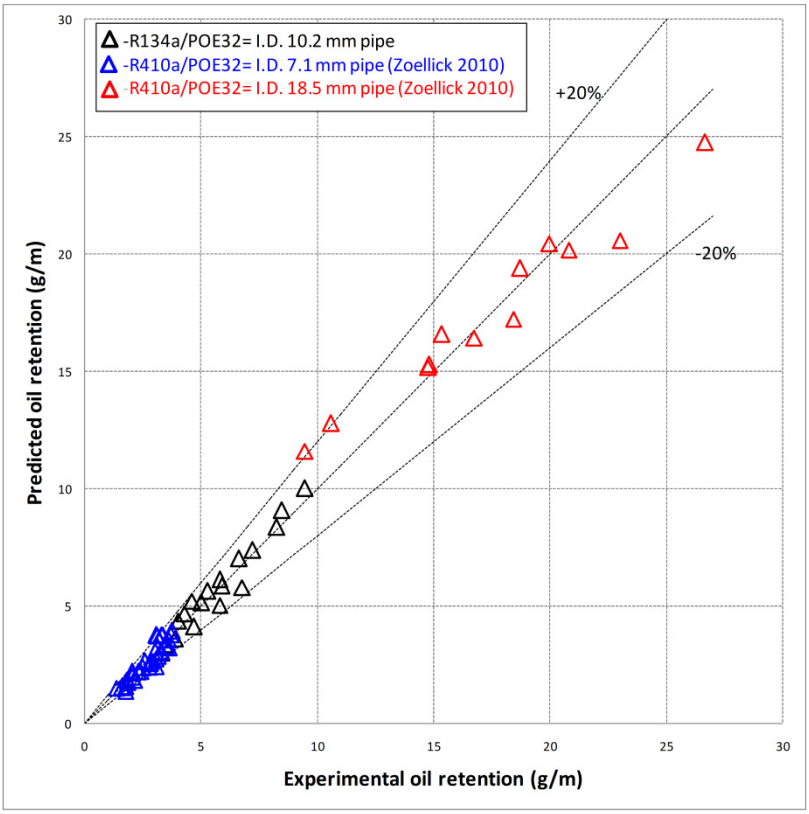


Figure 4.2 – Experimental validation of the model based on oil retention per unit length of vertical suction pipe

The experimental data from Zoellick and Hrnjak (2010) with R410A/POE 32 in 7.1 mm and 18.5 mm inside diameter pipes has also been included for validation of the model. It can be seen that the model predicts more than 90% of the oil retention data within ±20% for three different pipe diameters. Figures 4.3 shows the plot of predicted and experimental values for pressure drop in vertical suction pipe. It can be observed that the model predicts more than 90% of the pressure drop within ±30% of the experimental values. Tables 4.1 and 4.2 show the statistical comparison between measured data and predictions by different models. A total of 64 data points consisting

of the experimental data obtained for R134a/POE in this study and for R410/POE from Zoellick and Hrnjak (2010) were used to construct the tables. Radermacher et al. (2006) model was only used for predictions of oil retention data as the friction factor developed by them was used for prediction of oil retention data only.

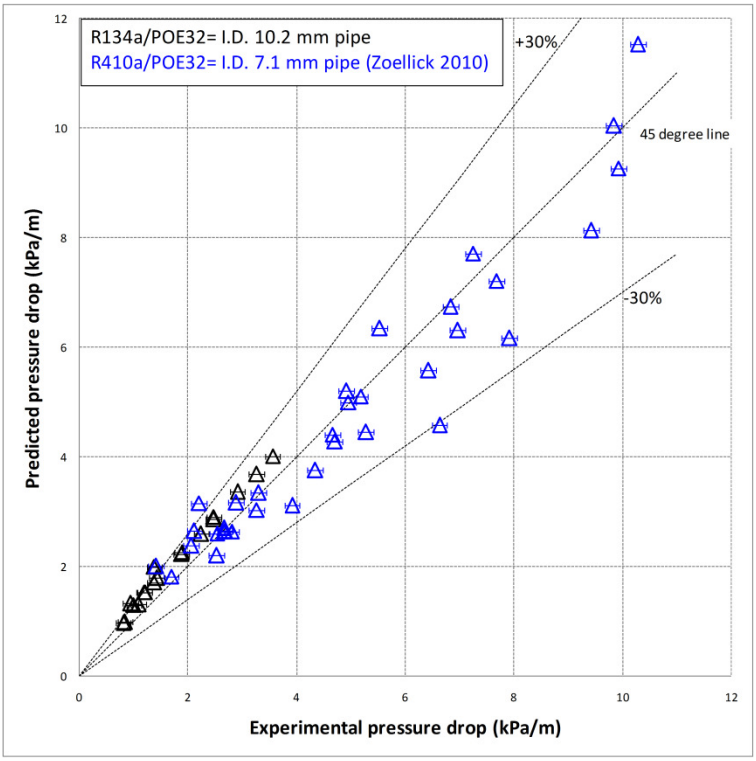


Figure 4.3 – Pressure drop model validation for unit length of vertical suction pipe

Figure 4.4 shows the model predictions for variation of oil retention with mass flux along with experimental data at a saturation temperature of 13$^{o}$C and superheat of 15$^{o}$C. The model predicts the trend well; however, since the model was developed for annular flow regime, it under predicts the oil retention near the Jacobs limit as the flow transitions to churn flow.

Table 4.1- Statistical comparison between experimental data and model predictions for oil retention

| | (1) | (2) | (3) |
|---|---|---|---|
| Radermacher et al. (2006) | 72.4 | -72.4 | 0 |
| Zoellick and Hrnjak (2010) | 11.5 | -0.9 | 83 |
| Proposed correlation | 7.9 | 0.1 | 95 |

(1) Mean absolute percentage error (%) $\frac{100}{n}\sum_1^n \frac{|(oil\ retention)_{pred}-(oil\ retention)_{exp}|}{(oil\ retention)_{exp}}$

(2) Mean percentage error (%) $\frac{100}{n}\sum_1^n \frac{(oil\ retention)_{pred}-(oil\ retention)_{exp}}{(oil\ retention)_{exp}}$

(3) Percentage of experimental data predicted within ± 20%

Table 4.2- Statistical comparison between experimental data and model predictions for pressure drop

| | (1) | (2) | (3) |
|---|---|---|---|
| Zoellick and Hrnjak (2010) | 82.7 | 82.7 | 0 |
| Proposed correlation | 15.4 | 7.9 | 92 |

(1) Mean absolute percentage error (%) $\frac{100}{n}\sum_1^n \frac{|(pressure\ drop)_{pred}-(pressure\ drop)_{exp}|}{(pressure\ drop)_{exp}}$

(2) Mean percentage error (%) $\frac{100}{n}\sum_1^n \frac{(pressure\ drop)_{pred}-(pressure\ drop)_{exp}}{(pressure\ drop)_{exp}}$

(3) Percentage of experimental data predicted within ± 30%

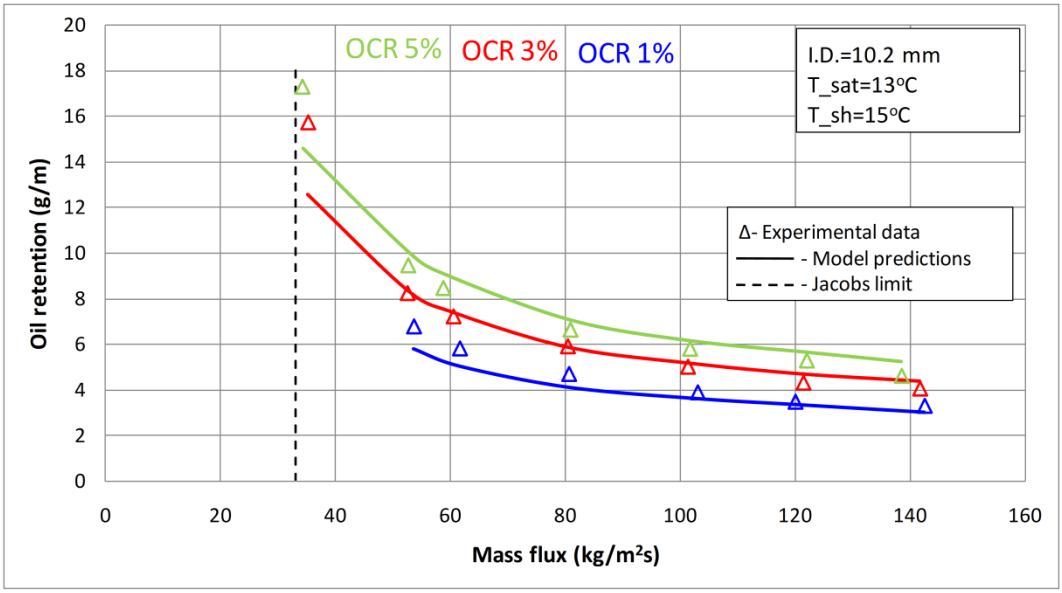


Figure 4.4- Model predictions with experimental data for oil retention as a function of mass flux for three OCRs in vertical pipe for R134a/POE

Figure 4.5 shows the model predictions for variation of oil retention with OCR along with experimental data.

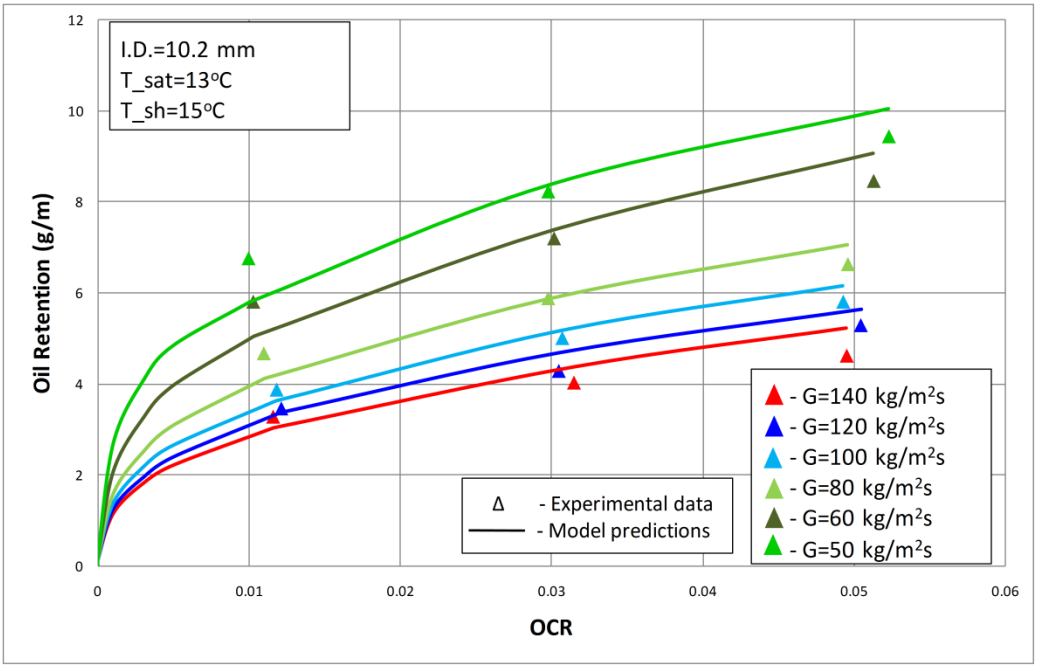


Figure 4.5- Model predictions with experimental data for oil retention as a function of OCR and mass flux as parameter in vertical pipe for R134a/POE

Figure 4.6 shows model predictions for variation of pressure drop with mass flux along with experimental data. It can be observed that the model predicts the increase in pressure drop as the liquid film reversal begins which was observed to happen at mass flux between 60 kg/m$^2$s and 50 kg/m$^2$s.

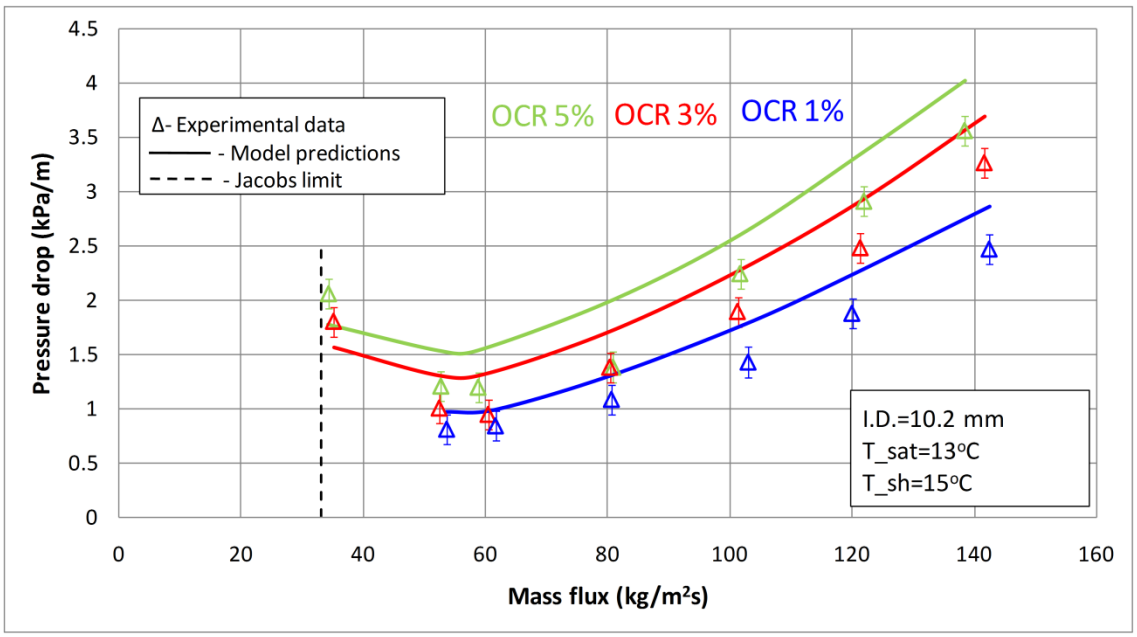


Figure 4.6- Model predictions with experimental data for pressure drop as a function of mass flux for three OCRs in vertical pipe for R134a/POE

Similar plots for R410A/POE data from Zoellick and Hrnjak (2010) are shown in Figures 4.7 to 4.10. The model predicts the oil retention trend well for both 7.1 mm and 18.5 mm internal diameter pipes.

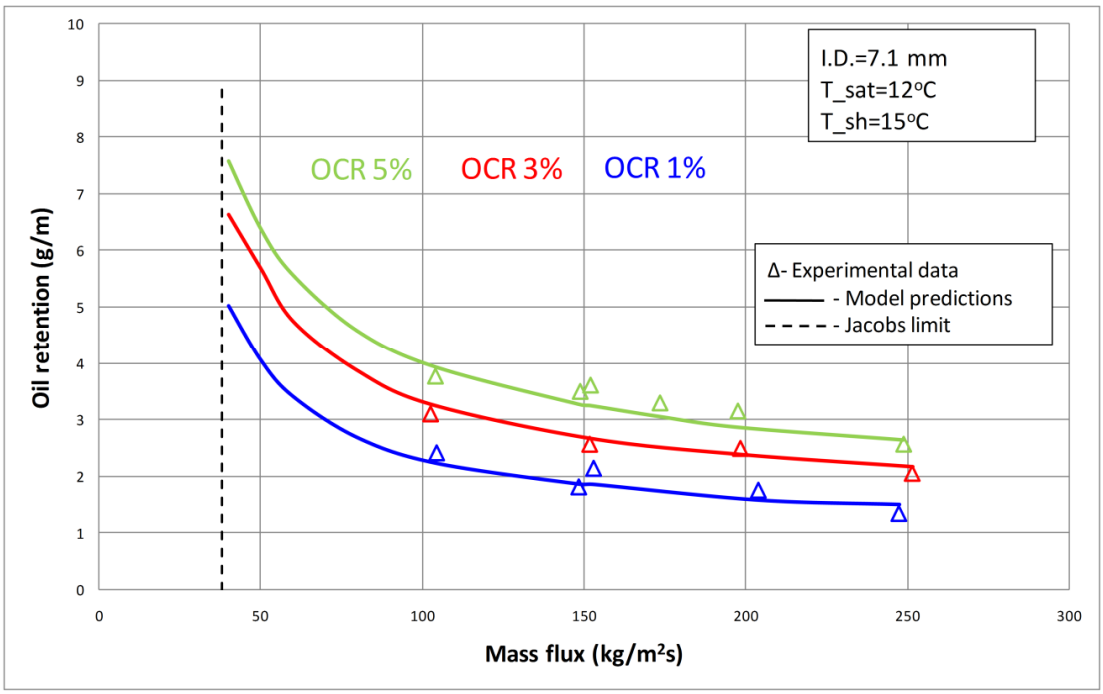


Figure 4.7- Model predictions with experimental data for oil retention as a function of mass flux for three OCRs in 7.1 mm I.D. vertical pipe for R410A/POE

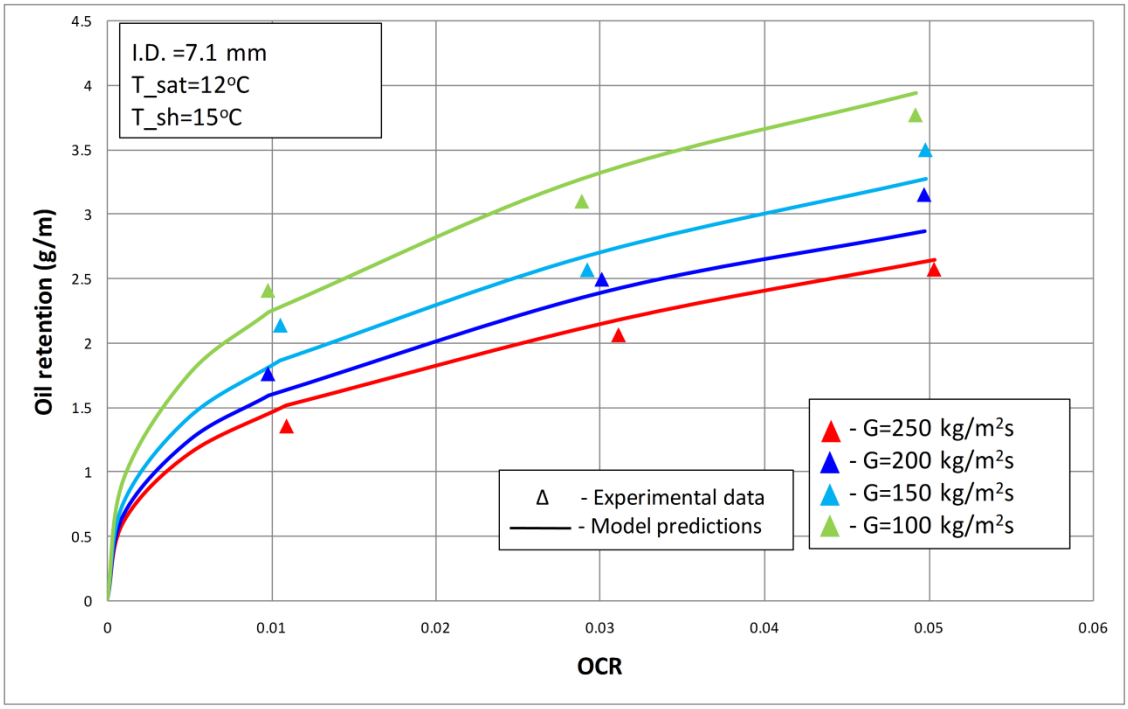


Figure 4.8- Model predictions with experimental data for oil retention as a function of OCR and mass flux as parameter in 7.1 mm I.D. vertical pipe for R410A/POE

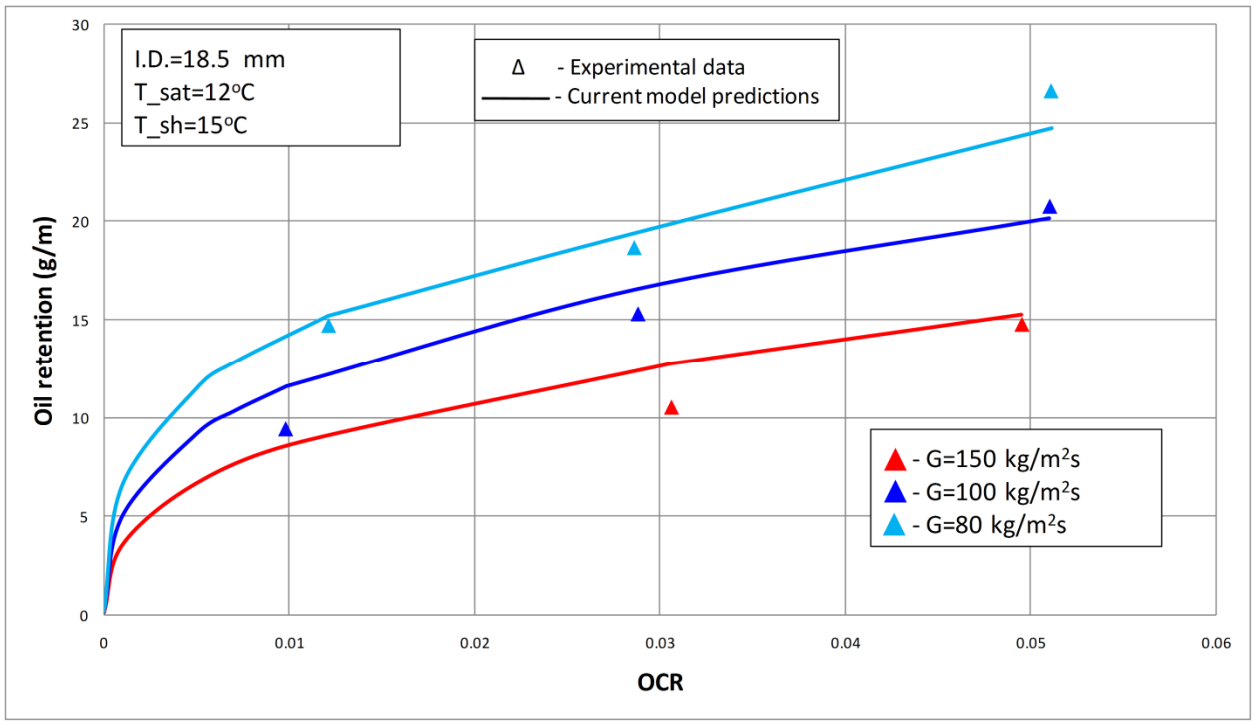


Figure 4.9- Model predictions with experimental data for oil retention as a function of OCR and mass flux as parameter in 18.5 mm I.D. vertical pipe for R410A/POE

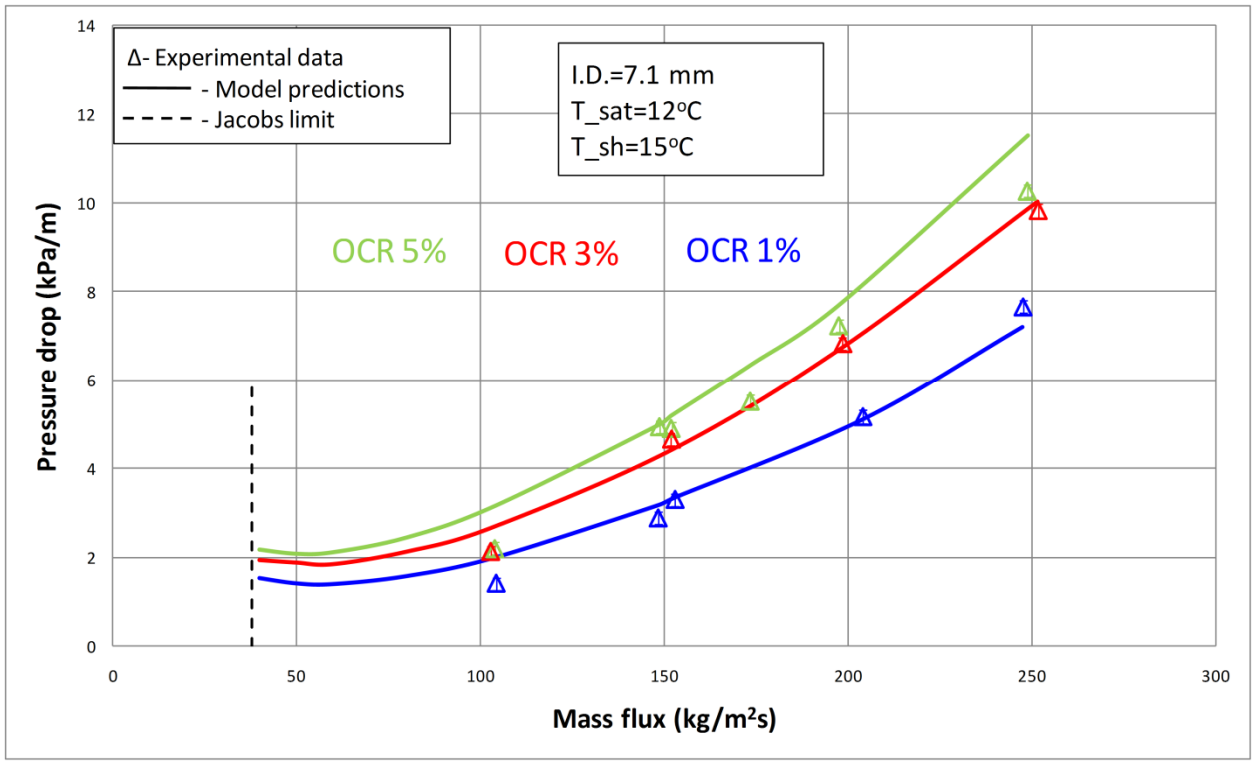


Figure 4.10- Model predictions with experimental data for pressure drop as a function of mass flux for three OCRs in vertical pipe for R410A/POE

Figure 4.11 shows experimental data for R22/MO from Cremaschi et al. (2005). The model predictions from Radermacher et al. (2006) and the proposed model are also depicted on the same plot.

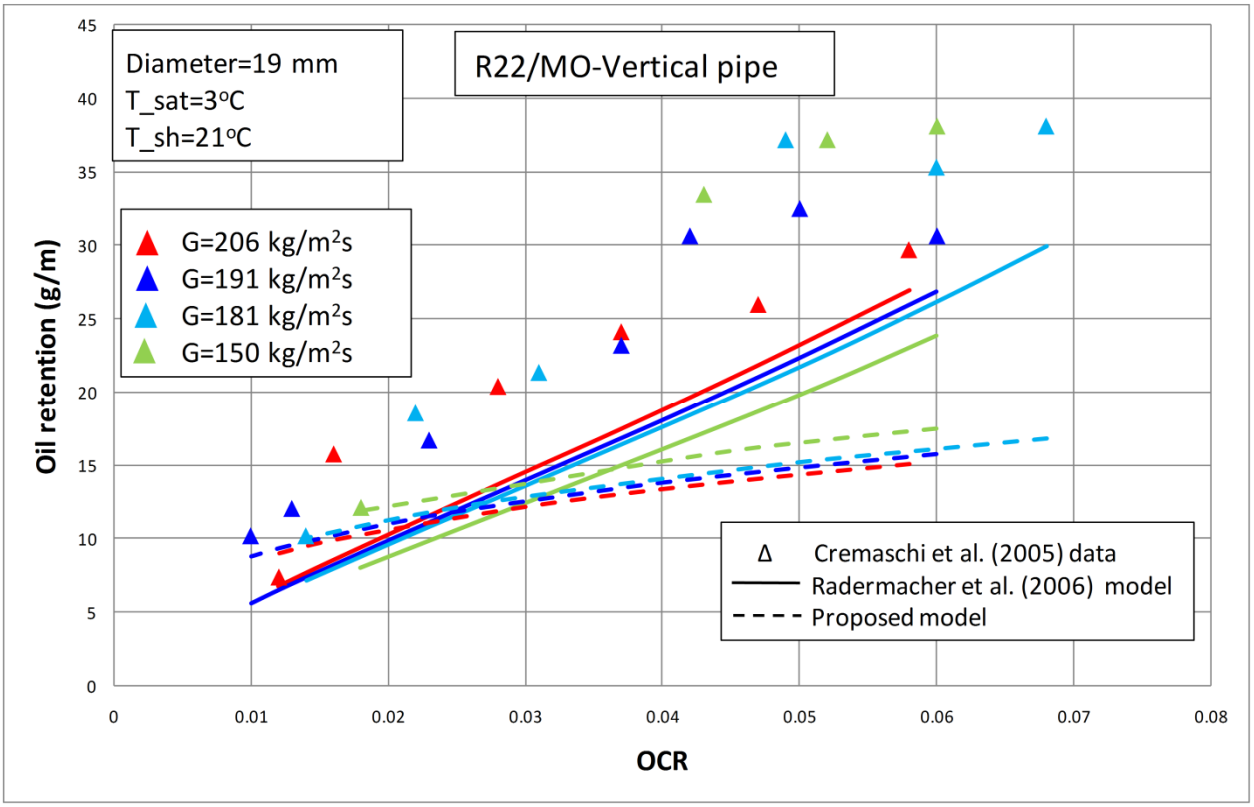


Figure 4.11- Comparison of Radermacher et al. (2006) and proposed model for R22/MO data from Cremaschi et al. (2005)

It is observed that the proposed model predicts the trend of the mass flux influence correctly but does not predict the variation with OCR correctly. The experimental data for R22/MO from Cremaschi et al. (2005) shows greater sensitivity to OCR than the experimental data for R1234yf /POE and R134a/POE from this study and for R410A/POE from Zoellick and Hrnjak (2010). This might be due to difference in experimental procedure. Cremaschi et al. (2005) used injection-extraction technique for studying oil retention in suction lines whereas direct

measurement was used in this study and Zoellick and Hrnjak (2010). Future work should try to focus on resolving the discrepancy in the sensitivity of oil retention to OCR by these different techniques. The model has been developed and validated in the following ranges:

Vertical Pipe

- $0.01 \leq \frac{\delta}{D} \leq 0.07$
- $48{,}000 \leq Re_v \leq 210{,}000$
- $0.3 \leq Re_l \leq 10$

## 4.3 Parametric Study

### 4.3.1 Effect of reducing the cooling capacity

Figure 4.12 shows the effect of reduction of cooling capacity at part load operation on oil retention and pressure drop in vertical suction lines. The graph has been plotted for R134a/POE 32 mixture at a condensing temperature of 40$^{o}$C with 5$^{o}$C of subcooling, evaporation temperature of 10$^{o}$C with 5$^{o}$C of superheat, OCR of 0.5% and inner pipe diameter of 16 mm. It can be seen that the model predicts an increase in oil retention and reduction in pressure drop as the cooling capacity is reduced. However, below a cooling capacity of 2.6 kW the oil retention increases sharply and pressure drop also starts to increase. This is because at this cooling capacity liquid film near the wall starts to reverse and a lot of oil is retained in the suction line. The pressure drop starts to increase because of increase in hydrostatic component of pressure drop which is the dominant factor in deciding overall pressure drop as the flow regime starts transitioning to churn flow. It can be seen that as the Jacobs limit is reached, oil retention and pressure drop increase significantly. This indicates that Jacobs limit may not be appropriate for design of suction risers. The pressure drop in suction line is minimum at the point of liquid film reversal

near the wall. Hence, this might be an appropriate limit for design of suction lines. This approach is adopted in developing a model for prediction of minimum mass flux for oil return in vertical suction lines and will be discussed later.

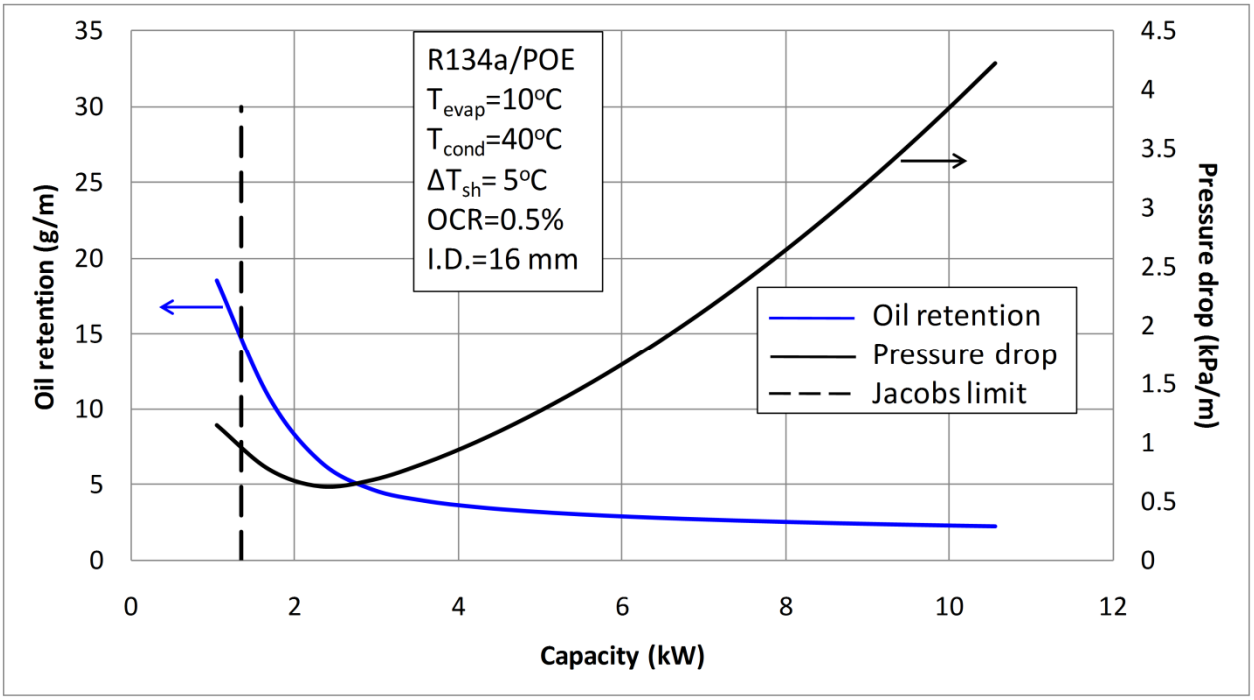


Figure 4.12- Effect of cooling capacity reduction on oil retention and pressure drop based on the proposed model

### 4.3.2 Effect of pipe diameter

Figure 4.13 shows the effect of increase in pipe diameter on oil retention and pressure drop. The graph was plotted for a system cooling capacity of 10.6 kW and other conditions being similar to Figure 4.12. The oil retention increases as the pipe diameter is increased due to reduction of refrigerant vapor velocity. The pressure drop increases as the pipe diameter is reduced because of increase in refrigerant vapor velocity which leads to higher frictional pressure drop, which is the dominant factor in overall pressure drop at high vapor velocities. However, as the pipe diameter is increased beyond 30 mm there is a sharp increase in oil retention due to flow reversal and transition of flow to churn flow regime. The pressure drop also increases as the pipe diameter increased beyond 30 mm due to sharp increase in oil retention. Plots similar to Figure 4.13 could

be a useful tool for design of suction lines depending on whether oil retention or pressure drop is more critical for system reliability and performance.

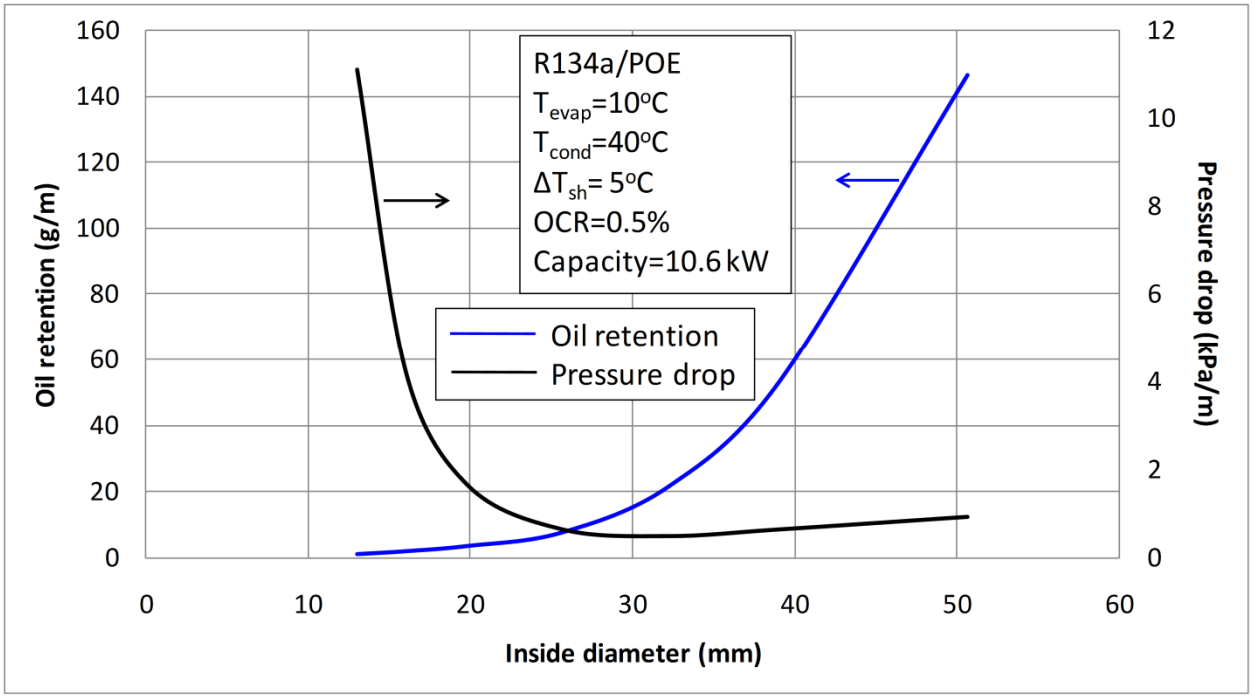


Figure 4.13- Effect of diameter on oil retention and pressure drop based on the proposed model

### 4.3.3 Effect of suction line superheat

The effect of superheat on oil retention and pressure drop in shown in Figure 4.14. The plot is depicted for a fixed mass flux of 330 kg/m$^2$s. Both oil retention and pressure drop increase as the superheat is increased. The liquid film viscosity increases as the superheat in increased due to reduction in amount of refrigerant in the liquid film. This increase is liquid film viscosity is responsible for increase in oil retention. The liquid film becomes thicker as the oil retention is increased which leads to increased waviness on the film surface. The vapor velocity also increases at same mass flux due to the thicker film. Both these factors lead to an increase in pressure drop as the superheat is increased. Table 4.3 shows the variation of refrigerant vapor density and liquid film viscosity with superheat at an evaporation temperature of 10°C for

R134a/POE 32 mixture. It is important to note that the model does not account for the effect of change in surface tension on pressure drop.

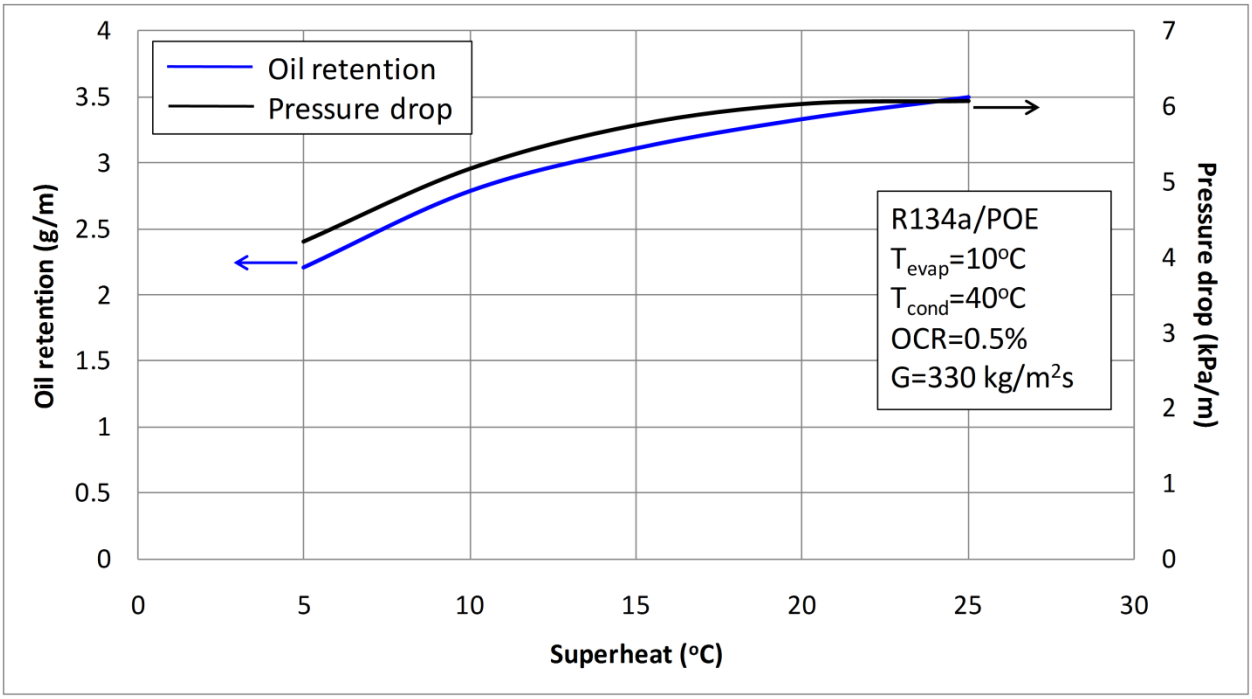


Figure 4.14- Effect of suction line superheat on oil retention and pressure drop based on the proposed model

Table 4.3- Density of refrigerant vapor and viscosity of liquid film at different superheats at 10°C evaporation temperature for R134a/POE ISO 32 mixture

| Superheat (°C) | Vapor density (kg/m$^3$) | Liquid film viscosity (cP) |
|---|---|---|
| **5** | 19.71 | 3.3 |
| **10** | 19.21 | 5.9 |
| **15** | 18.75 | 7.9 |
| **20** | 18.33 | 9.4 |
| **25** | 17.93 | 10.3 |

## 4.4 Model for prediction of minimum refrigerant mass flux for oil return

The minimum refrigerant mass flux is generally used for sizing of vertical suction risers. It is generally believed to be the mass flux below which oil return is not expected. It was found that though the oil returns at the minimum mass flux recommended by Jacobs et al. (1976) but oil retention in the pipe increases sharply at lower mass flux. In the current study it was observed that the oil retention increased sharply as the liquid film near the wall started to flow down. In this study an approach similar to Mehendale and Radermacher (2000) was followed and the friction factor correlation developed for prediction of oil retention and pressure drop was used for predicting the minimum refrigerant mass flux for oil return.

### 4.4.1 Development of Model

The film reversal begins when the wall shear stress goes to zero.

The shear stress at the wall is given by

$$\tau_w = \tau_i \frac{(R-\delta)}{R} - \frac{1}{2}\left(\frac{dP}{dz} + \rho_l g_z\right)\left(\frac{R^2-(R-\delta)^2}{R}\right) \tag{4.33}$$

Equating wall shear stress to zero the following equation is obtained

$$\tau_i \frac{(R-\delta)}{\delta} = \frac{1}{2}\left(\frac{dP}{dz} + \rho_l g_z\right)(2R-\delta) \tag{4.34}$$

Figures (4.15) and (4.16) illustrate oil retention and pressure drop data for R134a/POE 32 oil for 10.2 mm vertical suction pipe. Various minimum refrigerant mass flux criterions are shown on the same plot to evaluate them based on experimental oil retention and pressure drop data.

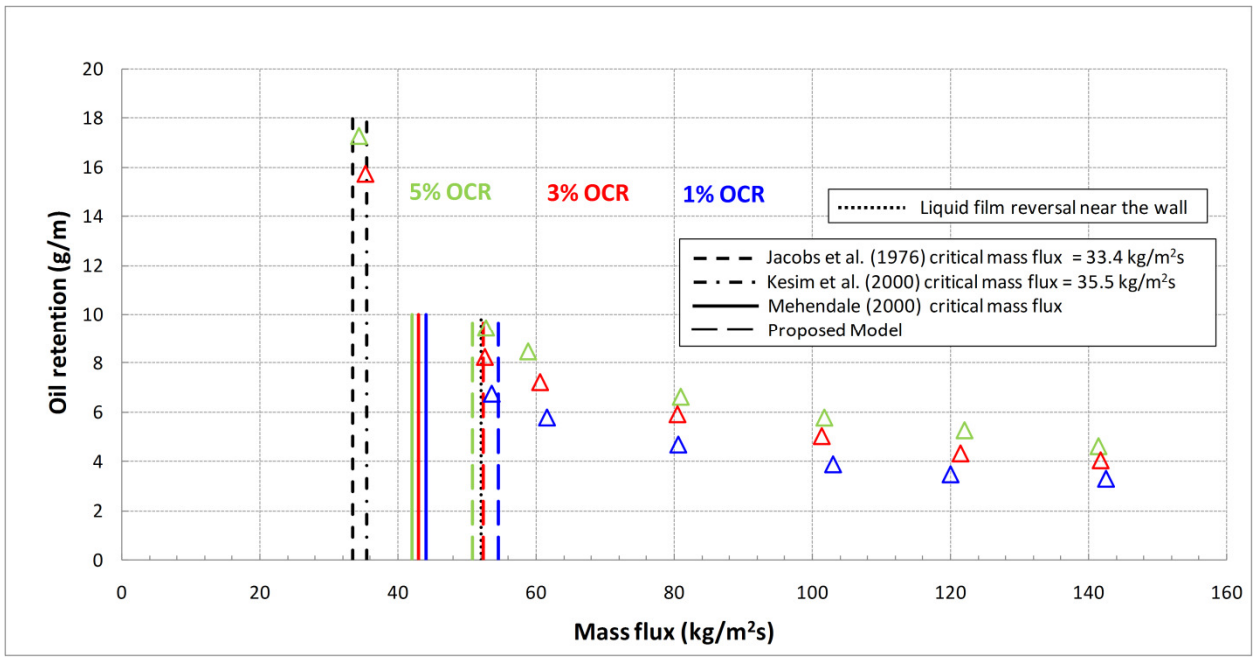


Figure 4.15- Oil retention data for R134a/POE 32 in 10.2 mm I.D. vertical pipe with various minimum mass flux limits

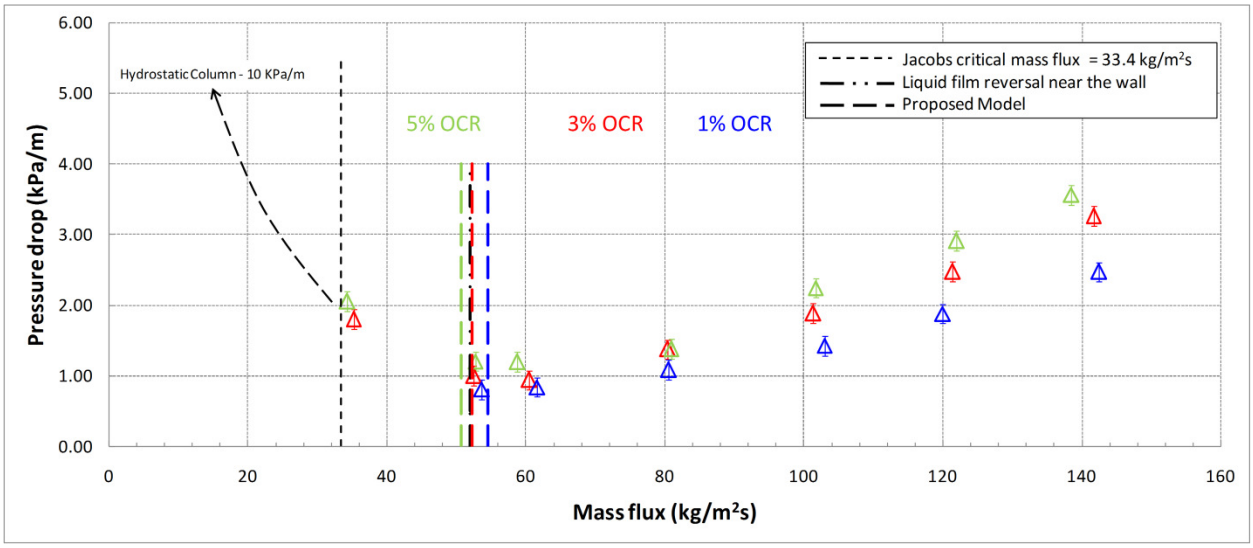


Figure 4.16- Pressure drop data for R134a/POE 32 in 10.2 mm I.D. vertical pipe with various minimum mass flux limits

It can be seen that the oil retention increases sharply even before the Jacobs et al. (1976) limit is reached because of liquid film reversal in the vertical suction pipe. Further, the pressure drop in the vertical suction pipe starts to increase even before the Jacobs limit is reached due to an

increase in oil retention. This indicates that Jacobs limit may not appropriate for design of vertical suction lines as it may lead to high oil retention and pressure drop in system under part load conditions. Minimum mass flux proposed by Kesim et al. (2000) is only slightly higher than the Jacobs limit and hence may not be appropriate for design of vertical suction lines.

The critical mass flux criterion proposed by Mehendale and Radermacher (2000) is based on the point of liquid film reversal and predicts a higher minimum mass flux than Jacobs but does not predict the point of liquid film reversal accurately. This may be due to the fact that they used interfacial friction proposed by Wallis (1969) which is not accurate for thick liquid films as would be observed near the point of flow reversal. It was observed that as the mass flux was reduced below the point of liquid film reversal the oil retention and pressure drop both started to increase. The proposed model predicts the minimum mass flux at the point of liquid film reversal and the oil retention is reasonable under these conditions. It can be observed that at minimum mass flux predicted by the proposed model, the pressure drop in suction line was minimum as illustrated by Figure (4.16). The proposed model also takes into account the effect of OCR and liquid film viscosity on minimum refrigerant mass flux. The properties for refrigerant oil mixtures were obtained from ASHRAE 2002 refrigeration handbook. The minimum mass flux predicted by the model was converted to an equivalent system cooling capacity. Table 4.4 shows the minimum cooling capacity requirements for R134a/POE ISO 32 oil for various pipe diameters and thermodynamic conditions. An OCR of 0.3% was assumed for constructing Table 4.4. Tables 4.5 and 4.6 show the minimum capacities for OCR's of 0.5% and 1% respectively. These capacities have been calculated assuming saturated conditions at condenser and evaporator outlet. Condensing temperature of 40$^{o}$C was assumed for the calculations of minimum capacities. For other liquid temperatures the correction multipliers are also provided at the bottom of Table

4.4. Similar tables for R1234yf/POE could not be constructed as the thermo-physical properties of the refrigerant and oil mixture were not available. The minimum capacity tables have been proposed based on the experiments carried out in PVC test sections. The extensions of these results for copper tubing may be justified as the surface would be completely wet in both cases because the flow regime is annular. Further any difference is surface roughness of the two materials may not affect the results as the liquid film is expected to be laminar. It should be noted that any increase in velocity in the suction line leads to a reduction in pipe diameter and an increase pressure drop.

Table 4.4- Minimum Refrigeration Capacity in kW for Oil Entrainment up Suction Risers based on the proposed model (OCR 0.3%)
(Copper Tubing, ASTM 88M Type B, Metric Size)

| Refrig-erant | Saturated Temp., °C | Suction Gas Temp., °C | Tube Nominal OD, mm | | | | | | | | | | | | |
|---|---|---|---|---|---|---|---|---|---|---|---|---|---|---|---|
| | | | 10 | 12 | 15 | 18 | 22 | 28 | 35 | 42 | 54 | 67 | 79 | 105 | 130 |
| 134a | -10 | -5 | 0.336 | 0.532 | 0.942 | 1.536 | 2.534 | 4.630 | 7.925 | 12.410 | 22.813 | 38.066 | 56.123 | 110.299 | 183.961 |
| | | 5 | 0.221 | 0.349 | 0.616 | 1.001 | 1.646 | 2.993 | 5.098 | 7.949 | 14.526 | 24.111 | 35.404 | 69.075 | 114.562 |
| | | 15 | 0.206 | 0.325 | 0.575 | 0.933 | 1.534 | 2.789 | 4.750 | 7.405 | 13.529 | 22.451 | 32.962 | 64.293 | 106.608 |
| | -5 | 0 | 0.366 | 0.580 | 1.027 | 1.673 | 2.760 | 5.041 | 8.627 | 13.505 | 24.818 | 41.397 | 61.017 | 119.857 | 199.826 |
| | | 10 | 0.260 | 0.411 | 0.726 | 1.179 | 1.939 | 3.526 | 6.009 | 9.372 | 17.131 | 28.445 | 41.778 | 81.550 | 135.300 |
| | | 20 | 0.238 | 0.376 | 0.663 | 1.078 | 1.772 | 3.221 | 5.486 | 8.555 | 15.632 | 25.947 | 38.100 | 74.334 | 123.284 |
| | 5 | 10 | 0.443 | 0.700 | 1.239 | 2.018 | 3.327 | 6.073 | 10.384 | 16.246 | 29.826 | 49.710 | 73.223 | 143.669 | 239.310 |
| | | 20 | 0.344 | 0.544 | 0.960 | 1.561 | 2.567 | 4.670 | 7.961 | 12.421 | 22.720 | 37.744 | 55.459 | 108.336 | 179.845 |
| | | 30 | 0.316 | 0.500 | 0.883 | 1.434 | 2.358 | 4.289 | 7.311 | 11.406 | 20.858 | 34.645 | 50.896 | 99.393 | 164.960 |
| | 10 | 15 | 0.485 | 0.766 | 1.356 | 2.209 | 3.641 | 6.643 | 11.354 | 17.758 | 32.587 | 54.289 | 79.943 | 156.766 | 261.013 |
| | | 25 | 0.389 | 0.614 | 1.084 | 1.762 | 2.897 | 5.272 | 8.989 | 14.027 | 25.661 | 42.638 | 62.658 | 122.424 | 203.267 |
| | | 35 | 0.363 | 0.573 | 1.013 | 1.646 | 2.706 | 4.922 | 8.390 | 13.090 | 23.940 | 39.766 | 58.424 | 114.109 | 189.407 |

| | | Liquid Temperature, °C | | |
|---|---|---|---|---|
| | Refrigerant | 20 | 30 | 50 |
| Correction Multipliers | 134a | 1.20 | 1.10 | 0.89 |

Table 4.5- Minimum Refrigeration Capacity in kW for Oil Entrainment up Suction Risers based on the proposed model (OCR 0.5%)
(Copper Tubing, ASTM 88M Type B, Metric Size)

| Refrig-erant | Saturated Temp., °C | Suction Gas Temp., °C | Tube Nominal OD, mm | | | | | | | | | | | | |
|---|---|---|---|---|---|---|---|---|---|---|---|---|---|---|---|
| | | | 10 | 12 | 15 | 18 | 22 | 28 | 35 | 42 | 54 | 67 | 79 | 105 | 130 |
| 134a | -10 | -5 | 0.352 | 0.558 | 0.989 | 1.612 | 2.659 | 4.859 | 8.315 | 13.016 | 23.918 | 39.891 | 58.789 | 115.450 | 192.429 |
| | | 5 | 0.219 | 0.346 | 0.611 | 0.994 | 1.636 | 2.977 | 5.075 | 7.916 | 14.471 | 24.025 | 35.282 | 68.844 | 114.180 |
| | | 15 | 0.203 | 0.321 | 0.568 | 0.924 | 1.521 | 2.767 | 4.716 | 7.356 | 13.445 | 22.318 | 32.772 | 63.933 | 106.017 |
| | -5 | 0 | 0.383 | 0.606 | 1.073 | 1.749 | 2.886 | 5.271 | 9.018 | 14.114 | 25.925 | 43.225 | 63.687 | 125.009 | 208.286 |
| | | 10 | 0.259 | 0.409 | 0.723 | 1.176 | 1.935 | 3.522 | 6.005 | 9.368 | 17.130 | 28.447 | 41.783 | 81.558 | 135.303 |
| | | 20 | 0.235 | 0.372 | 0.658 | 1.070 | 1.760 | 3.203 | 5.460 | 8.517 | 15.569 | 25.849 | 37.960 | 74.069 | 122.843 |
| | 5 | 10 | 0.458 | 0.725 | 1.284 | 2.093 | 3.451 | 6.299 | 10.770 | 16.846 | 30.917 | 51.508 | 75.846 | 148.716 | 247.577 |
| | | 20 | 0.345 | 0.545 | 0.963 | 1.567 | 2.578 | 4.693 | 8.003 | 12.490 | 22.848 | 37.958 | 55.771 | 108.927 | 180.792 |
| | | 30 | 0.316 | 0.499 | 0.882 | 1.435 | 2.361 | 4.298 | 7.238 | 11.436 | 20.917 | 34.744 | 51.043 | 99.671 | 165.400 |
| | 10 | 15 | 0.500 | 0.791 | 1.410 | 2.282 | 3.762 | 6.864 | 11.731 | 18.345 | 33.653 | 56.046 | 82.504 | 161.685 | 269.060 |
| | | 25 | 0.390 | 0.616 | 1.089 | 1.772 | 2.916 | 5.308 | 9.053 | 14.129 | 25.851 | 42.952 | 63.114 | 123.291 | 204.661 |
| | | 35 | 0.363 | 0.574 | 1.014 | 1.650 | 2.714 | 4.941 | 8.425 | 13.147 | 24.047 | 39.946 | 58.687 | 114.606 | 190.197 |

| Correction Multipliers | Refrigerant | Liquid Temperature, °C | | |
|---|---|---|---|---|
| | | 20 | 30 | 50 |
| | 134a | 1.20 | 1.10 | 0.89 |

Table 4.6- Minimum Refrigeration Capacity in kW for Oil Entrainment up Suction Risers based on the proposed model (OCR 1%)
(Copper Tubing, ASTM 88M Type B, Metric Size)

| Refrig-erant | Saturated Temp., °C | Suction Gas Temp., °C | Tube Nominal OD, mm | | | | | | | | | | | | |
|---|---|---|---|---|---|---|---|---|---|---|---|---|---|---|---|
| | | | 10 | 12 | 15 | 18 | 22 | 28 | 35 | 42 | 54 | 67 | 79 | 105 | 130 |
| 134a | -10 | -5 | 0.370 | 0.587 | 1.041 | 1.698 | 2.804 | 5.123 | 8.767 | 13.723 | 25.207 | 42.021 | 61.904 | 121.464 | 202.305 |
| | | 5 | 0.213 | 0.337 | 0.598 | 0.975 | 1.607 | 2.930 | 5.001 | 7.809 | 14.289 | 23.739 | 34.876 | 68.088 | 112.958 |
| | | 15 | 0.197 | 0.312 | 0.554 | 0.903 | 1.489 | 2,714 | 4.632 | 7.232 | 13.234 | 21.985 | 32.297 | 63.047 | 104.584 |
| | -5 | 0 | 0.400 | 0.634 | 1.124 | 1.834 | 3.026 | 5.530 | 9.461 | 14.807 | 27.189 | 45.315 | 66.741 | 130.903 | 217.957 |
| | | 10 | 0.253 | 0.401 | 0.712 | 1.159 | 1.911 | 3.483 | 5.946 | 9.283 | 16.990 | 28.229 | 41.476 | 80.991 | 134.387 |
| | | 20 | 0.229 | 0.363 | 0.643 | 1.049 | 1.729 | 3.151 | 5.378 | 8.397 | 15.365 | 25.527 | 37.502 | 73.216 | 121.462 |
| | 5 | 10 | 0.474 | 0.750 | 1.331 | 2.170 | 3.581 | 6.540 | 11.183 | 17.492 | 32.098 | 53.461 | 78.699 | 154.212 | 256.580 |
| | | 20 | 0.340 | 0.539 | 0.955 | 1.557 | 2.565 | 4.677 | 7.982 | 12.466 | 22.818 | 37.922 | 55.728 | 108.863 | 180.688 |
| | | 30 | 0.310 | 0.491 | 0.871 | 1.419 | 2.339 | 4.265 | 7.281 | 11.370 | 20.811 | 34.585 | 50.821 | 99.265 | 164.741 |
| | 10 | 15 | 0.514 | 0.814 | 1.444 | 2.354 | 3.883 | 7.090 | 12.121 | 18.956 | 34.771 | 57.896 | 85.207 | 166.892 | 277.581 |
| | | 25 | 0.386 | 0.611 | 1.083 | 1.765 | 2.908 | 5.302 | 9.050 | 14.133 | 25.871 | 42.999 | 63.194 | 123.460 | 204.935 |
| | | 35 | 0.358 | 0.567 | 1.004 | 1.636 | 2.697 | 4.915 | 8.389 | 13.099 | 23.976 | 39.842 | 58.546 | 114.353 | 189.784 |

| Correction Multipliers | Liquid Temperature, °C | | |
|---|---|---|---|
| Refrigerant | 20 | 30 | 50 |
| 134a | 1.20 | 1.10 | 0.89 |

### 4.4.2 Procedure for calculating minimum refrigerant mass flux for vertical suction lines

1. The inputs required for calculating minimum refrigerant mass flux are the saturation pressure, suction line inlet temperature, oil in circulation ratio (OCR), the diameter of the suction line, and the vapor and liquid thermophysical properties.
2. The quality and local oil concentration in the liquid film can be estimated from equations (4.28) to (4.31).
3. The mass flow rate of refrigerant vapor and the vapor quality are defined by the equations (4.35) and (4.36).

$$\dot{m}_v = \pi \rho_v \alpha \frac{D^2}{4} u_v \tag{4.35}$$

$$x = \frac{\dot{m}_v}{\dot{m}_v + \dot{m}_l} \tag{4.36}$$

4. Equations (4.34), (4.35) and (4.36) are solved in conjunction with Equations (4.14), (4.16), (4.17) and (4.19) to (4.27) to obtain the total mass flux of refrigerant when the wall shear stress goes to zero. This mass flux should be taken as the minimum mass flux for designing the vertical suction lines.

# CHAPTER 5- SUMMARY AND CONCLUSIONS

## 5.1 Conclusions from experimental study

In summary in this work the oil retention in horizontal, vertical and inclined suction lines was studied by using method of direct measurement. High speed videos of the flow were taken to study the flow regimes and to relate oil retention to flow regimes. The oil retention and pressure drop behavior of R1234yf was compared with R134a under similar conditions. The conclusions of the current experimental work are as follows:

- In horizontal suction lines, annular and stratified flow regimes were observed at high and low mass fluxes respectively. The transition from annular to stratified-wavy flow regime depends on OCR. A modified Baker's map was found to predict the flow regime and transition region reasonably well.
- In vertical suction lines, the flow regime was annular at high mass flux and transitioned to churn at low mass flux. Jacobs limit was found to be coincident with the mass flux at which the flow transitions from annular flow to churn flow.
- In inclined suction lines the flow regime was annular at high mass flux and changed to intermittent at very low mass flux. It was observed that for $45^{o}$ inclined pipes the flow regime was stratified-wavy at intermediate mass flux. However, for pipes at $60^{o}$ inclination stratified-wavy flow regime was not observed at intermediate mass flux and flow regime transitioned directly from annular flow to intermittent flow. The churn flow regime was completely suppressed in inclined pipes.
- Oil retention increases as the mass flux is reduced or the OCR is increased. The oil retention in vertical pipe increases sharply as the mass flux is reduced below the point of liquid film reversal and eventually the flow become churny. In the horizontal pipe oil retention was

observed to decrease as the flow regime transitioned from annular to stratified-wavy flow and increased only at very low mass flux.

- Inclined pipes were found to retain more oil than horizontal or vertical pipes. It was found that oil retention reaches a maximum value at angle of inclination somewhere between $45^{o}$ to $90^{o}$.
- The pressure drop in vertical suction lines decreases in the annular flow, reaches a minimum value and increases again in the churn flow regime as the mass flux is reduced. The pressure drop in horizontal suction pipes decreases continuously as the mass flux is reduced. The pressure drop in both horizontal and vertical suction pipes increases as the OCR is increased.
- At similar system cooling capacities in the same diameter suction line, R1234yf has similar oil retention but 20 to 30% higher pressure drop in both vertical and horizontal suction lines. This can have a negative effect on the overall system performance.

## 5.2 Conclusions from modeling efforts

A semi-empirical model for prediction of oil retention and pressure drop in vertical suction lines was developed using experimental data for R134a with POE oil. The model was further validated using experimental data for R410A/POE mixture. A new model was also developed for prediction of minimum refrigerant mass flux for design of vertical suction lines. The conclusions of this study are as follows:

- A semi-empirical correlation for interfacial friction factor was developed expressing it as a function of the dimensionless liquid film thickness, vapor Reynolds number and liquid film Reynolds number.

- The model was further validated using R410A/POE data from Zoellick and Hrnjak (2010) and was found to predict more than 90% of the data for oil retention and pressure drop within ± 20% and ± 30% of the experimental values respectively.
- Parametric studies carried out using the model indicated that as the system cooling capacity is reduced, the oil retention increases. It was found that the oil retention increases sharply if the cooling capacity is reduced below a point where liquid film reversal near the wall begins. It was also found that the pressure drop in vertical suction lines is minimum near the point of liquid film reversal. The model also predicted an increase in oil retention and reduction in pressure drop as the diameter is increased. Further, both oil retention and pressure drop increased as the suction line superheat was increased.
- It was found that Jacobs et al. (1976) criterion may not be appropriate for design of suction lines as a sharp increase in oil retention and pressure drop was observed even when the mass flux was 60% higher than the Jacobs limit. Based on the Mehendale and Radermacher (2000) approach, a new model for prediction of minimum refrigerant mass flux for oil return was developed. The model was used to propose a modified table of minimum system cooling capacity as in ASHRAE (2002) for R134a/POE mixture.

# APPENDIX A

## Repeatability Tests

The repeatability of the oil retention tests was analyzed by repeating a test 5 times over the course of three weeks. This test was repeated for $45^{o}$ inclined test section for R1234yf/POE mixture. The operating conditions and the mass measurements are presented in Table A.1. The saturation temperature was calculated from the saturation pressure measured at the inlet of the test section. The total mass flux and OCR were maintained as close as possible. The temperature at the exit of the evaporator was measured in two locations, in the center of the tube, T_core, and on the outside of the tube wall, T_wall. The two temperatures are close together, indicating that the liquid and vapor phases are near equilibrium. The small difference in temperature has a minor effect on liquid properties and hence equilibrium conditions are assumed. The apparent superheat is the difference between the saturation temperature and the measured wall temperature, and is approximately 15°C for all cases. The average oil retention for the inclined tube under these conditions was 10.03 g. The standard deviation of each test was 0.10 g for the inclined tube. The standard deviation of the inclined tube is 1% of the average mass measurement for that tube. This variability stems from many sources. The error in the instruments contributed to the overall variation of each data point. If the valves were not closed at nearly the same time, some excess oil may have entered or left the test section, which could have generated errors in the measurements. The slight differences in mass flux, OCR, and saturation temperature could cause variation in the mass retention. All of these factors combined affect the repeatability of each test condition.

**Table A-1 Repeatability tests 10.2 mm tube**

| Saturation Temperature | Mass Flux | OCR | Temperature Vapor Core | Temperature Tube Wall | Mass of Oil Inclined Tube | Pressure drop |
|---|---|---|---|---|---|---|
| **[°C]** | [kg / $m^2$ s] | | [°C] | [°C] | [g] | [kPa] |
| **13.1** | 119.5 | 0.030 | 28.4 | 28.0 | 10.20 | 4.31 |
| **13.1** | 121.2 | 0.031 | 28.5 | 27.9 | 10.00 | 4.43 |
| **13.0** | 120.1 | 0.032 | 28.3 | 27.6 | 10.00 | 4.62 |
| **13.0** | 119.8 | 0.031 | 28.4 | 27.6 | 9.93 | 4.70 |
| **13.0** | 120.0 | 0.030 | 28.0 | 27.2 | 10.00 | 4.67 |

# APPENDIX B

EES code for estimation of oil retention and pressure drop in vertical suction line

```
{1. Input parameters}

G =153                          {Total mass flux kg/m^2 s}

Psat = 0.443 [MPa]              {System saturation pressure in MPa}

w_inlet = 0.0105                {Oil concentration ratio, OCR}

T_evap_out = 27.1               { Evaporator outlet temperature in C}

D=0.0102                        {Internal tube diameter in m}

L_vert = 1.89                   {Length in m of vertical test section}

nu_l_cst = 7                    {Viscosity of refrigerant oil mixture in cSt}

rho_l= 1010                     {Density of  refrigerant oil mixture in kg/m^3}


{(Thome 1995) method for calculating local oil concentration and quality}

{2. Determine local oil concentration in liquid}
{2.1 determine two saturation points just above and below Psat}
Pabove = Psat +.005
Pbelow = Psat - .005
Tabove=Temperature(R134a,P=Pabove,x=.1)
Tbelow=Temperature(R134a,P=Pbelow,x=.1)

{2.2 Calculate a_0 and b_0 with w_inlet = 0}
Tabove+273 = a_0 / (ln(Pabove) - b_0)
Tbelow+273 = a_0 / (ln(Pbelow) - b_0)

{2.3 Use new values of a_0 and b_0 in equations, keep original values of a_1 to b_4}
a_1 = 182.52
a_2 = -724.21
a_3 = 3868
a_4 = -5268.9

b_1 = -.72212
b_2 = 2.3914
b_3 = -13.779
b_4 = 17.066


{2.4 calculate w_local from T}
A_w_local = a_0 + a_1*w_local + a_2*w_local^3 + a_3*w_local^5 + a_4*w_local^7
B_w_local = b_0 + b_1*w_local + b_2*w_local^3 + b_3*w_local^5 + b_4*w_local^7
T_evap_out+273 = A_w_local / (ln(Psat) - B_w_local)
```

{3.Calculate quality inside of text sections}
w_local*(1-x)= w_inlet

{4. Calculate density of the refrigerant vapor}
rho_v=Density(R134a,T=T_evap_out,P=Psat)

{5. Calculate viscosity of the liquid and vapor portions}
mu_v=Viscosity(R134a,T=T_evap_out,P=Psat)
mu_r=Viscosity(R134a,T=T_evap_out,x=0)
mu_l=rho_l * nu_l

nu_v = mu_v/rho_v {Kinematic viscosity of the vapor}
nu_l = nu_l_cSt*10^(-6) {Kinematic viscosity of the liquid}

{6. Equations for estimation of oil retention and pressure drop}

G_l=G*(1-x)

G_v=G*x

mdot_l=(G_l)*(3.14*D^2*0.25)

mdot_l=a+b

a=(2*3.14*rho_l/mu_l)*((tau_i*(0.5*D-delta)+((0.5*D-delta)^(2)/2)*(dpdz+rho_l*9.81))*(((0.5*D)^2-(0.5*D-delta)^2)/4-((0.5*D-delta)^(2)/2)*ln(1/(1-delta_by_R))))

b=(-1*3.14*rho_l/(8*mu_l))*(dpdz+rho_l*9.81)*((0.5*D)^2-(0.5*D-delta)^2)^2

delta_by_R=delta/(0.5*D)

dpdz+rho_v*9.81+(4*tau_i/(D*(alpha)^(0.5)))=0

alpha=((D-2*delta)/D)^2

tau_i=0.5*f_i*rho_v*u_v^2

u_v=G_v/(rho_v*alpha)

delta_plus=delta/(nu_v)*(tau_i/rho_v)^(0.5)

f_i/f_s=1+0.0784*(delta_plus)^(1.4)*Re_v^(-0.3)*Re_lf^(-0.3)

f_s=0.046*Re_v^(-0.2)

Re_v=rho_v*u_v*D/mu_v

Re_lf=G*(1-x)*D/(4*mu_l)

Oil_retention_predicted=((3.14*D*delta*rho_l*w_local))*1000 {Oil retention in g/m}

EES code for estimation of minimum refrigerant mass flux

```
{1. Input parameters}

Psat = 0.443 [MPa]              {System saturation pressure in MPa}

w_inlet = 0.0105                  {Oil concentration ratio, OCR}

T_evap_out = 27.1               { Evaporator outlet temperature in C}

D=0.0102                          {Internal tube diameter in m}

nu_l_cst = 7                      {Viscosity of refrigerant oil mixture in cSt}

rho_l= 1010                       {Density of  refrigerant oil mixture in kg/m^3}


{(Thome 1995) method for calculating local oil concentration and quality}
{2. determine local oil concentration in liquid}
{2.1  determine two saturation points just above and below Psat}
Pabove = Psat +.005
Pbelow = Psat - .005
Tabove=Temperature(R134a,P=Pabove,x=.1)
Tbelow=Temperature(R134a,P=Pbelow,x=.1)

{2.2 Calculate a_0 and b_0 with w_inlet = 0}
Tabove+273 = a_0 / (ln(Pabove) - b_0)
Tbelow+273 = a_0 / (ln(Pbelow) - b_0)

{2.3 Use new values of a_0 and b_0 in equations, keep original values of a_1 to b_4}
a_1 = 182.52
a_2 = -724.21
a_3 = 3868
a_4 = -5268.9

b_1 = -.72212
b_2 = 2.3914
b_3 = -13.779
b_4 = 17.066


{2.4 Calculate w_local from T}
A_w_local = a_0 + a_1*w_local + a_2*w_local^3 + a_3*w_local^5 + a_4*w_local^7
B_w_local = b_0 + b_1*w_local + b_2*w_local^3 + b_3*w_local^5 + b_4*w_local^7
T_evap_out+273 = A_w_local / (ln(Psat) - B_w_local)


{3.Calculate quality inside of text sections}
w_local*(1-x)= w_inlet

{4. Calculate density of the vapor}
rho_v=Density(R134a,T=T_evap_out,P=Psat)

{5. Calculate viscosity of the liquid and vapor portions}
mu_v=Viscosity(R134a,T=T_evap_out,P=Psat)
```

```
mu_r=Viscosity(R134a,T=T_evap_out,x=0)
mu_l=rho_l  * nu_l

nu_v = mu_v/rho_v                    {Kinematic viscosity of the vapor}
nu_l = nu_l_cSt*10^(-6)              {Kinematic viscosity of the liquid}


{6. Equations for predicting minimum refrigerant mass flux}

tau_i*(0.5*D-delta)/delta=0.5*(dpdz+rho_l*9.81)*(D-delta)   {Equation obtained by equating wall shear stress to zero}

dpdz+rho_v*9.81+(4*tau_i/(D*(alpha)^(0.5)))=0

tau_i=0.5*f_i*rho_v*u_v^2

delta_plus=delta/(nu_v)*(tau_i/rho_v)^(0.5)

f_i/f_s=1+0.0784*(delta_plus)^(1.4)*Re_v^(-0.3)*Re_lf^(-0.3)

f_s=0.046*Re_v^(-0.2)

Re_v=rho_v*(u_v)*D/mu_v

Re_lf=G*(1-x)*D/(4*mu_l)

alpha=((D-2*delta)/D)^2

delta_by_R=delta/(0.5*D)

a=(2*3.14*rho_l/mu_l)*((tau_i*(0.5*D-delta)+((0.5*D-delta)^(2)/2)*(dpdz+rho_l*9.81))*(((0.5*D)^2-(0.5*D-delta)^2)/4-((0.5*D-delta)^(2)/2)*ln(1/(1-delta_by_R))))

b=(-1*3.14*rho_l/(8*mu_l))*(dpdz+rho_l*9.81)*((0.5*D)^2-(0.5*D-delta)^2)^2

mdot_l=a+b

x=mdot_v/(mdot_v+mdot_l)

mdot_v=rho_v*0.25*D^2*3.14*u_v*alpha

G_critical=((mdot_v+mdot_l*(1-w_local))/(0.25*3.14*D^2))
```

# APPENDIX C

## R134a/POE 32 raw data – 10.2 mm pipe diameter

| P_sat | T_sat | Total Mass Flux | OCR | T_ref_evap_out | T_r_e_wall | Mass oil | Mass oil | Pressure drop (ho) | Pressure drop (vert) |
|---|---|---|---|---|---|---|---|---|---|
| ± 9 kpa | ± 0.3 °C | (kg/m$^2$-s) | | ± 0.5 °C | ± 0.5 °C | (ho) | (vert) | ± 0.1 kPa | ± 0.26 kPa |
| 457 | 12.9 | 141.4 | 0.0495 | 27.4 | 26.8 | 9.08 | 8.74 | 5.76 | 6.73 |
| 460 | 13.1 | 141.7 | 0.0315 | 27.5 | 26.9 | 7.56 | 7.60 | 5.48 | 6.16 |
| 458 | 13.0 | 142.5 | 0.0116 | 27.8 | 27.2 | 5.90 | 6.22 | 4.19 | 4.67 |
| 460 | 13.1 | 80.9 | 0.0496 | 28.1 | 27.3 | 9.59 | 12.53 | 1.48 | 2.61 |
| 460 | 13.1 | 80.4 | 0.0298 | 27.5 | 27 | 7.59 | 11.14 | 1.33 | 2.6 |
| 459 | 13.1 | 80.6 | 0.011 | 28.1 | 27.6 | 5.05 | 8.85 | 1.19 | 2.05 |
| 459 | 13.1 | 101.7 | 0.0493 | 27.9 | 27.2 | 10.34 | 10.93 | 2.92 | 4.24 |
| 459 | 13 | 101.3 | 0.0307 | 27.8 | 27.2 | 8.22 | 9.46 | 2.43 | 3.57 |
| 458 | 13 | 103 | 0.0118 | 28.1 | 27.5 | 5.37 | 7.33 | 1.74 | 2.7 |
| 460 | 13.1 | 122 | 0.0505 | 28 | 27.2 | 10.07 | 9.96 | 4.42 | 5.5 |
| 459 | 13 | 121.4 | 0.0305 | 27.9 | 27.2 | 8.14 | 8.13 | 3.97 | 4.68 |
| 459 | 13.1 | 120 | 0.0121 | 28.1 | 27.5 | 6.32 | 6.56 | 2.99 | 3.55 |
| 478 | 14.3 | 34.3 | 0.0525 | 28.7 | 27.7 | 19.20 | 32.64 | | 3.89 |
| 477 | 14.3 | 35.2 | 0.0333 | 28.4 | 27.2 | 15.22 | 29.74 | | 3.4 |
| 475 | 14.2 | 58.8 | 0.0513 | 28 | 27.2 | 9.65 | 16.01 | 0.79 | 2.26 |
| 476 | 14.2 | 60.5 | 0.0302 | 28 | 27.4 | 7.39 | 13.61 | 0.58 | 1.78 |
| 475 | 14.2 | 61.6 | 0.0103 | 28.2 | 27.5 | 4.74 | 10.93 | 0.55 | 1.59 |
| 475 | 14.1 | 52.7 | 0.0523 | 28.4 | 27.7 | 9.67 | 17.84 | 0.5 | 2.28 |
| 473 | 14 | 52.5 | 0.0298 | 28 | 27.4 | 7.56 | 15.55 | 0.48 | 1.89 |
| 477 | 14.3 | 53.6 | 0.01 | 28.4 | 27.8 | 4.72 | 12.76 | 0.35 | 1.53 |

# R1234yf/POE 32 raw data – 10.2 mm pipe diameter

| P_sat | T_sat | Total Mass Flux | OCR | T_ref_evap_out | T_r_e_wall | Mass oil | Mass oil | Pressure drop (ho) | Pressure drop (vert) |
|---|---|---|---|---|---|---|---|---|---|
| ± 9 kpa | ± 0.3 °C | (kg/m$^2$-s) | | ± 0.5 °C | ± 0.5 °C | (ho) | (vert) | ± 0.1 kPa | ± 0.26 kPa |
| 481 | 13.2 | 142.2 | 0.0507 | 28.0 | 27.2 | 11.12 | 10.93 | 5.34 | 6.70 |
| 477 | 13.0 | 141.1 | 0.0301 | 28.1 | 27.4 | 9.12 | 9.00 | 4.94 | 5.92 |
| 479 | 13.0 | 142.1 | 0.01 | 27.9 | 27.5 | 6.66 | 6.63 | 3.63 | 4.22 |
| 479 | 13.1 | 173.1 | 0.0526 | 28 | 27.2 | 10.44 | 10.11 | 7.96 | 9.35 |
| 478 | 13 | 171.9 | 0.0304 | 28 | 27.4 | 8.37 | 8.31 | 7.3 | 8.25 |
| 478 | 13 | 170.6 | 0.0102 | 28.1 | 27.7 | 5.88 | 5.93 | 5.43 | 6.04 |
| 480 | 13.2 | 122.1 | 0.0508 | 28 | 27.2 | 11.80 | 11.99 | 3.98 | 5.37 |
| 478 | 13 | 122.3 | 0.0303 | 28.1 | 27.5 | 9.68 | 9.87 | 3.7 | 4.63 |
| 480 | 13.1 | 120 | 0.0099 | 28.3 | 27.9 | 5.91 | 7.41 | 2.26 | 3.28 |
| 479 | 13 | 103.1 | 0.0499 | 28.2 | 27.4 | 11.54 | 13.10 | 2.38 | 4.37 |
| 479 | 13.1 | 101.5 | 0.0308 | 28.2 | 27.5 | 9.03 | 10.89 | 2.05 | 3.66 |
| 479 | 13.1 | 102.7 | 0.0108 | 28.2 | 27.7 | 5.44 | 8.45 | 1.62 | 2.49 |
| 477 | 13 | 80.1 | 0.0514 | 28 | 27.1 | 11.41 | 15.38 | 1.37 | 3.08 |
| 479 | 13.1 | 80.4 | 0.0309 | 28 | 27.3 | 8.78 | 12.92 | 1.23 | 2.59 |
| 479 | 13.1 | 82.4 | 0.011 | 28.1 | 27.6 | 5.39 | 10.17 | 1.01 | 1.9 |
| 478 | 13 | 62.3 | 0.0507 | 28.2 | 27.3 | 12.55 | 19.25 | 0.78 | 2.53 |
| 479 | 13.1 | 62 | 0.0311 | 28.5 | 27.9 | 8.89 | 16.17 | 0.58 | 1.99 |
| 478 | 13 | 61.5 | 0.0117 | 28 | 27.4 | 6.16 | 13.87 | 0.52 | 1.55 |
| 479 | 13.1 | 51.4 | 0.0499 | 28.2 | 27.4 | 12.47 | 21.58 | 0.46 | 2.35 |
| 479 | 13.1 | 52.1 | 0.0309 | 28.2 | 27.5 | 10.00 | 19.17 | 0.45 | 1.93 |
| 478 | 13 | 52.6 | 0.0122 | 28.1 | 27.4 | 6.52 | 16.13 | 0.33 | 1.51 |
| 494 | 14.1 | 39.5 | 0.0532 | 28 | 27 | 18.58 | 32.67 | 0.25 | 3.65 |
| 492 | 14.1 | 35.7 | 0.0333 | 28.2 | 27.4 | 19.91 | 32.80 | 0.15 | 3.38 |
| 491 | 13.9 | 35 | 0.0125 | 28 | 27.5 | 16.34 | 30.71 | 0.19 | 3.03 |

## R1234yf/POE 32 raw data – 10.2 mm pipe diameter, 45° inclination

| P_sat | T_sat | Total Mass Flux | OCR | T_ref_evap_out | T_r_e_wall | Mass oil | Pressure drop (vert) |
|---|---|---|---|---|---|---|---|
| ± 9 kpa | ± 0.3 °C | (kg/m$^2$-s) | | ± 0.5 °C | ± 0.5 °C | (vert) | ± 0.26 kPa |
| 481 | 13.2 | 170.0 | 0.0320 | 28.4 | 27.7 | 8.58 | 7.97 |
| | | | | | | | |
| 478 | 13.0 | 169.0 | 0.0102 | 28.2 | 27.7 | 6.06 | 5.76 |
| | | | | | | | |
| 479 | 13.1 | 101.4 | 0.0301 | 28.1 | 27.4 | 11.03 | 3.11 |
| | | | | | | | |
| 479 | 13.1 | 104.6 | 0.0141 | 28.2 | 27.6 | 8.30 | 2.68 |
| | | | | | | | |
| 478 | 13 | 64.3 | 0.0319 | 28.4 | 27.7 | 15.37 | 1.94 |
| | | | | | | | |
| 480 | 13.1 | 61.4 | 0.0117 | 28.1 | 27.6 | 10.50 | 1.36 |
| | | | | | | | |
| 480 | 13.1 | 52.8 | 0.0294 | 28.5 | 27.8 | 21.73 | 2.25 |
| | | | | | | | |
| 478 | 13 | 50.9 | 0.0113 | 28.2 | 27.5 | 18.67 | 2.07 |
| | | | | | | | |
| 492 | 14 | 36.6 | 0.0302 | 28.6 | 27.8 | 35.27 | 3.73 |
| | | | | | | | |
| 492 | 14 | 36.8 | 0.013 | 28.4 | 27.5 | 31.08 | 3.3 |

## R1234yf/POE 32 raw data – 10.2 mm pipe diameter, 60° inclination

| P_sat | T_sat | Total Mass Flux | OCR | T_ref_evap_out | T_r_e_wall | Mass oil | Pressure drop (vert) |
|---|---|---|---|---|---|---|---|
| ± 9 kpa | ± 0.3 °C | (kg/m$^2$-s) | | ± 0.5 °C | ± 0.5 °C | (vert) | ± 0.26 kPa |
| 477 | 13.0 | 172.8 | 0.0115 | 28.0 | 27.5 | 6.36 | 6.34 |
| | | | | | | | |
| 479 | 13.1 | 101.2 | 0.0109 | 28.0 | 27.6 | 8.72 | 2.39 |
| | | | | | | | |
| 480 | 13.1 | 64.6 | 0.0116 | 28.1 | 27.7 | 11.28 | 1.49 |
| | | | | | | | |
| 491 | 13.9 | 52.2 | 0.0117 | 28.2 | 27.7 | 19.91 | 2.1 |
| | | | | | | | |
| 494 | 14.1 | 34.3 | 0.0116 | 28.3 | 27.6 | 37.02 | 3.95 |
| | | | | | | | |
| 493 | 14.2 | 37.6 | 0.011 | 28.5 | 27.7 | 32.28 | 3.41 |
| | | | | | | | |
| 479 | 13.1 | 169.6 | 0.0344 | 28.1 | 27.5 | 9.27 | 7.67 |
| | | | | | | | |
| 480 | 13.1 | 98.7 | 0.0301 | 28.1 | 27.6 | 11.43 | 2.98 |
| | | | | | | | |
| 480 | 13.1 | 62.9 | 0.0309 | 28 | 27.3 | 17.21 | 1.98 |
| | | | | | | | |
| 479 | 13.1 | 53.5 | 0.03 | 28.1 | 27.5 | 21.10 | 2.25 |
| | | | | | | | |
| 492 | 14 | 38.6 | 0.0317 | 28.3 | 27.5 | 30.61 | 2.89 |
| | | | | | | | |
| 492 | 14 | 35.9 | 0.03 | 28.2 | 27.2 | 35.84 | 4.25 |
| | | | | | | | |

# REFERENCES


1. Asali, J.C., Hanratty, T.J., Andreussi, P., 1985. “Interfacial drag and film height for vertical annular flow”, *AIChE J.*, vol. 31, no. 6, pp. 895–902.
2. ASHRAE 1973. *Handbook and Product Directory, 1973 Systems*
3. ASHRAE 2002, "Lubricants in refrigerant systems" in *2002 ASHRAE Handbook—Refrigeration* American Society of Heating, Refrigerating and Air-Conditioning Engineers, Atlanta, pp. 7.1-7.26.
4. Baker, O. 1954, "Simultaneous Flow of Oil and Gas", *Oil and Gas Journal*, no. 53, pp. 185-190.
5. Beggs, H.D. & Brill, J.R. 1973, "Study of two-phase flow in inclined pipes", *JPT, Journal of Petroleum Technology,* vol. 25, pp. 607-617
6. Belt, R.J., Van't Westende, J.M.C. & Portela, L.M. 2009, "Prediction of the interfacial shear-stress in vertical annular flow", *International Journal of Multiphase Flow,* vol. 35, no. 7, pp. 689-697.
7. Collier J.G. & Thome J.R. 1994, *Convective Boiling and Condensation*, 3rd ed., Oxford University Press, New York, pp. 19-20.
8. Cremaschi, L., Hwang, Y. & Radermacher, R. 2005, "Experimental investigation of oil retention in air conditioning systems", *International Journal of Refrigeration*, vol. 28, no. 7, pp. 1018-1028.
9. Crompton, J.A., Newell, T.A. & Chato, J.C. 2004, “Experimental Measurement and Modeling of Oil Holdup*”*, ACRC TR 226, Air Conditioning and Refrigeration Center, University of Illinois at Urbana-Champaign, Urbana, IL
10. F-Chart. 2010. Engineering Equation Solver (EES) (academic version). Madison, WI: F-Chart.
11. Hager, W.H. 2003, "Blasius: A life in research and education", *Experiments in Fluids,* vol. 34, no. 5, pp. 566-571
12. Jacobs, M.L., Scheideman, F.C., Kazem, S.M. & Macken, N.A. 1976, "Oil Transport by Refrigerant Vapor", *ASHRAE Transactions,* vol. 82, no. pt 2, pp. 318-329.
13. Kesim, S.C., Albayrak, K. & Ileri, A. 2000, "Oil entrainment in vertical refrigerant piping", *International Journal of Refrigeration,* vol. 23, no. 8, pp. 626-631.
14. Knudsen, J.G. & Katz, D.L. 1958, *Fluid dynamics and heat transfer*, McGraw-Hill Book Company; New York, pp. 576
15. Lee, J., Hwang, Y., Radermacher, R. & Mehendale, S.S. 2001, "Experimental investigations on oil accumulation characteristics in a vertical suction line", *2001 ASME International Mechanical Engineering Congress and Exposition, November 11, 2001 - November 16,* American Society of Mechanical Engineers, New York, NY, United states, 2001, pp. 63.

16. Lee, J.P. 2003. “Experimental and theoretical investigation of oil retention in carbon dioxide air conditioning system”, PhD thesis, Center for Environmental Energy Engineering, University of Maryland, College Park, MD.
17. Mehendale, S.S. & Radermacher, R. 2000, "Experimental and theoretical investigation of annular film flow reversal in a vertical pipe: Application to oil return in refrigeration systems", *HVAC and R Research,* vol. 6, no. 1, pp. 55-74
18. Mukherjee, H. & Brill, J.P. 1983, "Liquid holdup correlations for inclined two-phase flow", *JPT, Journal of Petroleum Technology,* vol. 35, no. 5, pp. 1003-1008.
19. Pueker, S. and Hrnjak, P.S. 2010,”Experimental and Analytical Investigation of Refrigerant and Lubricant Migration”, ACRC TR 277, Air Conditioning and Refrigeration Center, University of Illinois at Urbana-Champaign, Urbana, IL
20. Radermacher, R., Cremaschi, L. & Schwentker, R.A. 2006, "Modeling of oil retention in the suction line and evaporator of air-conditioning systems", *HVAC and R Research*, vol. 12, no. 1, pp. 35-56.
21. Sundaresan, S.G. & Radermacher, R. 1996, "Oil return characteristics of refrigerant oils in split heat pump system", *ASHRAE Journal,* vol. 38, no. 8, pp. 57-61.
22. Taitel, Y., Barnea, D. & Dukler, A.E., 1980. Modeling flow pattern transition for steady upward gas-liquid flow in vertical tubes. *AICHE Journal*, vol. 26, pp. 345–354.
23. Taitel, Y. & Dukler, A.E. 1976, "A model for predicting flow regime transitions in horizontal and near horizontal gas-liquid flow", *AICHE Journal,* vol. 22, no. 1, pp. 47-55.
24. Takaishi, Y. & Oguchi, K. 1987, "Measurements of vapor pressures of R22/oil solution", *Proceedings of the 18th International Congress of Refrigeration*, pp. 217-222.
25. Thome, J.R. 1995, "Comprehensive thermodynamic approach to modeling refrigerant-lubricating oil mixtures", *HVAC&R Research,* vol. 1, no. 2, pp. 110-110.
26. van Rossum, J.J. 1959, "Experimental investigation of horizontal liquid films. Wave formation, atomization, film thickness", *Chemical Engineering Science,* vol. 11, no. 1, pp. 35-52.
27. Wallis, G. 1969, *One Dimensional Two-Phase Flow,* McGraw-Hill Book Company, Newyork.
28. Weisman, J. & Kang, S.Y. 1981, "Flow Pattern Transitions in Vertical and Upwardly Inclined Lines”, *International Journal of Multiphase Flow*, vol. 7, no. 3, pp. 271-291.
29. Zoellick, K.F. & Hrnjak, P.S. 2010, “Oil Retention and Pressure Drop in Horizontal and Vertical Suction Lines with R410A/POE”, ACRC TR 271, Air Conditioning and Refrigeration Center, University of Illinois at Urbana-Champaign, Urbana, IL